

**ΠΑΝΕΠΙΣΤΗΜΙΟ ΚΡΗΤΗΣ  
ΤΜΗΜΑ ΧΗΜΕΙΑΣ**

**ΜΕΤΑΠΤΥΧΙΑΚΟ ΠΡΟΓΡΑΜΜΑ  
ΕΠΙΣΤΗΜΕΣ ΚΑΙ ΜΗΧΑΝΙΚΗ ΠΕΡΙΒΑΛΛΟΝΤΟΣ**

**ΕΡΓΑΣΤΗΡΙΟ ΠΕΡΙΒΑΛΛΟΝΤΙΚΩΝ ΧΗΜΙΚΩΝ  
ΔΙΕΡΓΑΣΙΩΝ (Ε.ΠΕ.ΧΗ.ΔΙ)**



**ΜΕΤΑΠΤΥΧΙΑΚΟ ΔΙΠΛΩΜΑ ΕΙΔΙΚΕΥΣΗΣ**

**ΜΕΛΕΤΗ ΤΗΣ ΕΠΙΔΡΑΣΗΣ ΤΩΝ ΒΙΟΓΕΝΩΝ  
ΥΔΡΟΓΟΝΑΝΘΡΑΚΩΝ ΣΤΗΝ ΟΞΕΙΔΩΤΙΚΗ ΙΚΑΝΟΤΗΤΑ  
ΤΗΣ ΑΤΜΟΣΦΑΙΡΑΣ ΜΕ ΤΗ ΧΡΗΣΗ ΤΟΥ ΠΑΓΚΟΣΜΙΟΥ  
ΜΟΝΤΕΛΟΥ ΧΗΜΕΙΑΣ ΚΑΙ ΜΕΤΑΦΟΡΑΣ ΤΜ5**

**Γκουβούσης Άγγελος**

**ΗΡΑΚΛΕΙΟ 2019**

**UNIVERSITY OF CRETE  
DEPARTMENT OF CHEMISTRY**

**POSTGRADUATE PROGRAM  
ENVIRONMENTAL SCIENCES AND ENGINEERING**

**ENVIRONMENTAL CHEMICAL PROCESSES  
LABORATORY (ECPL)**



**Master Thesis**

**STUDY OF THE IMPACT OF BIOGENIC  
HYDROCARBONS ON ATMOSPHERIC OXIDATION  
CAPACITY WITH THE GLOBAL CHEMISTRY AND  
TRANSPORT MODEL TM5**

**Gkouvousis Angelos**

**HERAKLION 2019**

*...στην οικογένειά μου...*

*...to my family...*

## **Examining Committee**

**Kanakidou Maria (supervisor)**

*Professor, Department of Chemistry, University of Crete*

**Myriokefalitakis Stelios (co - supervisor)**

*Associate Researcher, Institute for Environmental Research & Sustainable Development  
(IERSD), National Observatory of Athens (NOA)*

**Mihalopoulos Nikolaos**

*Professor, Department of Chemistry, University of Crete*

## ACKNOWLEDGEMENTS

The present work was carried out at the Environmental Chemical Processes Laboratory of the Department of Chemistry, University of Crete. It was funded by the National Observatory of Athens research grant (no 5065 - Atmospheric Deposition Impacts on the Ocean System). I would like to thank the Chemistry Department for accepting me in the postgraduate program as a master student.

I would like to thank all the members of my examining committee. I would like to express my special thanks to my supervisor Professor Maria Kanakidou for her guidance and for giving me the opportunity to work with her and her team for the past years. I would also like to thank my co - supervisor Dr. Stelios Myriokefalitakis for everything he taught me on atmospheric modelling and his precious guidance and advice throughout the duration of my work. Finally, I would also like to thank Professor Nikolaos Mihalopoulos for accepting to review my thesis.

I would like to thank all the members of the Environmental Chemical Processes Laboratory for the excellent collaboration and the really nice and friendly environment in the lab. I would like to express my special thanks to my friends and colleagues, Ph.D. candidate Maria Tsagkaraki and Dr. Pavlos Zampas for their precious help and support inside and outside the lab.

I would like to thank the National Observatory of Athens for funding my thesis under the research program ADIOS and the GRNET – National Infrastructures for Research and Technology for providing computational time in the HPC facility ARIS to perform the simulations for the present work.

I would like to thank my family, my father Thodoris, my mother Valasia and my brother Dimitris who have always been supporting me and always been there for me all this time. Finally, I would like to thank all of my good friends inside and outside the university for their support.

# CURRICULUM VITAE

## Personal Details

---

<i>Full name:</i>	Angelos Gkouvousis
<i>Date of Birth:</i>	19 September 1992
<i>Work address:</i>	Department of Chemistry, University of Crete, 70013, Voutes, Heraklion, Greece
<i>Tel. (lab):</i>	(+30)2810-545111
<i>e-mail</i>	a.gouvousis@gmail.com

## Education

---

<i>2017-2019</i>	Master Thesis at Environmental Chemical Processes Laboratory, Department of Chemistry University of Crete. Title: "Study of the impact of biogenic hydrocarbons on the atmospheric oxidation capacity with the global chemistry and transport model TM5."
<i>2017</i>	Diploma in Chemistry, Department of Chemistry, University of Crete
<i>2016-2017</i>	Diploma Thesis at Environmental Chemical Processes Laboratory, Department of Chemistry University of Crete. Title: "Understanding the production and consumption processes of tropospheric O <sub>3</sub> by updating a reduced atmospheric chemistry scheme with KPP"
<i>Language Knowledge</i>	Greek (native language) English (Certificate of Proficiency in English - C1) German (Zertifikat Deutsch - B1)
<i>Computational Experience</i>	Operating systems: Linux, Windows Programming Languages: FORTRAN 90, Python

---

Web development languages: HTML, CSS

Built the website for the 21<sup>st</sup> Postgraduates' Conference on Chemistry, Department of Chemistry, University of Crete, 2019 :

<http://www.chemistry.uoc.gr/chemconf/home.html>

### Teaching Experience

---

*Feb. 2018-May 2018* Teaching Assistant in Analytical Chemistry I Laboratory

*Feb. 2019-May 2019* Teaching Assistant Environmental Computational Chemistry course

### Organizational/Managerial Experience

---

*2017-2019* Management of the Chemistry Outreach Group (COG), Department of Chemistry, University of Crete

*2019* Organizing committee of the 21<sup>st</sup> Postgraduates' Conference on Chemistry, Department of Chemistry, University of Crete

### Publications/Presentations

---

*Publications* Stelios Myriokefalitakis, Nikos Daskalakis, **Angelos Gkouvousis**, Andreas Hilboll, Twan P.C. van Noije, Jason Williams, Philippe Le Sager, Vincent Huijnen, Sander Houweling, Tommi Bergman, Mihalis Vrekoussis, Maria Kanakidou and Maarten C. Krol: Description and evaluation of a detailed gas-phase chemistry scheme in the TM5-MP global chemistry transport model (r112), Geosci. Model Dev. Discuss., <https://doi.org/10.5194/gmd-2020-110>, *in review*, 2020.

*Presentations* **Angelos Gkouvousis**, Stelios Myriokefalitakis, Maria Kanakidou: New isoprene chemistry in MOGUNTIA, 29th International TM5 meeting, November 2019

**Angelos Gkouvousis**, Stelios Myriokefalitakis, Maria Kanakidou: Isoprene chemistry in TM5, C-STACC seminars, December 2019





## ΠΕΡΙΛΗΨΗ

Οι βιογενείς υδρογονάνθρακες (BVOC) οξειδώνονται αρκετά εύκολα υπό την παρουσία ριζών υδροξυλίου, νιτρικών ριζών και όζοντος. Έτσι διαδραματίζουν σημαντικό ρόλο στον έλεγχο της οξειδωτικής ικανότητας της ατμόσφαιρας. Πρόσφατα, προκειμένου να εξηγηθούν παρατηρήσεις υψηλών συγκεντρώσεων ριζών OH σε περιοχές που επηρεάζονται από εκπομπές BVOC, πραγματοποιήθηκε σημαντική πρόοδος στην κατανόηση της χημείας οξείδωσης ισοπρενίου. Σε αυτή τη μελέτη, χρησιμοποιώντας το τρισδιάστατο μοντέλο χημείας και μεταφοράς TM5-MP, σε συνδυασμό με τον μεγάλης ακρίβειας επιλυτή Rosenbrock όπως παράχθηκε από το υπολογιστικό πρόγραμμα KPP, και το επικαιροποιημένο λεπτομερές χημικό σχήμα MOGUNTIA, αξιολογήσαμε την επίδραση του ισοπρενίου και των τερπενίων στην οξειδωτική ικανότητα της τροπόσφαιρας σε παγκόσμιο επίπεδο. Οι προσομοιώσεις πραγματοποιήθηκαν για το έτος 2006 λαμβάνοντας υπόψη, στην μία περίπτωση, και αγνοώντας στην άλλη, την χημεία του ισοπρενίου και των τερπενίων. Οι διαφορές μεταξύ των προσομοιώσεων που προέκυψαν από τη χημεία BVOC διερευνήθηκαν, εστιάζοντας στις συγκεντρώσεις των CO, O<sub>3</sub> και ριζών OH. Η απόδοση του μοντέλου αξιολογήθηκε με σύγκριση των αποτελεσμάτων με παρατηρήσεις πεδίου από τις βάσεις δεδομένων των WOUDC και NOAA.

**Λέξεις κλειδιά:** ατμοσφαιρικές διεργασίες, βιογενείς υδρογονάνθρακες, 3-διαστατο μοντέλο χημείας και μεταφοράς, οξειδωτική ικανότητα

## **ABSTRACT**

Biogenic hydrocarbons (BVOC) are highly reactive against hydroxyl and nitrate radicals and ozone. They thus play an important role in controlling the oxidation capacity of the atmosphere. Recently, in order to explain observations of high OH radicals in areas affected by BVOC emissions significant progress has been made in our understanding of isoprene oxidation chemistry. In this study, using the 3-dimensional chemistry and transport model TM5-MP, coupled with Rosenbrock solver as derived by the KPP software and the detailed updated MOGUNTIA chemical scheme we evaluated the impact of isoprene and terpenes on the oxidation capacity on the global troposphere. Simulations were performed for the year 2006 taking into consideration and neglecting isoprene and terpenes chemistry. The differences between these simulations resulting from the BVOC chemistry were investigated, focusing on the concentrations of CO, O<sub>3</sub> and OH radical. The performance of the model was evaluated by comparing the results with field observations from the WOUDC and NOAA.

**Keywords:** atmospheric processes, biogenic hydrocarbons, isoprene, 3D global chemistry and transport model, oxidation capacity

# Table of Contents

<b>1</b>	<b><i>Introduction</i></b> .....	<b>1</b>
<b>1.1</b>	<b>Atmospheric Chemistry</b> .....	<b>3</b>
1.1.1	Tropospheric Oxidants .....	3
1.1.2	Volatile Organic Compounds .....	6
<b>1.2</b>	<b>Isoprene</b> .....	<b>9</b>
1.2.1	Isoprene Oxidation .....	9
<b>1.3</b>	<b>Aim of the study</b> .....	<b>11</b>
<b>1.4</b>	<b>References</b> .....	<b>13</b>
<b>2</b>	<b><i>Model Description</i></b> .....	<b>16</b>
<b>2.1</b>	<b>Meteorology</b> .....	<b>19</b>
<b>2.2</b>	<b>Emissions</b> .....	<b>19</b>
<b>2.3</b>	<b>Deposition</b> .....	<b>21</b>
<b>2.4</b>	<b>Advection – Convection</b> .....	<b>22</b>
<b>2.5</b>	<b>Stratospheric Boundary Conditions</b> .....	<b>23</b>
<b>2.6</b>	<b>The Kinetic PreProcessor</b> .....	<b>23</b>
<b>2.7</b>	<b>The MOGUNTIA chemical scheme</b> .....	<b>24</b>
2.7.1	Updates on the chemical scheme .....	26
<b>2.8</b>	<b>Computational Resources</b> .....	<b>27</b>
<b>2.9</b>	<b>References</b> .....	<b>28</b>
<b>3</b>	<b><i>Simulations</i></b> .....	<b>33</b>
<b>3.1</b>	<b>Ozone</b> .....	<b>33</b>
3.1.1	Comparison between the UPDATED and the OLD scheme .....	34
<b>3.2</b>	<b>Comparison to observations (O<sub>3</sub>)</b> .....	<b>35</b>
<b>3.3</b>	<b>Hydroxyl radicals</b> .....	<b>36</b>
3.3.1	Comparison between the UPDATED and the OLD scheme .....	39
3.3.2	Comparison to other modelling studies .....	41

<b>3.4</b>	<b>Carbon Monoxide</b> .....	<b>42</b>
3.4.1	Comparison between the UPDATED and the OLD scheme .....	43
3.4.2	Comparison to observations (CO).....	44
<b>3.5</b>	<b>Isoprene epoxydiols</b> .....	<b>45</b>
<b>3.6</b>	<b>Hydro peroxy aldehydes</b> .....	<b>47</b>
<b>3.7</b>	<b>Impact of biogenic hydrocarbons (BVOCs) on tropospheric chemistry</b> .....	<b>48</b>
3.7.1	Ozone.....	48
3.7.2	Hydroxyl Radical .....	49
3.7.3	Carbon monoxide .....	51
<b>3.8</b>	<b>References</b> .....	<b>53</b>
<b>4</b>	<b>Conclusions</b> .....	<b>54</b>
<b>5</b>	<b>Appendix</b> .....	<b>56</b>
5.1	References .....	75

# 1 Introduction

Earth's atmosphere is a system of high complexity and of vital importance for every living organism. It extends from the surface of the earth to approximately 500km and has four main layers, the troposphere, the stratosphere, the mesosphere and the thermosphere as shown in Figure 1.1. Its main constituents are nitrogen ( $N_2$ , 78%), oxygen ( $O_2$ , 21%) and various noble gases (0.098%, mainly argon, Ar) which have remained constant throughout the past 2.3 billion years. The remaining gaseous constituents are trace gases which represent less than 0.02% of the atmosphere (Seinfeld and Pandis, 2016). Even though trace gases constitute a small fraction of the atmosphere, they show high variability in composition and affect significantly the atmospheric processes.

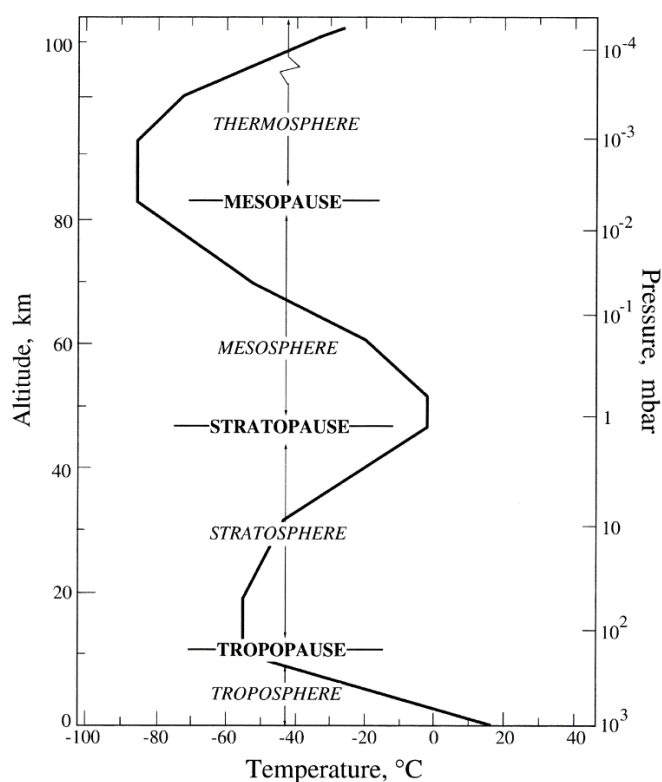


Figure 1.1: Schematic representation of atmospheric layers and temperature (Seinfeld and Pandis, 2016)

Atmospheric composition is affected by solar radiation, wind, clouds, ice, sea, flora, fauna and the earth's surface. It is also affected due to the chemical interactions of the emitted into the atmosphere trace compounds such as nitrogen oxides, volatile organics and carbon monoxide. This chemistry can take place in the gaseous, the particulate and as well as in the aqueous phase of the atmosphere and it is strongly impacted by meteorology and climate.

Gaseous and particulate compounds can be transported during air mass movements, absorb or scatter solar radiation, changing the earth's energy balance and therefore climate.

Trace compounds such as methane (CH<sub>4</sub>), water vapor (H<sub>2</sub>O), carbon dioxide (CO<sub>2</sub>), nitrous oxide (N<sub>2</sub>O) and ozone (O<sub>3</sub>) are some of those greenhouse gases (GHGs). They have the ability to absorb infrared radiation and thus heating earth's surface, creating a natural greenhouse effect and making the planet habitable. Without that effect, owing primarily to H<sub>2</sub>O and CO<sub>2</sub>, the planet would have a mean temperature of -18°C instead of 15°C that has currently. Humans have increased the GHG as well as the aerosols concentrations in the atmosphere, overall modified significantly the Earth's budget. The way that human induced changes in atmospheric composition has affected the Earth's balance since 1750, i.e. the radiative forcing, can be seen in **Figure 1.2**.

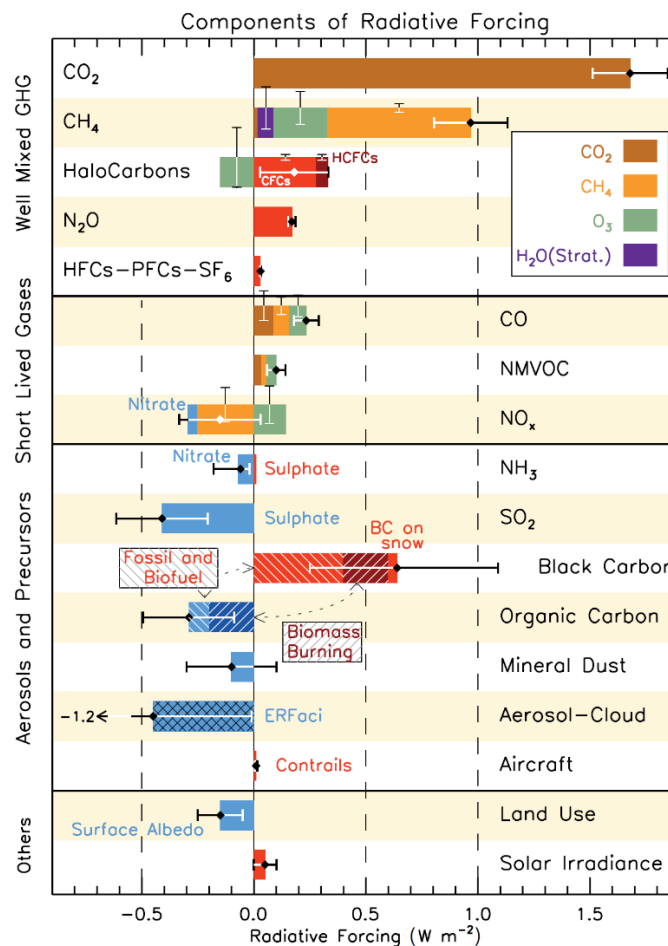


Figure 1.2: Bar chart for Radiative Forcing for the period 1750-2011 (IPCC, 2013)

## 1.1 Atmospheric Chemistry

Atmospheric chemical processes have drawn the attention of scientists and have been increasingly studied the last decades. Chemistry in the atmosphere can be split into two main categories, tropospheric and stratospheric, while mesospheric chemistry involves mainly radicals and ions. Tropospheric chemistry, that is the focus of the present study, takes places from Earth's surface up to 10-15km altitude depending on latitude and time of the year.

The troposphere acts like a chemical reservoir almost distinct from the stratosphere. Transport of trace compounds from the troposphere to the stratosphere, and vice versa, is much slower (about 1 year) than mixing within the troposphere itself. A factor critical for the chemistry in the troposphere is the high concentration of water vapor. Photochemical changes in the troposphere are sunlight driven. The direct interaction of sunlight with molecules in the air is the source of most of the atmospheric free radicals. Free radicals, in particular hydroxyl (OH) radicals act to transform most species in the troposphere.

### 1.1.1 Tropospheric Oxidants

Oxidation in the troposphere is driven mainly by three compounds, hydroxyl radicals (OH) during daytime, ozone (O<sub>3</sub>) during day and night and nitrate radical (NO<sub>3</sub>) during nighttime. These compounds, even though they exist in quite low mixing ratios, are responsible for the chemical degradation of most atmospheric species.

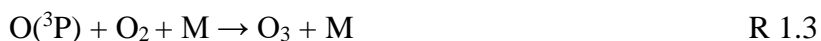
#### Hydroxyl radical

Hydroxyl radical is the key component of the oxidizing capacity of the troposphere, the so-called cleaning agent of the troposphere, responsible for the degradation of most reactive trace constituents of the troposphere. It is unreactive toward O<sub>2</sub>, once produced, so it survives to react with almost all reactive tropospheric trace species. The most abundant oxidizing agents in the atmosphere are O<sub>2</sub> and O<sub>3</sub> but their bond energy is high, making them unreactive except with certain free radicals and leaving OH as the primary oxidizing agent in troposphere. Hydroxyl radical is produced by the reaction of singlet oxygen (O<sup>1</sup>D) with water vapor where O<sup>1</sup>D is produced by O<sub>3</sub> photolysis.





The ground state  $\text{O}({}^3\text{P})$  rapidly reforms to  $\text{O}_3$  by the reaction with the existing  $\text{O}_2$  molecules.



Reaction R1.1 followed by reaction R1.3 can be called a null cycle since there is no net chemical effect. A portion of  $\text{O}({}^1\text{D})$  undergoes transition into its ground state by colliding with air molecules (M), usually  $\text{N}_2$  and  $\text{O}_2$ , which remove its excess of energy. The remaining  $\text{O}({}^1\text{D})$  will react with  $\text{H}_2\text{O}$  vapors to produce two OH radicals.



At 80% relative humidity, almost 40% of the  $\text{O}({}^1\text{D})$  formed by R1.1 produces OH radicals (Seinfeld and Pandis, 2016). Although, they cannot react with the most abundant gases in the atmosphere such as  $\text{O}_2$ ,  $\text{N}_2$ ,  $\text{CO}_2$ , or  $\text{H}_2\text{O}$ , they react with most of the reactive trace compounds in the troposphere. Their high reactivity, however, combined with their relatively high concentration makes them important to tropospheric chemistry. Furthermore, when they react with trace compounds they are regenerated through catalytic cycles, maintaining their daylight mean concentration on the order of  $10^6$  molecules  $\text{cm}^{-3}$ . Finally, the two main pathways of OH destruction in the global troposphere are reactions with  $\text{CH}_4$  and  $\text{CO}$ .



### **Ozone and nitrate radical**

Another important oxidizing agent of the troposphere is  $\text{O}_3$  which also acts as a greenhouse gas. The stratosphere acts as a source of  $\text{O}_3$  in troposphere is through downward transport. Tropospheric  $\text{O}_3$  levels though cannot be explained by only taking into account the



flux from the stratosphere. In the presence of NO<sub>x</sub> (sum of nitric oxide (NO) and nitrogen dioxide (NO<sub>2</sub>)) during daytime, ozone production is initiated by photolysis of NO<sub>2</sub>.



Triplet oxygen generated from reaction R1.8 will then react with O<sub>2</sub> to produce O<sub>3</sub> according to reaction R1.3. Nitric oxide (NO) can also react with O<sub>3</sub> to generate NO<sub>2</sub> overall resulting null cycle for O<sub>3</sub>. In order to have O<sub>3</sub> production, NO needs to be converted to NO<sub>2</sub> without consumption of O<sub>3</sub>. When organic compounds are present, the RO<sub>2</sub> radicals formed by volatile organic compound (VOC) oxidation can convert NO to NO<sub>2</sub> without destroying O<sub>3</sub> through reactions that are described in Sect. 1.1.2. Nitrogen dioxide can also react with O<sub>3</sub> in order to produce another oxidant, NO<sub>3</sub> radical. Finally, NO<sub>3</sub> itself can react with NO<sub>2</sub> producing nitrogen pentoxide (N<sub>2</sub>O<sub>5</sub>). Production of NO<sub>3</sub> is favored during nighttime since during daytime quickly decomposes NO<sub>3</sub> back to NO or NO<sub>2</sub> as shown in reactions R1.12 and R1.13.



Nitrogen oxides are removed from the atmosphere through the formation of N<sub>2</sub>O<sub>5</sub> and its further reaction with water vapor or wet surfaces. In addition, reaction of NO<sub>2</sub> with OH radicals, is another way of NO<sub>x</sub> removal through nitric acid (HNO<sub>3</sub>) production. Nitric acid can be removed from the atmosphere by wet deposition.



A summary of the main reactions taking place in the troposphere without details about the organic chemistry can be seen in **Figure 1.3**.

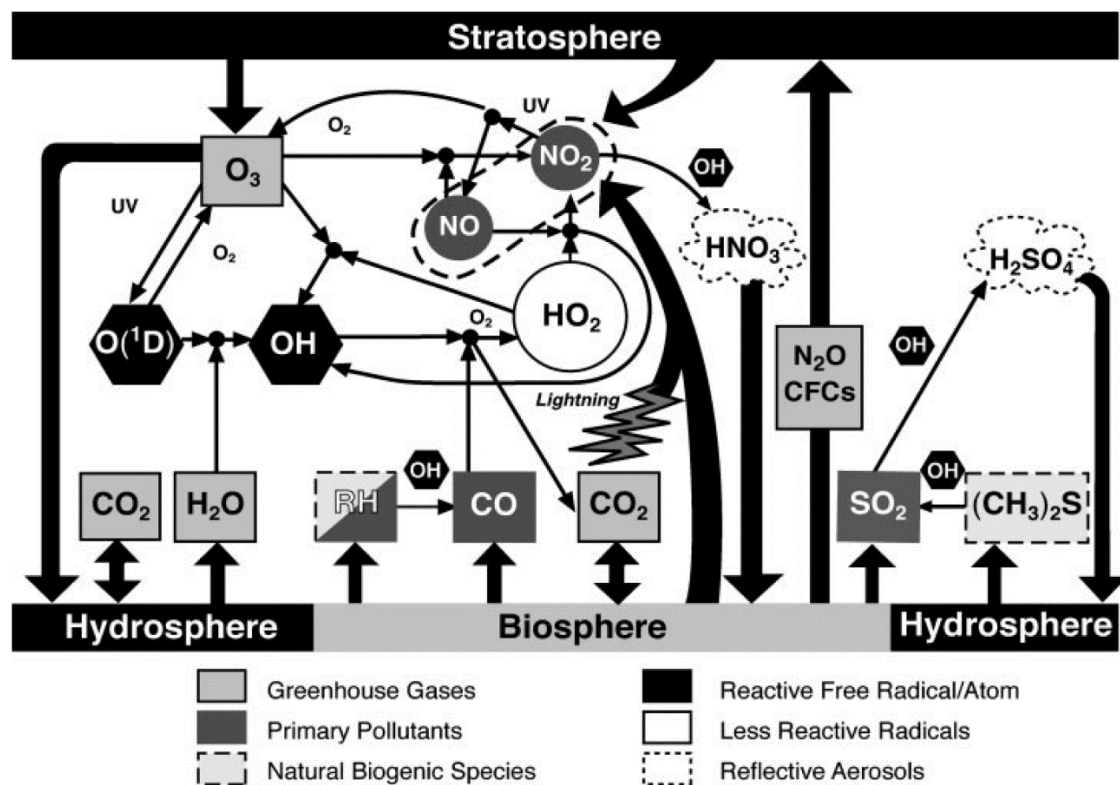


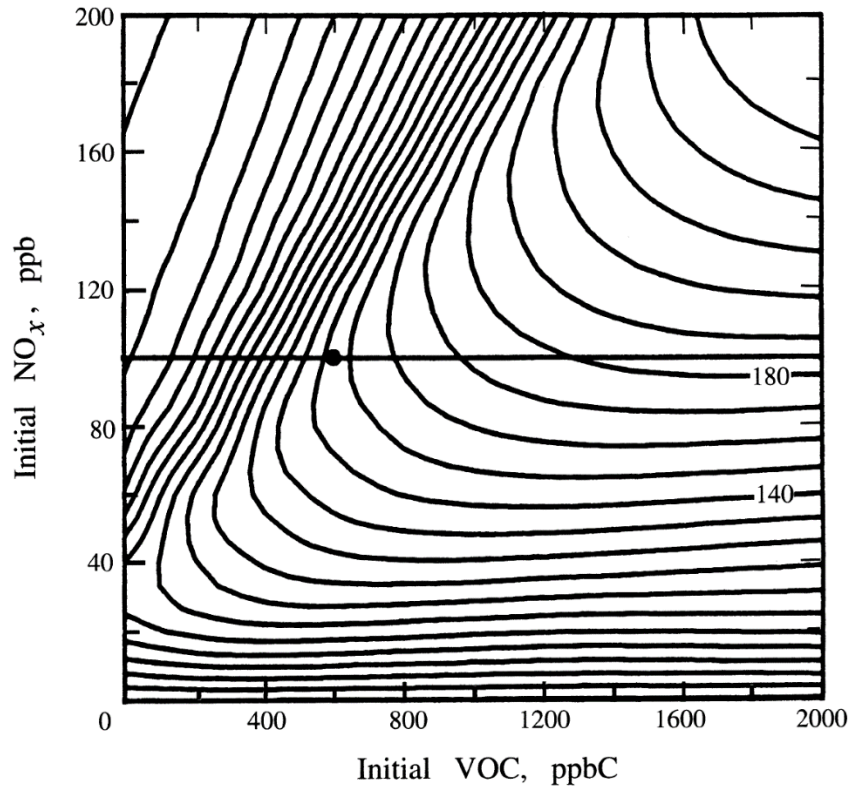
Figure 1.3: Summary of the oxidation processes taking place in the troposphere oversimplifying the chemistry of organics (Prinn, 2003)

### 1.1.2 Volatile Organic Compounds

A volatile organic compound (VOC) is defined by the US Environmental Protection Agency (EPA) as ‘any compound of carbon, excluding carbon monoxide, carbon dioxide, carbonic acid, metallic carbides or carbonates, and ammonium carbonate, which participates in atmospheric photochemical reactions’ (source: [www.epa.gov/](http://www.epa.gov/)). The sources of VOC in the atmosphere can be either anthropogenic or biogenic. The most abundant VOC in the troposphere is methane which has a lifetime of about 9 years.

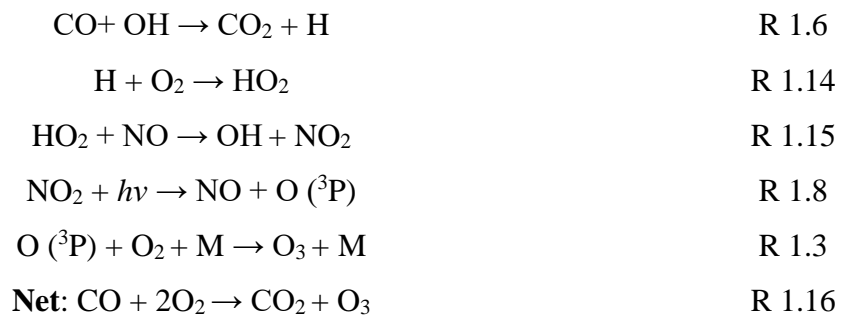
Oxidation of VOC takes place through reactions with  $O_3$ ,  $OH$  radicals and  $NO_3$  radicals, the main oxidizing agents in the troposphere. VOCs are oxidized into carbonylic compounds (aldehydes, ketones) and other organic products, degrading to carbon dioxide ( $CO_2$ ) as the final product of oxidation. Throughout the course of oxidation, hydroperoxy ( $HO_2$ ) and organic-peroxy ( $RO_2$ ) radicals which have the ability of oxidizing  $NO$  to  $NO_2$  are produced, with the simplest in structure being alkyl-peroxy radicals (Atkinson, 2000). As mentioned in Sect. 1.1.1,

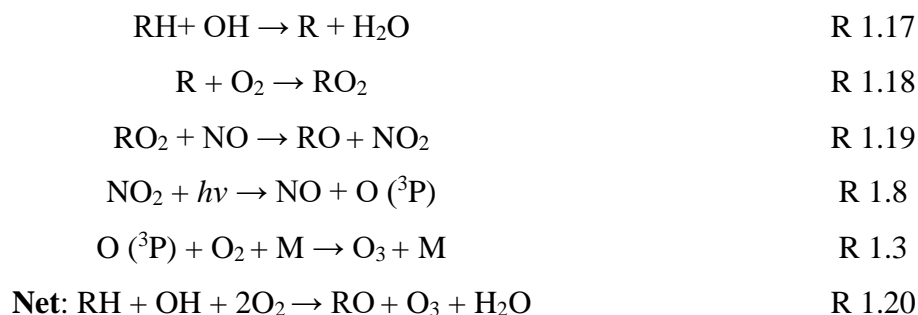
NO<sub>x</sub> are important to O<sub>3</sub> production. VOC reacting with OH radicals is initiating for the oxidation sequence. However, there is a competition between NO<sub>x</sub> and VOCs for the OH radical. The O<sub>3</sub> production highly depends on the VOC/NO<sub>x</sub> ratio. This dependence is frequently represented by means of an ozone isopleth diagram (**Figure 1.4**).



**Figure 1.4:** Isopleth plot based on simulations of chemistry along air trajectories in Atlanta (Seinfeld and Pandis, 2016). O<sub>3</sub> isopleths are spaced every 10 ppb, and increase as one moves upward and to the right.

Under sufficient NO<sub>x</sub> concentrations, the following reaction cycles take place which lead to O<sub>3</sub> production.





Besides the path shown above, the  $\text{RO}_2$  radicals when reacting with  $\text{NO}_x$  can produce organonitrate compounds ( $\text{RC(O)O}_2\text{NO}_2$ ,  $\text{RONO}_2$ ,  $\text{RO}_2\text{NO}_2$ ), capable to carry and transfer  $\text{NO}_x$  to large distances, where  $\text{NO}_x$  get released during the decomposition of these compounds mixture, more stable than  $\text{NO}_x$ .  $\text{RO}_2$  can also react with  $\text{HO}_2$  radicals to form of hydroperoxides ( $\text{ROOH}$ ). A simplified schematic of OH initiating reactions of VOC can be seen in **Figure 1.5**.

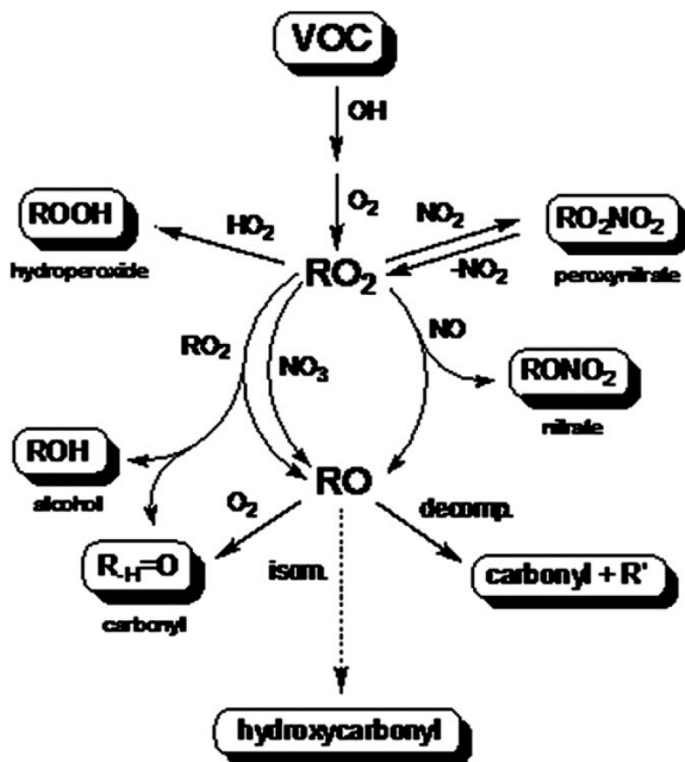


Figure 1.5: Simplified scheme of OH initiated oxidation of VOCs to first generation products (Monks, 2005)

To summarize, hydrocarbons impact the oxidizing capacity of the troposphere, since they affect the quantities of O<sub>3</sub>, CO and NO<sub>x</sub> (Poisson et al., 2000) and also consume OH and NO<sub>3</sub> radicals. In addition, there is a difference between the reaction rates of non-methane VOC (NMVOC) and CH<sub>4</sub> with the OH radical. That difference is greater than an order of magnitude which explains why NMVOC amounts in the atmosphere are smaller than those of CH<sub>4</sub> even though NMVOC emissions are nearly triple (Nriagu, 1992). NMVOC photo-oxidation in the presence NO<sub>x</sub>, leads to the formation of secondary compounds (gases and aerosols), such as, O<sub>3</sub>, aldehydes, ketones, secondary aerosol (SOA), which are considered to be responsible for the photochemical smog (Kanakidou et al., 2005; Poisson et al., 2000; Seinfeld and Pandis, 2016).

## 1.2 Isoprene

Isoprene (2-methyl-1,3-butadiene) is the most abundant biogenic NMVOC emitted to the atmosphere by plants. Its annual emissions globally are estimated to be around 500 Tg, i.e. comparable to those of methane (Guenther et al., 2012). Its lifetime in the atmosphere is ~1h against oxidation by OH radicals, i.e. almost 5 orders of magnitude shorter than that of CH<sub>4</sub>. The high reactivity of isoprene and its oxidation products are of high importance for tropospheric O<sub>3</sub> (Squire et al., 2015) and the OH radicals (Lelieveld et al., 2008). Isoprene is also important for SOA formation (Kanakidou et al., 2005).

### 1.2.1 Isoprene Oxidation

Oxidation processes of isoprene are complex and consist of almost 2000 reactions (Jenkin et al., 2015). Isoprene oxidation cascade initiated by OH radical results in the production of isoprene peroxy radicals (ISOPO<sub>2</sub>), the fate of which depends on NO<sub>x</sub> levels. A simplified representation of the oxidation process and first-generation products is shown in **Figure 1.6**. While NO<sub>x</sub> is present, the favored reaction pathway of ISOPO<sub>2</sub> is with NO, producing methyl vinyl ketone (MVK), methacrolein (MACR) and formaldehyde (HCHO) (Paulson and Seinfeld, 1992). Furthermore, a small portion of the ISOPO<sub>2</sub> reacting with NO<sub>x</sub> may lead to organic nitrate formation (ISOPN) (F. Paulot et al., 2009a). In the absence of NO<sub>x</sub>, in contrast, ISOPO<sub>2</sub> can react with RO<sub>2</sub> or HO<sub>2</sub> or it is capable of isomerization. Reaction of ISOPO<sub>2</sub> with HO<sub>2</sub> produces isoprene hydroperoxides (ISOPOOH) (F. Paulot et al., 2009b), while reaction with RO<sub>2</sub> leads mainly to small oxygenated VOCs (MVK, MACR, HCHO) (Saunders et al., 2003). ISOPO<sub>2</sub> is also able to isomerize via intramolecular hydrogen transfer, to be more precise, via either 1,6-H or 1,5-H shift (Peeters et al., 2009). Isomerization via 1,6-H shift forms

hydroperoxyl aldehydes (HPALD), which then undergo photolysis to produce small VOCs and regenerate OH radicals (Crouse et al., 2011; Peeters and Müller, 2010).

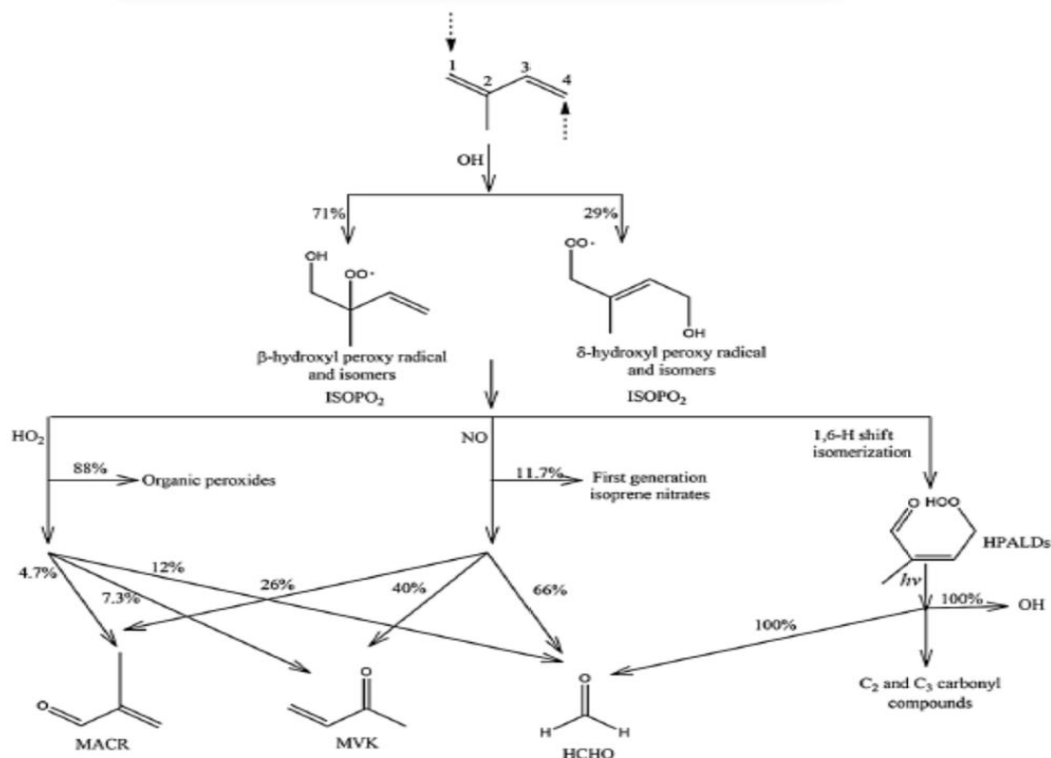


Figure 1.6: Schematic of the first stage of isoprene oxidation mechanism initiated by OH (Mao et al., 2013)

The 1,5-H shift produces an unstable intermediate that undergoes degradation to form HCHO, MACR and MVK. Finally, ISOPOOH formed by the reaction of ISOPO<sub>2</sub> with HO<sub>2</sub> radicals, may react with OH radicals producing cis- and trans- isomers of isoprene epoxydiols (IEPOX) and recycling OH radicals (Figure 1.7).

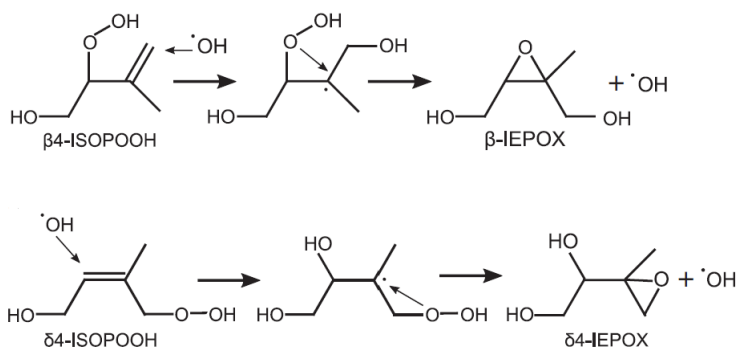
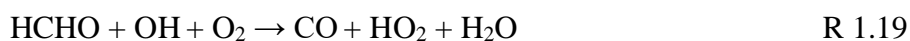
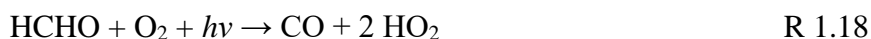


Figure 1.7: Example of two different IEPOX isomer formation through ISOPOOH reaction with OH and OH regeneration (F. Paulot et al., 2009b)

Formaldehyde (HCHO) is the major product of the isoprene oxidation chain reactions. It is produced not only from the first-generation products but also from the consecutive chemistry of other oxidation products such as methacrolein (MACR) and methyl vinyl ketone (MVK). Production of HCHO through isoprene oxidation is highly dependent on NO<sub>x</sub> levels (Wolfe et al., 2016). The presence of NO<sub>x</sub> is beneficial for the formation of both HCHO and O<sub>3</sub>. As shown in the following reactions during daytime HCHO decomposes to CO and HO<sub>2</sub> which contribute to the production of tropospheric O<sub>3</sub> as described in the previous section.



Also, very important is the other photolysis path



and reaction with OH radical



### 1.3 Aim of the study

Biogenic hydrocarbons (BVOCs) are highly reactive compounds against hydroxyl and nitrate radicals and play an important role controlling the oxidation capacity of the atmosphere. Lelieveld et al. (2008) have shown a remarkable impact of BVOCs on the OH radicals in areas with high biogenic activity like a tropical forest was by where they discovered unexpected high concentrations of OH radicals. Shortly after this discovery, Hofzumahaus et al. (2009) reported 3-5 times higher concentrations of OH than expected during a field campaign in Pearl-River, China, and proposed a mechanism of OH regeneration during VOC oxidation that is independent of NO<sub>x</sub> levels. Further studies showed that OH radicals were regenerated through isoprene oxidation under low NO<sub>x</sub> conditions (Fuchs et al., 2013) and proposed specific chemical pathways that have been documented since then (Paulot et al., 2009; Peeters and Müller, 2010).

The focus of this work is on BVOC chemistry and how this affects the oxidation capacity of the atmosphere. More specifically we implemented an updated and more detailed chemical scheme regarding isoprene, in the MOGUNTIA chemistry scheme (Poisson et al., 2000; Myriokefalitakis et al., 2008; Daskalakis et al., 2015) in order to take into consideration the latest finding of isoprene chemistry and OH regeneration (Browne et al., 2014). Using the MOGUNTIA chemistry scheme in the 3-dimensional global chemistry and transport model TM5-MP (Krol et al., 2005; Huijnen et al., 2010; Williams et al., 2017), we aim to study the impact of BVOC chemistry on the oxidation capacity of the troposphere as well as of isoprene's oxidation products, isoprene epoxydiols (IEPOX) and hydro peroxy aldehydes (HPALD) on O<sub>3</sub> and OH levels. For this we perform a global 3-d model simulation:

- 1) With the full updated MOGUNTIA chemistry scheme
- 2) Without the BVOC chemistry
- 3) Without the chemistry of IEPOX and HPALD

In addition, the performance of the new scheme is evaluated by comparison of the results to field measurements.



## 1.4 References

- Atkinson, R., 2000. Atmospheric chemistry of VOCs and NO(x). *Atmos. Environ.* 34, 2063–2101. [https://doi.org/10.1016/S1352-2310\(99\)00460-4](https://doi.org/10.1016/S1352-2310(99)00460-4)
- Browne, E.C., Wooldridge, P.J., Min, K.E., Cohen, R.C., 2014. On the role of monoterpene chemistry in the remote continental boundary layer. *Atmos. Chem. Phys.* <https://doi.org/10.5194/acp-14-1225-2014>
- Crouse, J.D., Paulot, F., Kjaergaard, H.G., Wennberg, P.O., 2011. Peroxy radical isomerization in the oxidation of isoprene. *Phys. Chem. Chem. Phys.* 13, 13607–13613. <https://doi.org/10.1039/c1cp21330j>
- Daskalakis, N., Myriokefalitakis, S., Kanakidou, M., 2015. Sensitivity of tropospheric loads and lifetimes of short lived pollutants to fire emissions. *Atmos. Chem. Phys.* <https://doi.org/10.5194/acp-15-3543-2015>
- Fuchs, H., Hofzumahaus, A., Rohrer, F., Bohn, B., Brauers, T., Dorn, H.P., Häseler, R., Holland, F., Kaminski, M., Li, X., Lu, K., Nehr, S., Tillmann, R., Wegener, R., Wahner, A., 2013. Experimental evidence for efficient hydroxyl radical regeneration in isoprene oxidation. *Nat. Geosci.* 6, 1023–1026. <https://doi.org/10.1038/ngeo1964>
- Guenther, A.B., Jiang, X., Heald, C.L., Sakulyanontvittaya, T., Duhl, T., Emmons, L.K., Wang, X., 2012. The model of emissions of gases and aerosols from nature version 2.1 (MEGAN2.1): An extended and updated framework for modeling biogenic emissions. *Geosci. Model Dev.* <https://doi.org/10.5194/gmd-5-1471-2012>
- Hofzumahaus, A., Rohrer, F., Lu, K., Bohn, B., Brauers, T., Chang, C.C., Fuchs, H., Holland, F., Kita, K., Kondo, Y., Li, X., Lou, S., Shao, M., Zeng, L., Wahner, A., Zhang, Y., 2009. Amplified trace gas removal in the troposphere. *Science* (80-. ). <https://doi.org/10.1126/science.1164566>
- Huijnen, V., Williams, J., Van Weele, M., Van Noije, T., Krol, M., Dentener, F., Segers, A., Houweling, S., Peters, W., De Laat, J., Boersma, F., Bergamaschi, P., Van Velthoven, P., Le Sager, P., Eskes, H., Alkemade, F., Scheele, R., Nédélec, P., Pätz, H.W., 2010. The global chemistry transport model TM5: Description and evaluation of the tropospheric chemistry version 3.0. *Geosci. Model Dev.* 3, 445–473. <https://doi.org/10.5194/gmd-3-445-2010>
- IPCC, 2013. Working Group I Contribution to the IPCC Fifth Assessment Report, Climate Change 2013: The Physical Science Basis. IPCC.
- Jenkin, M.E., Young, J.C., Rickard, A.R., 2015. The MCM v3.3.1 degradation scheme for isoprene. *Atmos. Chem. Phys.* <https://doi.org/10.5194/acp-15-11433-2015>
- Kanakidou, M., Seinfeld, J.H., Pandis, S.N., Barnes, I., Dentener, F.J., Facchini, M.C., Van Dingenen, R., Ervens, B., Nenes, A., Nielsen, C.J., Swietlicki, E., Putaud, J.P., Balkanski, Y., Fuzzi, S., Horth, J., Moortgat, G.K., Winterhalter, R., Myhre, C.E.L., Tsigaridis, K., Vignati, E., Stephanou, E.G., Wilson, J., 2005. Organic aerosol and global climate modelling: a review. *Atmos. Chem. Phys.* 5, 1053–1123. <https://doi.org/10.5194/acp-5-1053-2005>
- Krol, M., Houweling, S., Bregman, B., van den Broek, M., Segers, A., van Velthoven, P., Peters, W., Dentener, F., Bergamaschi, P., 2005. The two-way nested global chemistry-

- transport zoom model TM5: algorithm and applications. *Atmos. Chem. Phys.* 5, 417–432. <https://doi.org/10.5194/acp-5-417-2005>
- Lelieveld, J., Butler, T.M., Crowley, J.N., Dillon, T.J., Fischer, H., Ganzeveld, L., Harder, H., Lawrence, M.G., Martinez, M., Taraborrelli, D., Williams, J., 2008. Atmospheric oxidation capacity sustained by a tropical forest. *Nature*. <https://doi.org/10.1038/nature06870>
- Mao, J., Paulot, F., Jacob, D.J., Cohen, R.C., Crouse, J.D., Wennberg, P.O., Keller, C.A., Hudman, R.C., Barkley, M.P., Horowitz, L.W., 2013. Ozone and organic nitrates over the eastern United States: Sensitivity to isoprene chemistry. *J. Geophys. Res. Atmos.* <https://doi.org/10.1002/jgrd.50817>
- Monks, P.S., 2005. Gas-phase radical chemistry in the troposphere. *Chem. Soc. Rev.* 34, 376. <https://doi.org/10.1039/b307982c>
- Myriokefalitakis, S., Vrekoussis, M., Tsigaridis, K., Wittrock, F., Richter, A., Brühl, C., Volkamer, R., Burrows, J.P., Kanakidou, M., 2008. The influence of natural and anthropogenic secondary sources on the glyoxal global distribution. *Atmos. Chem. Phys.* <https://doi.org/10.5194/acp-8-4965-2008>
- Paulot, F., Crouse, J.D., Kjaergaard, H.G., Kroll, J.H., Seinfeld, J.H., Wennberg, P.O., 2009a. Isoprene photooxidation: New insights into the production of acids and organic nitrates. *Atmos. Chem. Phys.* <https://doi.org/10.5194/acp-9-1479-2009>
- Paulot, Fabien, Crouse, J.D., Kjaergaard, H.G., Kürten, A., Clair, J.M.S., Seinfeld, J.H., Wennberg, P.O., 2009. Unexpected epoxide formation in the gas-phase photooxidation of isoprene. *Science* (80-. ). 325, 730–733. <https://doi.org/10.1126/science.1172910>
- Paulot, F., Kjaergaard, H.G., Seinfeld, J.H., St. Clair, J.M., Crouse, J.D., Wennberg, P.O., Kurten, A., 2009b. Unexpected Epoxide Formation in the Gas-Phase Photooxidation of Isoprene. *Science* (80-. ). 325, 730–733. <https://doi.org/10.1126/science.1172910>
- Paulson, S.E., Seinfeld, J.H., 1992. Development and evaluation of a photooxidation mechanism for isoprene. *J. Geophys. Res.*
- Peeters, J., Müller, J.F., 2010. HO<sub>x</sub> radical regeneration in isoprene oxidation via peroxy radical isomerisations. II: Experimental evidence and global impact. *Phys. Chem. Chem. Phys.* 12, 14227–14235. <https://doi.org/10.1039/c0cp00811g>
- Peeters, J., Nguyen, T.L., Vereecken, L., 2009. HO<sub>x</sub> radical regeneration in the oxidation of isoprene. *Phys. Chem. Chem. Phys.* <https://doi.org/10.1039/b908511d>
- Poisson, N., Kanakidou, M., Crutzen, P.J., 2000. Impact of non-methane hydrocarbons on tropospheric chemistry and the oxidizing power of the global troposphere: 3-Dimensional modelling results. *J. Atmos. Chem.* 36, 157–230. <https://doi.org/10.1023/A:1006300616544>
- Prinn, R.G., 2003. THE CLEANSING CAPACITY OF THE ATMOSPHERE. *Annu. Rev. Environ. Resour.* 28, 29–57. <https://doi.org/10.1146/annurev.energy.28.011503.163425>
- Saunders, S.M., Jenkin, M.E., Derwent, R.G., Pilling, M.J., 2003. Protocol for the development of the Master Chemical Mechanism, MCM v3 (Part A): Tropospheric degradation of non-aromatic volatile organic compounds. *Atmos. Chem. Phys.* [14](https://doi.org/10.5194/acp-3-</a></p>
</div>
<div data-bbox=)

- Seinfeld, J.H., Pandis, S.N., 2016. *Atmospheric Chemistry and Physics: From Air Pollution to Climate Change*, 3rd ed, Wiley.
- Squire, O.J., Archibald, A.T., Griffiths, P.T., Jenkin, M.E., Smith, D., Pyle, J.A., 2015. Influence of isoprene chemical mechanism on modelled changes in tropospheric ozone due to climate and land use over the 21st century. *Atmos. Chem. Phys.* <https://doi.org/10.5194/acp-15-5123-2015>
- Williams, J.E., Folkert Boersma, K., Le Sager, P., Verstraeten, W.W., 2017. The high-resolution version of TM5-MP for optimized satellite retrievals: Description and validation. *Geosci. Model Dev.* 10, 721–750. <https://doi.org/10.5194/gmd-10-721-2017>
- Wolfe, G.M., Kaiser, J., Hanisco, T.F., Keutsch, F.N., De Gouw, J.A., Gilman, J.B., Graus, M., Hatch, C.D., Holloway, J., Horowitz, L.W., Lee, B.H., Lerner, B.M., Lopez-Hilifiker, F., Mao, J., Marvin, M.R., Peischl, J., Pollack, I.B., Roberts, J.M., Ryerson, T.B., Thornton, J.A., Veres, P.R., Warneke, C., 2016. Formaldehyde production from isoprene oxidation across NO<sub>x</sub> regimes. *Atmos. Chem. Phys.* <https://doi.org/10.5194/acp-16-2597-2016>

## 2 Model Description

TM5-MP (Tracer Model, version 5, Massively Parallel version) is a 3D global chemistry and transport model (CTM). The model has evolved from its predecessors, the original TM2 model (Heimann et al., 1988), to TM3 ( Houweling et al., 1998; Dentener et al., 2003; Tsigaridis and Kanakidou, 2003), to TM4 (van Noije et al., 2004; Myriokefalitakis et al., 2008; Daskalakis et al., 2015) and TM5 (Krol et al., 2005; Huijnen et al., 2010; Williams et al., 2017) models. It is an off-line model which means that it does not calculate meteorology but instead reads it as an input from observations assimilated by the European Centre for Medium-Range Weather Forecasts (ECMWF) model. Since no meteorological calculations take place, there is a gain in computational time which is used for chemistry and transport calculations. To compute, the model splits the atmosphere into grid boxes (**Figure 2.1**) and every process is calculated separately in each box in every model timestep (30min). Boxes communicate with each other via air mass transport.

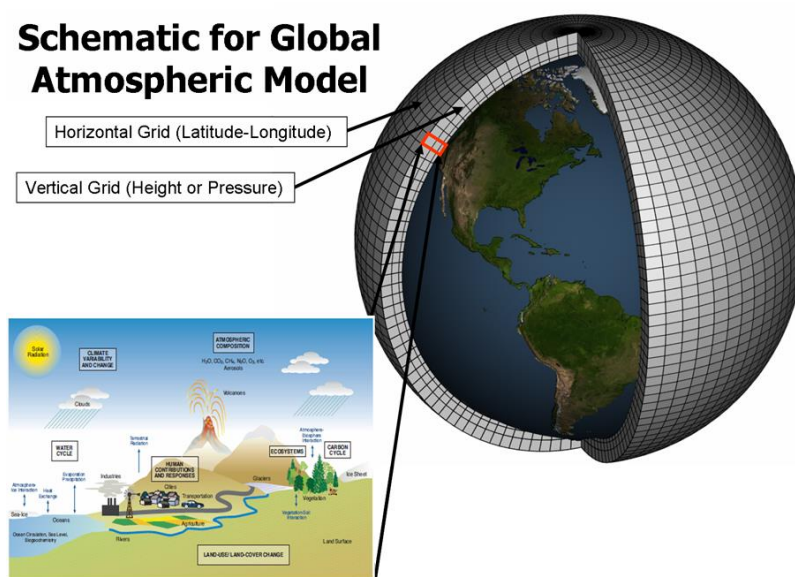
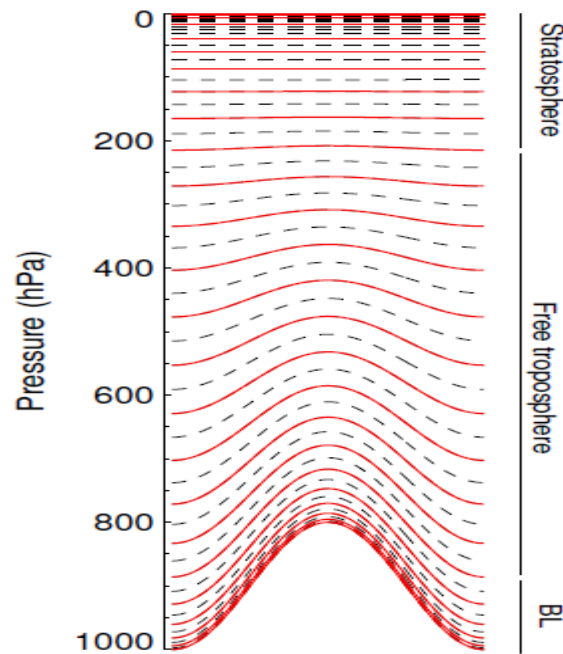


Figure 2.1: Representation of the grid box splitting of the atmosphere in a global model (source:

<https://www.gfdl.noaa.gov/climate-modeling/>)

TM5-MP can run simulations in three different horizontal resolutions, a high resolution that splits the atmosphere every 1° in longitude and 1° in latitude (1°x1°), a medium resolution that splits the atmosphere every 3° in longitude and 2° in latitude (3°x2°) and a low resolution that splits the atmosphere every 6° in longitude and 4° in latitude (6°x4°). Vertically, the model may use 60 hybrid sigma-pressure levels as in the ECMWF ERA-Interim reanalysis. However,

it typically uses 34 vertical levels with the model top being at 0.1hPa. A representation of the hybrid sigma-pressure, terrain following, layers is shown in **Figure 2.2**.



**Figure 2.2:** Representation of the vertical layers employed by the TM5 model (Krol et al., 2005)

The pressure of each level is calculated by the following equation

$$pres = (a(l) + a(l + 1) + p_s \cdot (b(l) + b(l + 1)))/2$$

Where  $p_s$  = surface pressure

$l$  = level

$a$  and  $b$  constants defined in the table below

**Table 2.1:** Values of the constants  $a$  and  $b$  used to calculate pressure in TM5

Level	$a$	$b$
1	0	1
2	7.367743	0.994019
3	210.3939	0.979663
4	855.3618	0.951822
5	2063.78	0.907884

---

6	3850.913	0.847375
7	6144.315	0.771597
8	8802.356	0.683269
9	11632.76	0.586168
10	14411.12	0.484772
11	16899.47	0.383892
12	17961.36	0.335155
13	18864.75	0.288323
14	19584.33	0.243933
15	20097.4	0.202476
16	20384.48	0.164384
17	20429.86	0.130023
18	20222.21	0.099675
19	19755.11	0.073534
20	19027.7	0.05169
21	18045.18	0.034121
22	16819.47	0.020678
23	15379.81	0.011143
24	13775.33	0.005081
25	12077.45	0.001815
26	10376.13	0.000461
27	8765.054	7.58E-05
28	7306.631	0
29	6018.02	0
30	3960.292	0
31	1680.64	0
32	713.2181	0
33	298.4958	0
34	95.63696	0

---

## 2.1 Meteorology

All the meteorological data needed by the model are acquired from the ERA-Interim reanalysis (Dee et al., 2011) or from the ECMWF operational forecast data for the recent years. Normally data are preprocessed onto a global  $1^\circ \times 1^\circ$  grid and stored on a 3-hourly frequency. The data that are used are then either time averaged or hourly interpolated.

## 2.2 Emissions

Anthropogenic and biomass burning (BB) emissions of CO, nitrogen oxides ( $\text{NO}_x$ ), black carbon aerosol (BC), particulate organic carbon (OC), sulfur dioxide and sulfates ( $\text{SO}_x$ ), as well as speciated non-methane volatile organic compounds (NMVOCs) are considered, such as emissions of ethane, methanol, ethanol, propane, acetylene, ethane, propene, isoprene, monoterpenes, benzene, toluene, xylene and other aromatics, higher alkenes, higher alkanes, HCHO, acetaldehyde, acetone, dimethyl sulfide (DMS), formic acid, acetic acid, methyl ethyl ketone (MEK), methylglyoxal (MGLY), and hydroxy acetaldehyde. Emissions from anthropogenic activities and BB are acquired from the sectoral and gridded historical inventory developed for the Coupled Model Intercomparison Project phase 6 (CMIP6; Eyring et al., 2016). These include emissions by aircraft, agricultural waste burning, fires used in deforestation, boreal forest fires, peat fires and temperate forest fires (Van Marle et al., 2017).

Biogenic emissions from vegetation are based on the Model of Emissions of Gases and Aerosols from Nature (MEGAN) (Sindelarova et al., 2014) and take into account emissions of isoprene, terpenes, other VOCs and CO. For isoprene emissions, a diurnal cycle is imposed and for latitudes between  $20^\circ\text{S}$ - $20^\circ\text{N}$  they are distributed over the first ~50m. Furthermore, biogenic emissions from soils include  $\text{NO}_x$ ,  $\text{NH}_3$  and terrestrial DMS emissions. The model also considers  $\text{NO}_x$  production by lightning, that are tied to the convective activity in the model, with annual global emissions of  $6\text{Tg-N yr}^{-1}$  and emissions of  $\text{SO}_2$  from volcanoes with annual global emissions of  $10\text{Tg-S yr}^{-1}$ .

The chemical scheme used in the present study considers the emissions of all the aforementioned species. Higher alkanes ( $\text{C} \geq 5$ ) emissions are accounted for as  $n\text{C}_4\text{H}_{10}$  emissions. Higher alkenes ( $\text{C} \geq 4$ ) emissions are accounted for as equivalent  $\text{C}_3\text{H}_6$  emissions. Higher ketones from BB emissions are accounted as MEK. Benzene, toluene, xylene, trimethyl-benzene, and higher aromatics are represented as toluene. When emissions are added to a lumped species, corrections are made in order to ensure mass conservation and

atmospheric reactivity. Additional emissions that are usually not included in the emission databases (emissions of biofuel and BB of light carbonyls) are also considered by the model because of the explicit parameterization of these in the chemistry scheme. Emissions from biofuels use of 1.4Tg yr<sup>-1</sup>, 2.4Tg yr<sup>-1</sup>, and 1.6Tg yr<sup>-1</sup> are considered for GLYAL, GLY, and MGLY, respectively. BB emissions of 4.3Tg yr<sup>-1</sup>, 5.2Tg yr<sup>-1</sup> and 3.4Tg yr<sup>-1</sup> are considered for GLYAL, GLY and MGLY respectively following the emission rates based on Fu et al., 2008 and Myriokefalitakis et al., 2008. Global emissions of ~2Tg yr<sup>-1</sup> of MEK are also considered based on studies showing that its anthropogenic emissions are significant (Andreae and Merlet, 2001) and originate mainly from domestic burning (Rodigast et al., 2016). Finally, primary aerosol emissions of OC, BC, sea-salt and dust are also considered, with sea-salt and dust emissions calculated online, based on wind dependent parameterization (Vignati et al., 2010, van Noije et al., in preparation). A detailed list of the emissions used can be seen in table...

**Table 2.2: Global annual emissions used for the MOGUNTIA chemistry scheme in TM5-MP for the year 2006 in Tg yr<sup>-1</sup>**

Species	Long name	Emissions						total
		Anthropogenic <sup>&amp;</sup>	Biomass Burning	Biogenic	Soil	Oceanic	other	
CO	carbon monoxide	600.7	386.4	90.2	19.9			1097
HCHO	formaldehyde	2.4	5.2	4.7				12.3
HCOOH	formic acid	4.6	1.8	3.5				9.8
CH <sub>3</sub> OH	methanol	4.7	9.8	131.9				146.4
C <sub>2</sub> H <sub>6</sub>	ethane	6.2	3.4	0.3		1.0		10.9
C <sub>2</sub> H <sub>4</sub>	ethene	5.3	4.8	18.3		1.4		29.8
C <sub>2</sub> H <sub>2</sub>	acetylene	3.3						3.3
CH <sub>3</sub> CHO	acetaldehyde	1.2	4.4	21.9				27.5
CH <sub>3</sub> COOH	acetic acid	4.6	18.0	3.5				26.1
CH <sub>3</sub> CH <sub>2</sub> OH	ethanol	0.5	0.1	18.6				19.3
HOCH <sub>2</sub> CHO	glycol-aldehyde	1.4	4.3					5.7
CHOCHO	glyoxal	2.4	5.2					7.6
C <sub>3</sub> H <sub>8</sub>	propane	6.5	0.7	0.03		1.3		8.5
C <sub>3</sub> H <sub>6</sub>	propene and higher alkenes	8.3	4.8			1.5		31.2



CH <sub>3</sub> COCH <sub>3</sub>	acetone	2.7	1.7	37.7			42.1
CH <sub>3</sub> COCHO	Methylglyoxal	1.6	3.4				5.0
C <sub>4</sub> H <sub>10</sub>	butane and higher alkanes (including butane, pentane, hexane, higher alkanes, and other vocs)	52.8	0.5	0.1			53.4
CH <sub>3</sub> CH <sub>2</sub> COCH <sub>3</sub>	methyl-ethyl-ketone (including higher ketones except for acetone)	2.0	1.4	0.7			4.1
C <sub>5</sub> H <sub>8</sub>	isoprene			579.4			579.4
C <sub>10</sub> H <sub>16</sub>	monoterpenes			97.9			97.9
C <sub>7</sub> H <sub>8</sub>	toluene and aromatics (including toluene, xylene benzene, trimethylbenzene and higher aromatics)	25.3	4.0	1.5			30.8
NO <sub>x</sub> #	nitrogen oxides	42.3	6.6	5.0		6.0 *	59.9
NH <sub>3</sub>	ammonia	56.1	4.4	2.3	8.1		70.9
SO <sub>2</sub>	sulfur dioxide	120.5	2.3			9.3 §	132.1
CH <sub>3</sub> SCH <sub>3</sub>	dimethylsulphide			1.7	95.8		97.5

& including aircraft emissions

# in Tg-N yr<sup>-1</sup>

\* NO<sub>x</sub> production from lightning

§ SO<sub>2</sub> from volcanoes

## 2.3 Deposition

Removal of gaseous compounds and particles from the atmosphere depends on their physical and chemical properties. It can occur through either wet or dry deposition. Regarding dry deposition, the calculation in the model was made online based on a series of surface and atmospheric resistances on a 1°x1° spatial resolution (Ganzeveld et al., 1998; Ganzeveld and Lelieveld, 1995; Wesely, 1989). The aerodynamic resistance is calculated from the model boundary layer stability, wind speed and surface roughness, where a quasi-laminar boundary layer resistance is included. The model separates the uptake resistances for vegetation, soil, water, ice and snow, at surface level. The vegetation resistance is calculated using the in-canopy aerodynamic, soil, and leaf resistance. A seasonal and diurnal cycle appears for the calculated velocities, using 3-hourly meteorological and surface parameters.

Concerning wet deposition, the model takes into account both in-cloud and below-cloud scavenging of gases and aerosol by liquid and ice precipitation. In-cloud scavenging in stratiform precipitation makes use of the altitude dependent precipitation formation rate, describing the conversion of cloud water into rainwater. The amount of gases removed by precipitation depends on Henry’s law, together with the dissociation constants, temperature and liquid content. Aerosol and gases that are highly soluble, are assumed to be fully scavenged in the vigorous convective updrafts producing rainfall rates of >1mm/h.

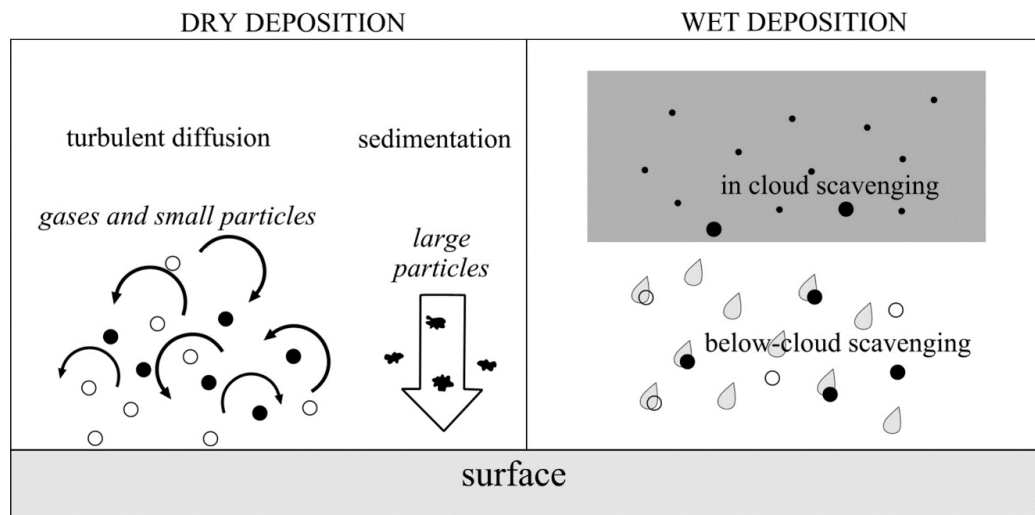


Figure 2.3: Schematic representation of wet and dry deposition (Leelőssy et al., 2014)

## 2.4 Advection – Convection

Atmospheric transport of tracers in TM5 is made by advection, cumulus convection and vertical diffusion. Tracer advection is described by either the first-order moments (slopes) algorithm developed by Russell and Lerner, (1981) or the second order moments scheme by Prather, (1986). Both schemes conserve the mass of the tracers. Convective tracer transport in TM5 is described by using a bulk mass flux approach, in which clouds are represented by a single pair of entraining and detraining plumes, describing the updraft and downdraft motions. Lastly, a first-order closure scheme is used to describe the vertical diffusion of the tracers. In the free troposphere it is computed based on wind shear and static stability following (Louis, 1979). In the boundary layer it is based on the Louis-Tiedke-Geleyn (LTG) scheme of Holtslag and Boville, (1993).

## 2.5 Stratospheric Boundary Conditions

TM5-MP contains no stratospheric chemistry, so constraints are applied above the tropopause in order to establish realistic stratosphere-troposphere exchange (STE) of O<sub>3</sub>. The overhead stratospheric profile of O<sub>3</sub> is nudged to the ozone data set provided for the Coupled Model Intercomparison Project phase 6 (CMIP6; van Noije et al., manuscript in preparation). Three separate bands are used for nudging O<sub>3</sub> fields, one between 30°S-30°N, one between 30°-66°S/N and one >66°S/N, where nudging occurs at pressure levels <45hPa, <95 hPa and <120 hPa, with relaxation times of 2.5, 3 and 4 days respectively.

CH<sub>4</sub> boundary conditions, for both lower troposphere and stratosphere, are also based on the global mean value provided for CMIP6 to scale the monthly 2-D climatological fields as derived from HALOE measurements (Groß and Russell, 2005) with the nudging heights and relaxation times being the same as for stratospheric O<sub>3</sub>. For stratospheric CO and HNO<sub>3</sub>, mixing ratios were constrained by using monthly mean ratios of CO/O<sub>3</sub> (Dupuy et al., 2004) and HNO<sub>3</sub>/O<sub>3</sub> (Jégou et al., 2008; Urban et al., 2009) based on climatology derived from ODIN observations. For the definition of the tropopause a mixing ratio of 150ppb for O<sub>3</sub> is applied as a threshold (e.g. Stevenson et al., 2006; van Noije et al., 2014).

## 2.6 The Kinetic PreProcessor

The Kinetic PreProcessor (KPP) (Damian et al., 2002; Sandu and Sander, 2006) is a software used in atmospheric chemistry simulations to assist in the solution of chemical kinetic problems. KPP provides a library with a variety of chemical mechanisms and provides the user the ability to create its own mechanism in a KPP specific format (**Figure 2.4**). The definition of the chemical species considered by the mechanism regarding their molecular weight is made in the model's modules and not in KPP. The software can then translate the chemical scheme into a FORTAN 90 code in order to solve the differential kinetic equations. KPP is able to use a number of numerical integrators that are either included in the software or custom-made by the user.

In the present work KPP v2.2.3 was coupled to the TM5-MP model to produce the FORTRAN code needed for the integration of the chemical scheme. KPP provides more versatility to changes in a scheme since it uses its own format and then translates it into FORTRAN code. However, thermal and photolysis reactions are not calculated by KPP but are instead calculated by the model's chemistry module. In summary, the reactions are initially

calculated by the model, then provided to KPP through a driver developed for KPP - TM5-MP coupling and finally the chemistry solver is employed by KPP for the numerical integration of the system. The numerical solver employed by KPP in this study is Rosenbrock (rosenbrock posdef). Rosenbrock solvers use a variable time step, making the integration of stiff numerical systems more accurate. Details regarding the mathematical approach that Rosenbrock solvers use, can be found in Sandu et al., (1997).

```

EQUATIONS {MOGUNTIA mechanism}
#
{=====}
{EMISSIONS}
{=====}
<E001> EMISSION = NO : 0.; {KNO_EMI}

{=====}
{PHOTOLYSIS}
{=====}
<J001> O3 + hv = 2 OH + BUDJO3 : 0.; {JO3d}
<J002> NO2 + hv = NO + O3 : 0.; {JNO2}
<J003> H2O2 + hv = 2 OH : 0.; {JH2O2}
<J004> HNO3 + hv = NO2 + OH : 0.; {JHNO3}
<J005> HNO4 + hv = NO2 + HO2 : 0.; {JHNO4}
<J006> N2O5 + hv = NO2 + NO3 : 0.; {JN2O5A}
<J007> N2O5 + hv = NO + NO3 : 0.; {JN2O5B}
<J008> CH2O + hv = CO : 0.; {JACH2O}
<J009> CH2O + hv = CO + 2 HO2 : 0.; {JBCH2O}
<J010> CH3O2H + hv = CH2O + OH + HO2 : 0.; {JMEPE}

<J011> NO3 + hv = NO2 + O3 : 0.; {JANO3}
<J012> NO3 + hv = NO : 0.; {JBNO3}
<J013> PAN + hv = C2O3 + NO2 : 0.; {JPANA}
<J014> PAN + hv = CH3O2 + NO3 : 0.; {JPANB}
<J015> ISOPNO3 + hv = CH2O + HO2 + NO2 + 0.64 MVK + 0.36 MACR : 0.; {JORGN}
<J016> CH3CHO + hv = CH3O2 + CO + 2 HO2 : 0.; {JALD2}
<J017> MGLY + hv = C2O3 + HO2 + CO : 0.; {JMGLY}
<J018> C2H5O2H + hv = CH3CHO + OH + HO2 : 0.; {JROOH}
<J019> O2 + hv = O3 : 0.; {JO2}
<J020> ISOP2OH + hv = CH2O + OH + HO2 + 0.64 MVK + 0.36 MACR : 0.; {JISPD}

```

Figure 2.4: Example of the MOGUNTIA chemical scheme in KPP format

## 2.7 The MOGUNTIA chemical scheme

The chemical scheme used in this work is a molecular lumping mechanism, initially developed for box (Poisson et al., 2000) and global modelling studies (Kanakidou and Crutzen, 1999; Poisson et al., 2001) and coupled to the global model MOGUNTIA (Model of the Global Universal Tracer transport In the Atmosphere; Zimmermann, 1988). The mechanism has been further developed since then and used for a number of studies coupled with the global CTM TM4 (Myriokefalitakis et al., 2008; Daskalakis et al., 2015;).

The MOGUNTIA mechanism is a rather detailed oxidation scheme as far as light alkanes (C1 – C3), light alkenes (C2 – C3) and isoprene are concerned. Organic compounds containing more than three carbon atoms are represented as n-butane (n-C<sub>4</sub>H<sub>10</sub>). In addition, second-generation products formed through oxidation of terpenes are considered to follow the oxidation pathway of isoprene and those formed through oxidation of aromatic species, the

oxidation pathway of n-C<sub>4</sub>H<sub>10</sub>. Species like CO<sub>2</sub>, H<sub>2</sub>O, O<sub>2</sub> and H<sub>2</sub> that are in high abundance in the atmosphere are not considered in the scheme.

In general, the reaction of an alkane (RH) with OH radicals, produces an alkoxy radical (RO) which will then react rapidly with O<sub>2</sub> to produce a peroxy radical (RO<sub>2</sub>). Since the reaction of RO with O<sub>2</sub> happens very fast and the concentration of O<sub>2</sub> is extremely high, it is considered that the RH will react with OH radicals to produce RO<sub>2</sub> radicals. RO<sub>2</sub> radicals will then react with either HO<sub>2</sub>, CH<sub>3</sub>O<sub>2</sub> or NO to produce hydroperoxy radicals (ROOH), carbonyl compounds and organic nitrates respectively. Further addition of NO to RO<sub>2</sub> leads to the formation of alkyl nitrates (RONO<sub>2</sub>). RONO<sub>2</sub> can be considered a sink or a source of NO<sub>x</sub>, depending on the NO<sub>x</sub> levels (sink in high NO<sub>x</sub>, source in low NO<sub>x</sub>) and atmospheric conditions that control their stability (for instance in the case of PAN), since their lifetime in the atmosphere is much longer than the one of NO<sub>x</sub> and can be transported to longer distances.

Alkenes considered in the mechanism are ethene (C<sub>2</sub>H<sub>4</sub>) and propene (C<sub>3</sub>H<sub>6</sub>). Alkenes may react with either OH, NO<sub>3</sub> or O<sub>3</sub> in production of hydroxy alkyl radicals, nitroalkyl radicals or carbonyl compounds respectively.

Concerning isoprene, the scheme considers a rather detailed oxidation. Isoprene can be oxidized by all three major atmospheric oxidants i.e. OH, NO<sub>3</sub> and O<sub>3</sub>. The reaction of isoprene with OH radicals, forms a variety of isoprene peroxide isomers which are lumped in the scheme as ISOPOO. Further oxidation leads to the formation of methyl vinyl ketone (MVK), methacrolein (MACR) and formaldehyde (HCHO), which are the main oxidation products of isoprene.

The rate coefficients for the reactions in the MOGUNTIA scheme were taken from the IUPAC kinetic data evaluation (Atkinson et al., 2003, 2006; Wallington et al., 2018) and the IUPAC website in combination with coefficients proposed by the JPL (Burkholder et al., 2015) when IUPAC recommendations are not available. Photolysis rates have been taken from the IUPAC database (Atkinson, 1997; Atkinson et al., 2003, 2006) as well. VOC reaction pathways follow the ones proposed by the Master Chemical Mechanism (MCM v3.3.1) (Bloss et al., 2005; Jenkin et al., 1997, 2003, 2015.; Saunders et al., 2003). The complete list of photochemical and thermal reactions that are currently included in the MOGUNTIA scheme can be found in the Appendix section.

### 2.7.1 Updates on the chemical scheme

A number of changes and updates have been made to the original MOGUNTIA chemical scheme in the current work. The entire chemical scheme underwent an update regarding the reaction rate coefficients of the thermal reactions, where needed, from the databases listed in paragraph 2.7. Furthermore, a lumped monoterpene species was implemented ( $C_{10}H_{16}$ ) to represent all terpenes and terpenoids, assuming 50:50  $\alpha$ -,  $\beta$ -pinene distribution. The previous version of the scheme distinguished between the oxidation of  $\alpha$ - and of  $\beta$ -pinene (e.g., Myriokefalitakis et al., 2008).

Regarding the aromatic species, a new lumped aromatic species was implemented, based on toluene, that represents benzene, toluene, xylene used previously (Myriokefalitakis et al., 2008). Toluene also represents trimethylbenzenes and higher aromatics.

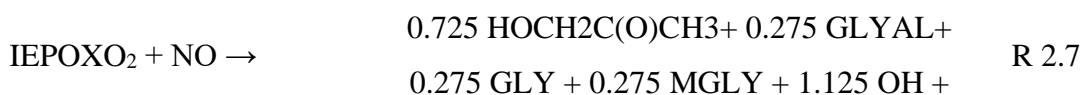
Finally, several additions were made to the isoprene oxidation mechanism to include the production of isoprene epoxydiols (IEPOX), hydro peroxy aldehydes (HPALD) and the  $HO_x$ -recycling mechanism under low- $NO_x$  conditions (Crouse et al., 2011; Paulot et al., 2009; Peeters and Müller, 2010). IEPOX and HPALD species consider all possible isomers of isoprene epoxydiols and hydro peroxy aldehydes respectively. The mechanism previously included reactions containing the lumped  $RO_2$  species which referred to oxidation products of isoprene hydro peroxy radicals. Those reactions can be seen below.

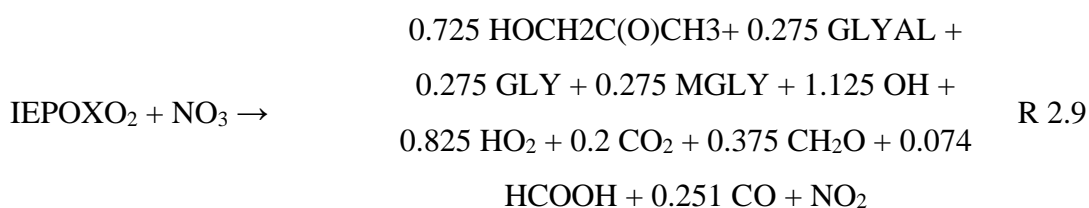
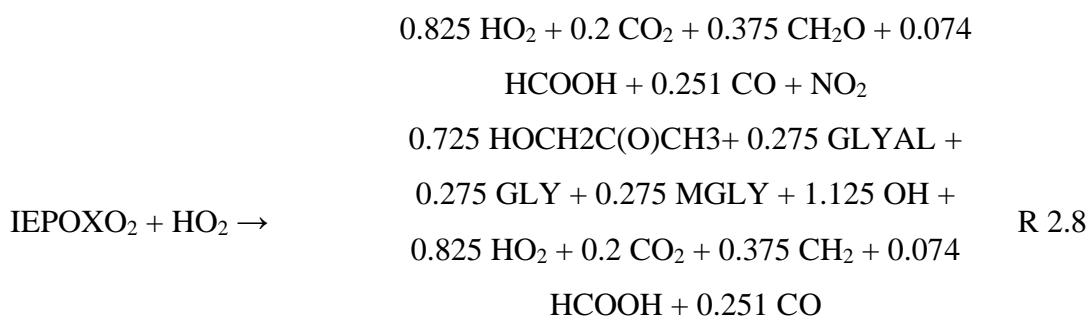


Where GLYAL: glycolaldehyde

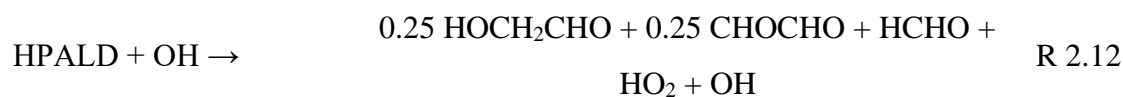
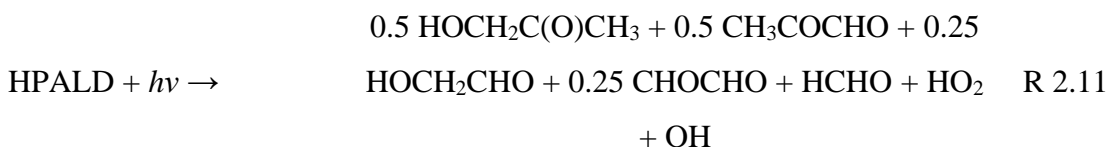
and MGLY: methylglyoxal

Reactions R 2.1 – 2.4 were replaced by the reactions R 2.5 – 2.8 respectively:





IEPOXO<sub>2</sub> is a lumped species of the peroxy oxidation products of IEPOX. Additionally, reactions regarding the production and degradation of HPALD were included.



## 2.8 Computational Resources

The simulations in the present work were performed in the National HPC facility ARIS, provided by the National Infrastructures for Research and Technology S.A. (GRNET S.A.) using 2 nodes of 20 cores (2.8GHz) each and memory of 64GB. A 3°x2° resolution was used for all the computations with 34 vertical layers. One-year simulation required ~30h for completion (~2.5h/month).

## 2.9 References

- Andreae, M.O., Merlet, P., 2001. Emission of trace gases and aerosols from biomass burning. *Global Biogeochem. Cycles*. <https://doi.org/10.1029/2000GB001382>
- Atkinson, R., 1997. Gas-phase tropospheric chemistry of volatile organic compounds: 1. Alkanes and alkenes. *J. Phys. Chem. Ref. Data*. <https://doi.org/10.1063/1.556012>
- Atkinson, R., Baulch, D.L., Cox, R.A., Crowley, J.N., Hampson, R.F., Hynes, R.G., Jenkin, M.E., Rossi, M.J., Troe, J., 2006. Evaluated kinetic and photochemical data for atmospheric chemistry: Volume II – gas phase reactions of organic species. *Atmos. Chem. Phys. Discuss.* 6, 3625–4055. <https://doi.org/10.5194/acpd-7-16349-2007>
- Atkinson, R., Baulch, D.L., Cox, R.A., Crowley, J.N., Hampson, R.F., Hynes, R.G., Jenkin, M.E., Rossi, M.J., Troe, J., 2003. Evaluated kinetic and photochemical data for atmospheric chemistry: Part 1 – gas phase reactions of Ox, HOx, NOx and SOx species. *Atmos. Chem. Phys. Discuss.* 3, 6179–6699. <https://doi.org/10.5194/acpd-3-6179-2003>
- Bloss, C., Wagner, V., Bonzanini, A., Jenkin, M.E., Wirtz, K., Martin-Reviejo, M., Pilling, M.J., 2005. Evaluation of detailed aromatic mechanisms (MCMv3 and MCMv3.1) against environmental chamber data. *Atmos. Chem. Phys.* 5, 623–639. <https://doi.org/10.5194/acp-5-623-2005>
- Burkholder, J.B., Sander, S.P., Abbatt, J.P.D., Barker, J.R., Huie, R.E., Kolb, C.E., Kurylo, M.J., Orkin, V.L., Wilmouth, D.M., Wine, P.H., 2015. Chemical Kinetics and Photochemical Data for Use in Atmospheric Studies Evaluation Number 18 NASA Panel for Data Evaluation.
- Crouse, J.D., Paulot, F., Kjaergaard, H.G., Wennberg, P.O., 2011. Peroxy radical isomerization in the oxidation of isoprene. *Phys. Chem. Chem. Phys.* <https://doi.org/10.1039/c1cp21330j>
- Damian, V., Sandu, A., Damian, M., Potra, F., Carmichael, G.R., 2002. The kinetic preprocessor KPP—a software environment for solving chemical kinetics. *Comput. Chem. Eng.* 26, 1567–1579. [https://doi.org/10.1016/S0098-1354\(02\)00128-X](https://doi.org/10.1016/S0098-1354(02)00128-X)
- Daskalakis, N., Myriokefalitakis, S., Kanakidou, M., 2015. Sensitivity of tropospheric loads and lifetimes of short lived pollutants to fire emissions. *Atmos. Chem. Phys.* <https://doi.org/10.5194/acp-15-3543-2015>
- Dee, D.P., Uppala, S.M., Simmons, A.J., Berrisford, P., Poli, P., Kobayashi, S., Andrae, U., Balmaseda, M.A., Balsamo, G., Bauer, P., Bechtold, P., Beljaars, A.C.M., van de Berg, L., Bidlot, J., Bormann, N., Delsol, C., Dragani, R., Fuentes, M., Geer, A.J., Haimberger, L., Healy, S.B., Hersbach, H., Hólm, E. V., Isaksen, I., Kållberg, P., Köhler, M., Matricardi, M., McNally, A.P., Monge-Sanz, B.M., Morcrette, J.J., Park, B.K., Peubey, C., de Rosnay, P., Tavolato, C., Thépaut, J.N., Vitart, F., 2011. The ERA-Interim reanalysis: Configuration and performance of the data assimilation system. *Q. J. R. Meteorol. Soc.* <https://doi.org/10.1002/qj.828>
- Dentener, F., Van Weele, M., Krol, M., Houweling, S., Van Velthoven, P., 2003. Trends and inter-annual variability of methane emissions derived from 1979-1993 global CTM simulations. *Atmos. Chem. Phys.* <https://doi.org/10.5194/acp-3-73-2003>



- Dupuy, É., Urban, J., Ricaud, P., Le Flochmoën, É., Lautié, N., Murtagh, D., De La Noë, J., El Amraoui, L., Eriksson, P., Forkman, P., Frisk, U., Jégou, F., Jiménez, C., Olberg, M., 2004. Strato-mesospheric measurements of carbon monoxide with the Odin sub-millimetre radiometer: Retrieval and first results. *Geophys. Res. Lett.* <https://doi.org/10.1029/2004GL020558>
- Eyring, V., Bony, S., Meehl, G.A., Senior, C.A., Stevens, B., Stouffer, R.J., Taylor, K.E., 2016. Overview of the Coupled Model Intercomparison Project Phase 6 (CMIP6) experimental design and organization. *Geosci. Model Dev.* <https://doi.org/10.5194/gmd-9-1937-2016>
- Fu, T.M., Jacob, D.J., Wittrock, F., Burrows, J.P., Vrekoussis, M., Henze, D.K., 2008. Global budgets of atmospheric glyoxal and methylglyoxal, and implications for formation of secondary organic aerosols. *J. Geophys. Res. Atmos.* <https://doi.org/10.1029/2007JD009505>
- Ganzeveld, L., Lelieveld, J., 1995. Dry deposition parameterization in a chemistry general circulation model and its influence on the distribution of reactive trace gases. *J. Geophys. Res.*
- Ganzeveld, L., Lelieveld, J., Roelofs, G.J., 1998. A dry deposition parameterization for sulfur oxides in a chemistry and general circulation model. *J. Geophys. Res. Atmos.* <https://doi.org/10.1029/97JD03077>
- Groß, J.U., Russell, J.M., 2005. Technical note: A stratospheric climatology for O<sub>3</sub>, H<sub>2</sub>O, CH<sub>4</sub>, NO<sub>x</sub>, HCl and HF derived from HALOE measurements. *Atmos. Chem. Phys.* <https://doi.org/10.5194/acp-5-2797-2005>
- Heimann, M., Monfray, P., Polian, G., 1988. Long range transport of Rn-222: A test for 3D tracer models. *Chem. Geol.* [https://doi.org/10.1016/0009-2541\(88\)90476-7](https://doi.org/10.1016/0009-2541(88)90476-7)
- Holtstlag, A.A.M., Boville, B.A., 1993. Local versus nonlocal boundary-layer diffusion in a global climate model. *J. Clim.* [https://doi.org/10.1175/1520-0442\(1993\)006<1825:LVNBLD>2.0.CO;2](https://doi.org/10.1175/1520-0442(1993)006<1825:LVNBLD>2.0.CO;2)
- Houweling, S., Dentener, F., Lelieveld, J., 1998. The impact of nonmethane hydrocarbon compounds on tropospheric photochemistry. *J. Geophys. Res. D Atmos.*
- Huijnen, V., Williams, J., Van Weele, M., Van Noije, T., Krol, M., Dentener, F., Segers, A., Houweling, S., Peters, W., De Laat, J., Boersma, F., Bergamaschi, P., Van Velthoven, P., Le Sager, P., Eskes, H., Alkemade, F., Scheele, R., Nédélec, P., Pätz, H.W., 2010. The global chemistry transport model TM5: Description and evaluation of the tropospheric chemistry version 3.0. *Geosci. Model Dev.* 3, 445–473. <https://doi.org/10.5194/gmd-3-445-2010>
- Jégou, F., Urban, J., De La Noë, J., Ricaud, P., Le Flochmoën, E., Murtagh, D.P., Eriksson, P., Jones, A., Petelina, S., Llewellyn, E.J., Lloyd, N.D., Haley, C., Lumpe, J., Randall, C., Bevilacqua, R.M., Catoire, V., Huret, N., Berthet, G., Renard, J.B., Strong, K., Davies, J., Mc Elroy, C.T., Goutail, F., Pommereau, J.P., 2008. Technical note: Validation of Odin/SMR limb observations of ozone, comparisons with OSIRIS, POAM III, ground-based and balloon-borne instruments. *Atmos. Chem. Phys.* <https://doi.org/10.5194/acp-8-3385-2008>
- Jenkin, M.E., Saunders, S.M., Pilling, M.J., 1997. The tropospheric degradation of volatile

- organic compounds: A protocol for mechanism development. *Atmos. Environ.* [https://doi.org/10.1016/S1352-2310\(96\)00105-7](https://doi.org/10.1016/S1352-2310(96)00105-7)
- Jenkin, M.E., Saunders, S.M., Wagner, V., Pilling, M.J., 2003. Protocol for the development of the Master Chemical Mechanism, MCM v3 (Part B): tropospheric degradation of aromatic volatile organic compounds. *Atmos. Chem. Phys.* 3, 181–193. <https://doi.org/10.5194/acp-3-181-2003>
- Jenkin, M.E., Young, J.C., Rickard, A.R., 2015. The MCM v3.3.1 degradation scheme for isoprene. *Atmos. Chem. Phys.* <https://doi.org/10.5194/acp-15-11433-2015>
- Kanakidou, M., Crutzen, P.J., 1999. The photochemical source of carbon monoxide: Importance, uncertainties and feedbacks. *Chemosph. - Glob. Chang. Sci.* [https://doi.org/10.1016/S1465-9972\(99\)00022-7](https://doi.org/10.1016/S1465-9972(99)00022-7)
- Krol, M., Houweling, S., Bregman, B., van den Broek, M., Segers, A., van Velthoven, P., Peters, W., Dentener, F., Bergamaschi, P., 2005. The two-way nested global chemistry-transport zoom model TM5: algorithm and applications. *Atmos. Chem. Phys.* 5, 417–432. <https://doi.org/10.5194/acp-5-417-2005>
- Leelőssy, Á., Molnár, F., Izsák, F., Havasi, Á., Lagzi, I., Mészáros, R., 2014. Dispersion modeling of air pollutants in the atmosphere: a review. *Cent. Eur. J. Geosci.* <https://doi.org/10.2478/s13533-012-0188-6>
- Louis, J.F., 1979. A parametric model of vertical eddy fluxes in the atmosphere. *Boundary-Layer Meteorol.* <https://doi.org/10.1007/BF00117978>
- Myriokefalitakis, S., Vrekoussis, M., Tsigaridis, K., Wittrock, F., Richter, A., Brühl, C., Volkamer, R., Burrows, J.P., Kanakidou, M., 2008. The influence of natural and anthropogenic secondary sources on the glyoxal global distribution. *Atmos. Chem. Phys.* <https://doi.org/10.5194/acp-8-4965-2008>
- Paulot, F., Crounse, J.D., Kjaergaard, H.G., Kroll, J.H., Seinfeld, J.H., Wennberg, P.O., 2009. Isoprene photooxidation: New insights into the production of acids and organic nitrates. *Atmos. Chem. Phys.* <https://doi.org/10.5194/acp-9-1479-2009>
- Peeters, J., Müller, J.F., 2010. HOx radical regeneration in isoprene oxidation via peroxy radical isomerisations. II: Experimental evidence and global impact. *Phys. Chem. Chem. Phys.* 12, 14227–14235. <https://doi.org/10.1039/c0cp00811g>
- Poisson, N., Kanakidou, M., Bonsang, B., Behmann, T., Burrows, J.P., Fischer, H., Gölz, C., Harder, H., Lewis, A., Moortgat, G.K., Nunes, T., Pio, C.A., Platt, U., Sauer, F., Schuster, G., Seakins, P., Senzig, J., Seuwen, R., Trapp, D., Volz-Thomas, A., Zenker, T., Zitzelberger, R., 2001. The impact of natural non-methane hydrocarbon oxidation on the free radical and ozone budgets above a eucalyptus forest. *Chemosph. - Glob. Chang. Sci.* 3, 353–366. [https://doi.org/10.1016/S1465-9972\(01\)00016-2](https://doi.org/10.1016/S1465-9972(01)00016-2)
- Poisson, N., Kanakidou, M., Crutzen, P.J., 2000. Impact of non-methane hydrocarbons on tropospheric chemistry and the oxidizing power of the global troposphere: 3-Dimensional modelling results. *J. Atmos. Chem.* 36, 157–230. <https://doi.org/10.1023/A:1006300616544>
- Prather, M.J., 1986. Numerical advection by conservation of second-order moments. *J. Geophys. Res.* <https://doi.org/10.1029/jd091id06p06671>

- Rodigast, M., Mutzel, A., Schindelka, J., Herrmann, H., 2016. A new source of methylglyoxal in the aqueous phase. *Atmos. Chem. Phys.* 16, 2689–2702. <https://doi.org/10.5194/acp-16-2689-2016>
- Russell, G.L., Lerner, J.A., 1981. A new finite-differencing scheme for the tracer transport equation. *J. Appl. Meteorol.* [https://doi.org/10.1175/1520-0450\(1981\)020<1483:ANFDSF>2.0.CO;2](https://doi.org/10.1175/1520-0450(1981)020<1483:ANFDSF>2.0.CO;2)
- Sandu, A., Sander, R., 2006. Technical note: Simulating chemical systems in Fortran90 and Matlab with the Kinetic PreProcessor KPP-2.1. *Atmos. Chem. Phys.* <https://doi.org/10.5194/acp-6-187-2006>
- Sandu, A., Verwer, J.G., Blom, J.G., Spee, E.J., Carmichael, G.R., Potra, F.A., 1997. Benchmarking stiff ode solvers for atmospheric chemistry problems II: Rosenbrock solvers. *Atmos. Environ.* 31, 3459–3472. [https://doi.org/10.1016/S1352-2310\(97\)83212-8](https://doi.org/10.1016/S1352-2310(97)83212-8)
- Saunders, S.M., Jenkin, M.E., Derwent, R.G., Pilling, M.J., 2003. Protocol for the development of the Master Chemical Mechanism, MCM v3 (Part A): Tropospheric degradation of non-aromatic volatile organic compounds. *Atmos. Chem. Phys.* <https://doi.org/10.5194/acp-3-161-2003>
- Sindelarova, K., Granier, C., Bouarar, I., Guenther, A., Tilmes, S., Stavrou, T., Müller, J.F., Kuhn, U., Stefani, P., Knorr, W., 2014. Global data set of biogenic VOC emissions calculated by the MEGAN model over the last 30 years. *Atmos. Chem. Phys.* <https://doi.org/10.5194/acp-14-9317-2014>
- Stevenson, D.S., Dentener, F.J., Schultz, M.G., Ellingsen, K., van Noije, T.P.C., Wild, O., Zeng, G., Amann, M., Atherton, C.S., Bell, N., Bergmann, D.J., Bey, I., Butler, T., Cofala, J., Collins, W.J., Derwent, R.G., Doherty, R.M., Drevet, J., Eskes, H.J., Fiore, A.M., Gauss, M., Hauglustaine, D.A., Horowitz, L.W., Isaksen, I.S.A., Krol, M.C., Lamarque, J.F., Lawrence, M.G., Montanaro, V., Müller, J.F., Pitari, G., Prather, M.J., Pyle, J.A., Rast, S., Rodriguez, J.M., Sanderson, M.G., Savage, N.H., Shindell, D.T., Strahan, S.E., Sudo, K., Szopa, S., 2006. Multimodel ensemble simulations of present-day and near-future tropospheric ozone. *J. Geophys. Res. Atmos.* <https://doi.org/10.1029/2005JD006338>
- Tsigaridis, K., Kanakidou, M., 2003. Global modelling of secondary organic aerosol in the troposphere: A sensitivity analysis. *Atmos. Chem. Phys.* <https://doi.org/10.5194/acp-3-1849-2003>
- Urban, J., Pommier, M., Murtagh, D.P., Santee, M.L., Orsolini, Y.J., 2009. Nitric acid in the stratosphere based on Odin observations from 2001 to 2009 - Part 1: A global climatology. *Atmos. Chem. Phys.* <https://doi.org/10.5194/acp-9-7031-2009>
- Van Marle, M.J.E., Kloster, S., Magi, B.I., Marlon, J.R., Daniou, A.L., Field, R.D., Arneth, A., Forrest, M., Hantson, S., Kehrwald, N.M., Knorr, W., Lasslop, G., Li, F., Mangeon, S., Yue, C., Kaiser, J.W., Van Der Werf, G.R., 2017. Historic global biomass burning emissions for CMIP6 (BB4CMIP) based on merging satellite observations with proxies and fire models (1750-2015). *Geosci. Model Dev.* <https://doi.org/10.5194/gmd-10-3329-2017>

- van Noije, T.P.C., Eskes, H.J., van Weele, M., van Velthoven, P.F.J., 2004. Implications of the enhanced Brewer-Dobson circulation in European Centre for Medium-Range Weather Forecasts reanalysis ERA-40 for the stratosphere-troposphere exchange of ozone in global chemistry transport models. *J. Geophys. Res. D Atmos.* <https://doi.org/10.1029/2004JD004586>
- Van Noije, T.P.C., Le Sager, P., Segers, A.J., Van Velthoven, P.F.J., Krol, M.C., Hazeleger, W., Williams, A.G., Chambers, S.D., 2014. Simulation of tropospheric chemistry and aerosols with the climate model EC-Earth. *Geosci. Model Dev.* <https://doi.org/10.5194/gmd-7-2435-2014>
- Vignati, E., Karl, M., Krol, M., Wilson, J., Stier, P., Cavalli, F., 2010. Sources of uncertainties in modelling black carbon at the global scale. *Atmos. Chem. Phys.* <https://doi.org/10.5194/acp-10-2595-2010>
- Wallington, T.J., Ammann, M., Cox, R.A., Crowley, J.N., H., H., Jenkin, M.E., McNeill, V., Mellouki, A., J., R.M., Troe, J., 2018. IUPAC Task group on atmospheric chemical kinetic data evaluation: Evaluated kinetic data.
- Wesley, M.L., 1989. Parameterization of Surface Resistances to Gaseous Dry Deposition in Regional-Scale Numerical Models. *Atmos. Environ.* [https://doi.org/10.1016/S0950-351X\(05\)80241-1](https://doi.org/10.1016/S0950-351X(05)80241-1)
- Williams, J.E., Folkert Boersma, K., Le Sager, P., Verstraeten, W.W., 2017. The high-resolution version of TM5-MP for optimized satellite retrievals: Description and validation. *Geosci. Model Dev.* 10, 721–750. <https://doi.org/10.5194/gmd-10-721-2017>

### 3 Simulations

In the present work, simulations using both the updated and the old version of the MOGUNTIA chemistry scheme, were performed to evaluate the impact of the applied updates on the simulated oxidant levels. In addition, an extra simulation was performed, where the chemistry of BVOCs was neglected from the scheme in order to evaluate the overran impact of BVOCs chemistry on atmospheric composition and particularly on O<sub>3</sub> and OH levels and budget terms. The simulation year was 2006, which was also used in the benchmarking studies by Huijnen et al. (2010) and Williams et al. (2013, 2017). The results derived from the model simulations are presented in the following sections alongside the evaluation of the model against surface observations. Observational data for the evaluation of O<sub>3</sub> were derived by the World Ozone and Ultraviolet Radiation Data Centre (WOUDC) and the European Monitoring Evaluation Program (EMEP). For the evaluation of CO, data as taken from the National Oceanic and Atmospheric Administration (NOAA) database were used.

#### 3.1 Ozone

Ozone is a major atmospheric oxidant as explained in detail in Chapter 1. Its production and consumption are affected by photochemical reactions and a variety of meteorological factors such as temperature, humidity, solar radiation and chemical factors such as NO<sub>x</sub>, CO and VOC concentrations.

The simulated by the model near-surface O<sub>3</sub> concentration global distribution can be seen in **Figure 3.1** (annual mean). Computed ozone concentrations are higher in the Northern Hemisphere (NH) and in the tropics. The high O<sub>3</sub> values in the NH can be explained by the important human and industrial activity there, that caused an increase in the emissions of NO<sub>x</sub> and VOCs, contributing to O<sub>3</sub> production. In the tropics, the major contributor of O<sub>3</sub> is biomass burning.

Zonal mean O<sub>3</sub> values (**Figure 3.1; right**) increase from the equator to high latitudes (NH), attributed as already explained to increased human activity. The high values in the upper model levels are attributed to the stratosphere-troposphere exchanges of air masses.

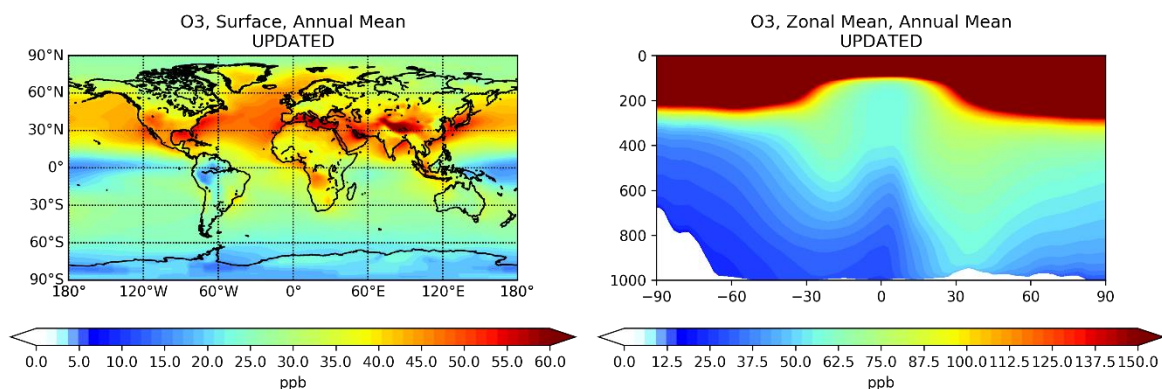


**Figure 3.1: Annual mean O<sub>3</sub> concentrations simulated using the updated MOGUNTIA scheme. Surface annual mean (left) and zonal annual mean (right).**

### 3.1.1 Comparison between the UPDATED and the OLD scheme

In this section the differences in O<sub>3</sub> concentrations between the simulations using the UPDATED and the OLD MOGUNTIA scheme are presented.

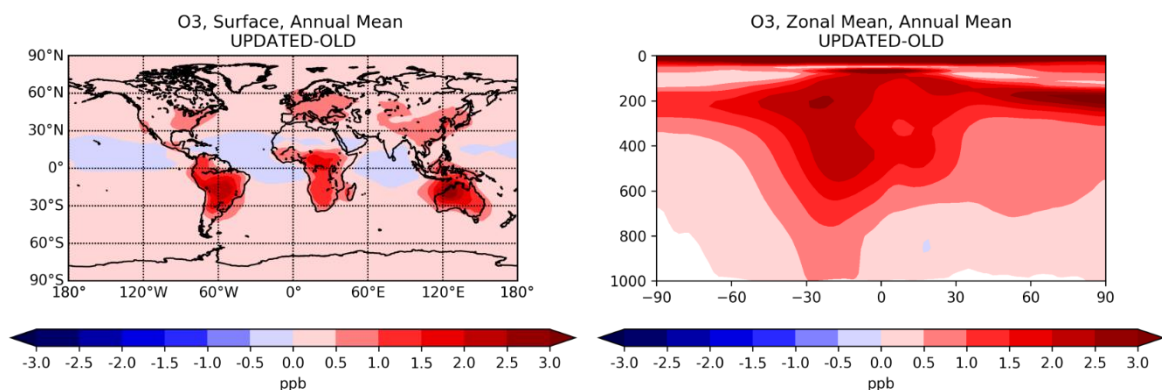


**Figure 3.2: Difference between the UPDATED and the OLD MOGUNTIA scheme for O<sub>3</sub>. Surface annual mean difference (left) and zonal annual mean difference (right).**

In **Figure 3.2** the red color indicates higher O<sub>3</sub> concentrations in the updated scheme compared to the old chemical scheme. The largest difference (~2.5-3ppb) is calculated for continental areas of the SH (South America, Central-South Africa, Australia). These areas have intense BVOC emissions. Therefore, at these locations the updated chemistry of isoprene oxidation that is now implemented in the model results in increased HO<sub>2</sub> radicals which may contribute to O<sub>3</sub> production by reacting with NO. However, the differences observed do not exceed 2.5ppb.

**Table 3.1** presents the impact of the updated chemistry on O<sub>3</sub> budgets. The updated scheme leads to higher O<sub>3</sub> tropospheric burden which results from both higher photochemical production and destruction but also higher influx from the stratosphere.

Table 3.1: Tropospheric budget of O<sub>3</sub> for the year 2006.

Production terms Tg(O <sub>3</sub> ) yr <sup>-1</sup>	OLD	UPDATED	Loss terms Tg(O <sub>3</sub> ) yr <sup>-1</sup>	OLD	UPDATED
Stratospheric inflow*	423	432	Deposition	912	927
Trop. chem. production	5723	5897	Trop. chem. loss	5233	5401
Trop. burden	375	382	Trop. lifetime (days)	22.3	22

\*sum of the deposition and the tropospheric chemical loss minus the production

### 3.2 Comparison to observations (O<sub>3</sub>)

Model results for O<sub>3</sub> concentrations have been evaluated against surface observations both for the OLD and the UPDATED chemistry scheme for the year 2006. In **Figure 3.3** are presented the results of the evaluation for some of the studied stations, covering the NH, the tropics, the SH and Antarctica (top to bottom). The model in general overestimates O<sub>3</sub> concentrations for most of the NH stations such as Barrow (USA) and Mace Head (Ireland) presenting a bias of ~3-8ppb. The model results show a smaller bias for the stations of Mauna Loa (USA) and Viznar (Spain) (i.e. 0.2-1.3ppb). For stations of the SH (e.g. Cape Point, South Africa; Lauder, New Zealand) the model results show a positive bias against observations of ~6.5-10ppb. At Antarctica (i.e. Neumayer and Syowa station) the model presents a negative bias of ~4ppb but a very good correlation (R=0.9).

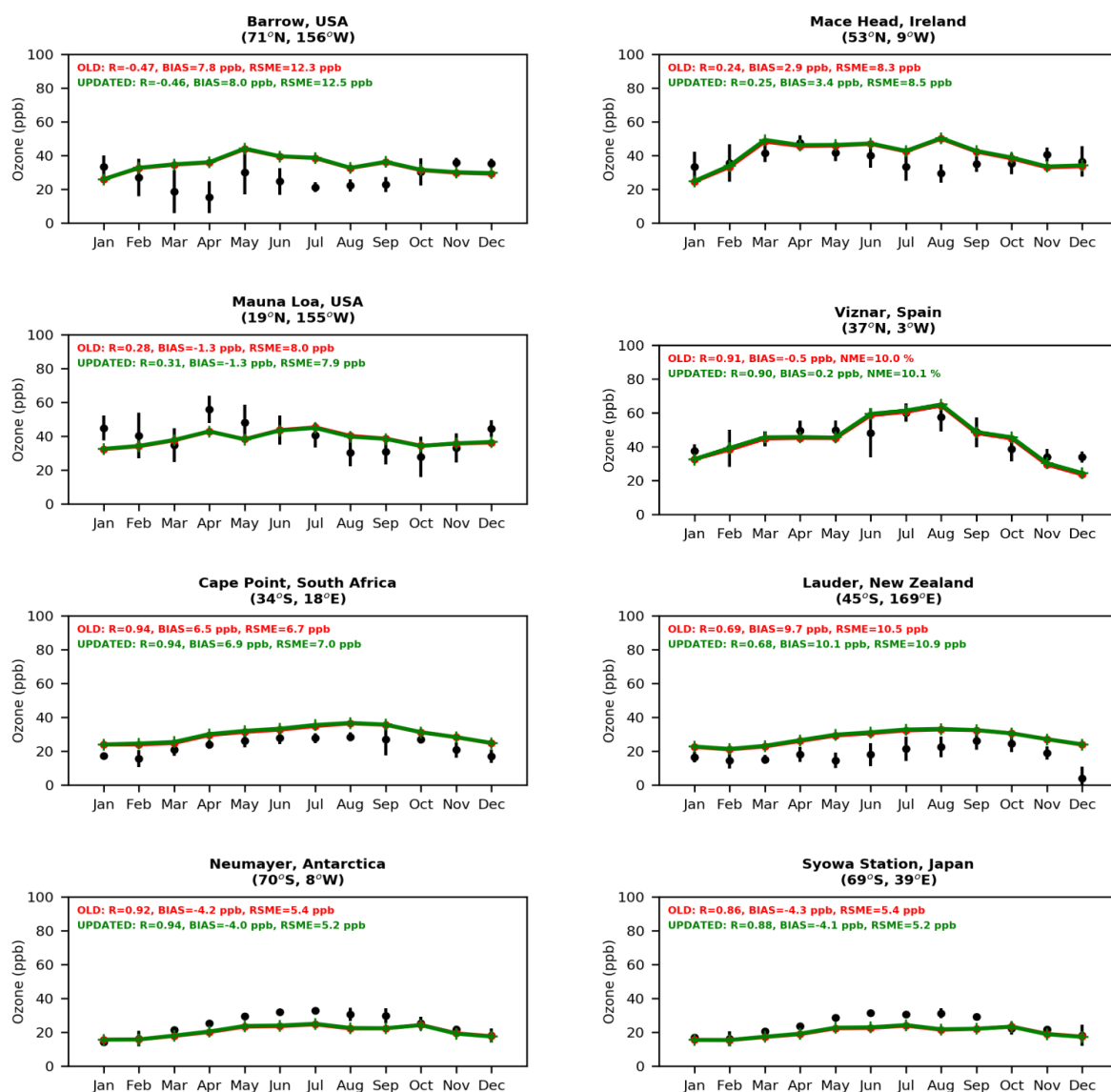


**Figure 3.3:** Monthly mean comparison of TM5-MP surface O<sub>3</sub> (ppb) against surface observations (black dots) from EMEP and WOUDC databases for the two chemistry schemes, OLD (red line) and UPDATED (green line).

Overall, the model presents a mean overestimation against O<sub>3</sub> surface observations globally of ~7ppb (~16%). Finally, the mean bias that the two different chemistry schemes is 6.7ppb for the OLD scheme and 7.3ppb for the UPDATED scheme. The difference between those two is negligible.

### 3.3 Hydroxyl radicals

Hydroxyl radicals are the main oxidant in the atmosphere during daytime. During nighttime their concentrations are significantly lower since their production is mainly



photochemical. **Figure 3.4** and **Figure 3.5**, illustrate the seasonal mean (boreal winter and summer) and the annual mean distribution of OH radicals respectively, as simulated by the model.

As can be seen in **Figure 3.4**, the highest surface concentrations of OH radicals appear in the NH due to higher human activity. More specifically, during the boreal summer (JJA) increased OH concentrations are observed because of high photochemical activity and higher O<sub>3</sub> concentrations. Moreover, the seasonal shift in OH concentrations in high latitudes (>40° S or N) can be seen, with higher concentrations calculated, during each hemisphere summertime, again because of increased photochemistry. In areas such as the open ocean, the high amounts of OH radicals are addressed to marine traffic. The highest concentrations are visible above shipping routes, due to NO<sub>x</sub> emissions which contribute to O<sub>3</sub> production, especially in the Northern Atlantic Ocean, the Indian Ocean, the Persian Gulf, the Panama Gulf and the Sea of Japan with seasonal mean concentrations >5x10<sup>6</sup> radicals cm<sup>-3</sup>. In oceanic areas that are more remote and less visited by humans, the OH concentrations are much lower (< 1x10<sup>6</sup> radicals cm<sup>-3</sup>). In forested areas and areas with increased vegetation, OH concentrations remain in relatively low levels (~1x10<sup>6</sup> radicals cm<sup>-3</sup> or lower). In areas with increased biogenic activity (e.g. tropical forests), the model simulates relatively low concentrations of OH as well, although the HO<sub>x</sub> recycling mechanism has been implemented. This is because the high amounts of biogenic VOCs which consume the OH radicals.

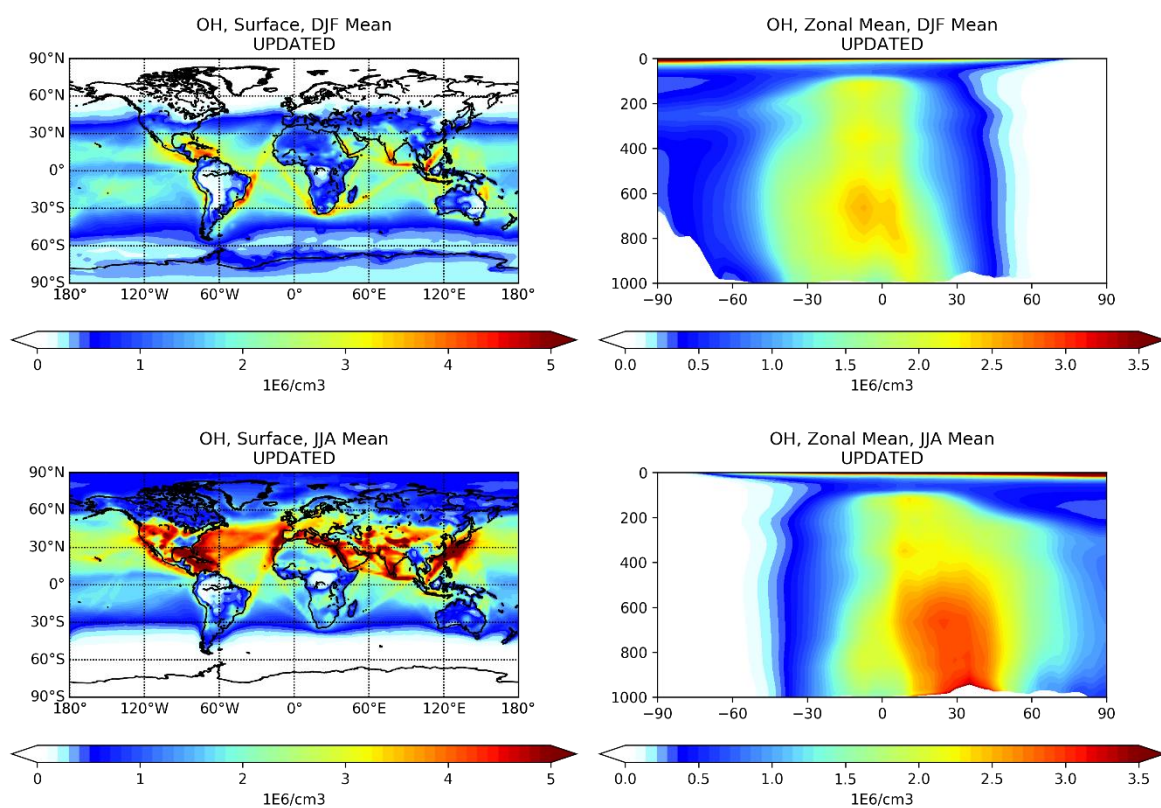


**Figure 3.4: Simulated seasonal mean values of OH radical concentrations for the updated MOGUNTIA scheme. Surface and zonal mean for December-January-February (DJF; top row) and for June-July-August (bottom row; JJA)**

Zonal mean concentrations appear to be higher in the tropics and the NH. The highest values are calculated from the surface up to  $\sim 600$ hPa for the NH summer and at  $\sim 600$ hPa for SH summer. In general, annually the highest concentrations are calculated for the tropics at  $\sim 600$ hPa and another peak appears at  $\sim 200$ hPa (**Figure 3.5**). The increased solar radiations that the tropics receive in combination with the high humidity lead to the production of OH radicals. In the tropics the maxima appear in the upper levels of the atmosphere because of VOC emissions from vegetation near the surface, which tend to consume OH radicals.

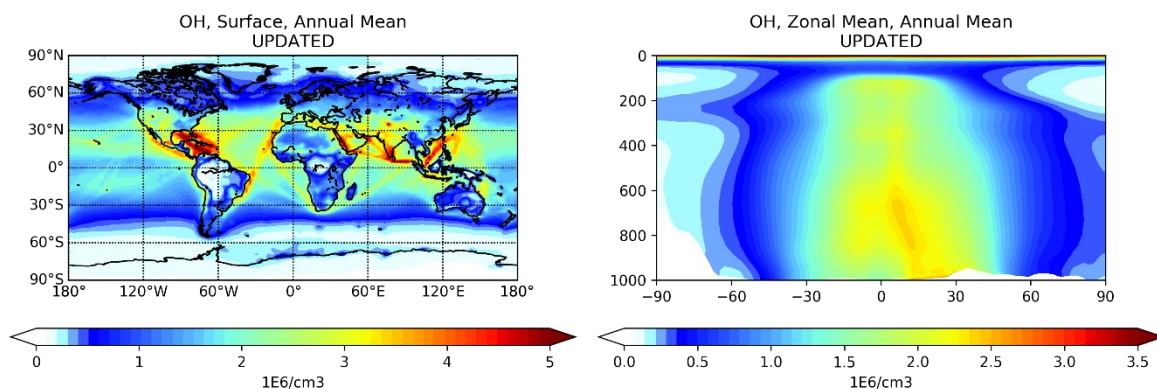


**Figure 3.5: Simulated annual mean values of OH radical concentrations for the updated MOGUNTIA scheme. Surface annual mean (left) and zonal annual mean (right)**

### 3.3.1 Comparison between the UPDATED and the OLD scheme

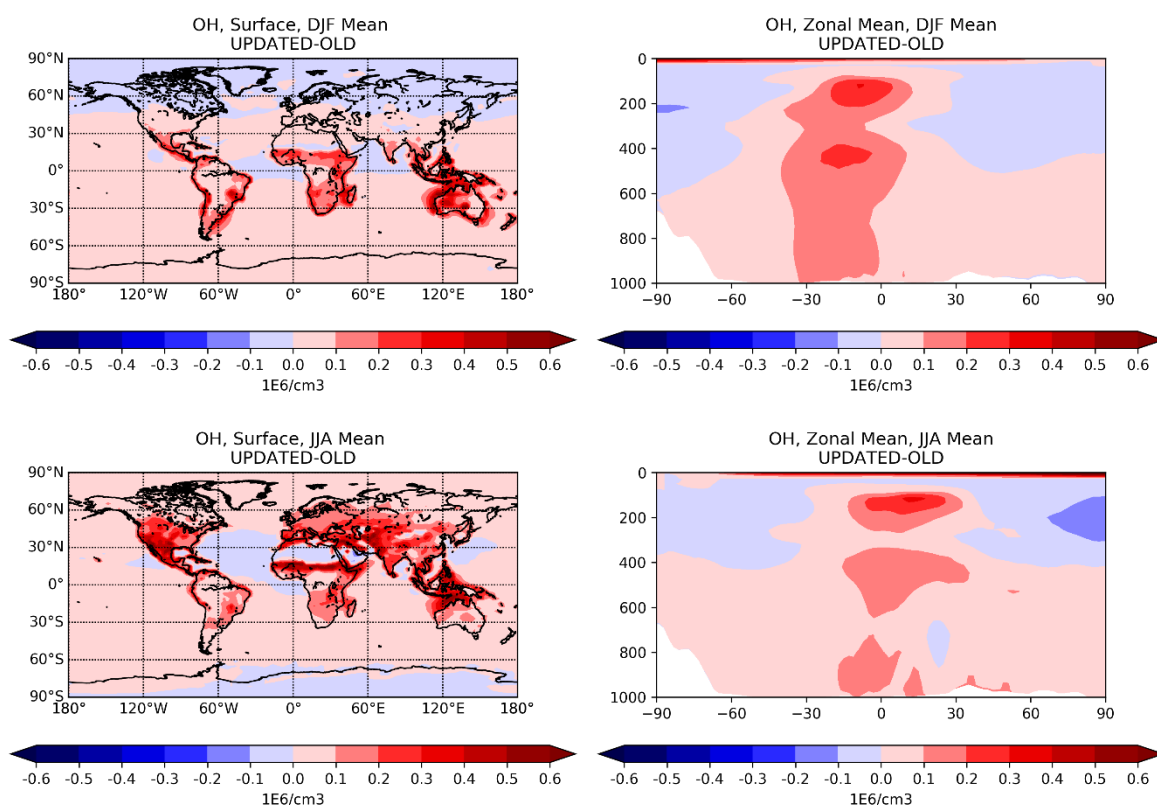


**Figure 3.6: Difference between the UPDATED and the OLD MOGUNTIA scheme for OH. Surface seasonal mean difference (left) and zonal seasonal mean difference (right).**

In **Figure 3.7** the difference in OH radicals' concentrations (surface and zonal) for the two simulations are presented. Again, the red color indicates that the UPDATED scheme calculates higher OH concentrations. This is expected since the implementation of the new scheme included the recycling of OH. As can be seen, the highest differences appear in the tropics and the SH and in general, in areas with high isoprene emissions.

Regarding zonal mean OH, the highest concentration differences appear in the tropics and the SH with the maximum being ~200hPa. This maximum is explained by the production of OH from IEPOX which can also be transported in the upper levels of the troposphere. The lifetime of OH is higher at that altitude as calculated by Lelieveld et al. (2016). The difference between the two chemical mechanisms results (zonal distribution) can be seen in **Table 3.2**

**Table 3.2 Mean annual OH concentration differences for the OLD and the UPDATED scheme**

<b>10<sup>6</sup> radicals/cm<sup>3</sup></b>	<b>OLD</b>	<b>UPDATED</b>	<b>Difference</b>
<b>North Hemisphere (&gt;30°N)</b>	0.79	0.8	<b>1%</b>
<b>Tropics (30°N-30°S)</b>	1.68	1.75	<b>4%</b>
<b>South Hemisphere (&gt;30°S)</b>	0.44	0.44	<b>0%</b>
<b>Global</b>	1.02	1.05	<b>3%</b>

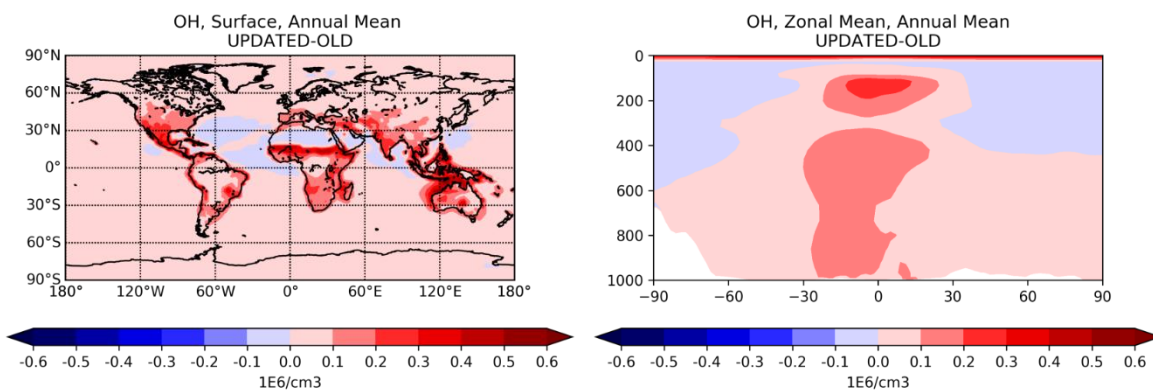


**Figure 3.7: Difference between the UPDATED and the OLD MOGUNTIA scheme for OH. Surface annual mean difference (left) and zonal annual mean difference (right).**

**Table 3.3** illustrates the major production and consumption reactions of OH radicals as simulated by TM5-MP for the two scheme configurations.

**Table 3.3: Tropospheric budget of OH radicals for the year 2006**

<b>Production terms</b> <b>Tg(OH) yr<sup>-1</sup></b>			<b>Loss terms</b>		
	<b>OLD</b>	<b>UPDATED</b>	<b>Tg(OH)</b> <b>yr<sup>-1</sup></b>	<b>OLD</b>	<b>UPDATED</b>
<b>O(<sup>1</sup>D) + H<sub>2</sub>O</b>	1888	1907	<b>OH + CO</b>	1788	1819
<b>NO + HO<sub>2</sub></b>	1424	1487	<b>OH + CH<sub>4</sub></b>	635	655
<b>O<sub>3</sub> + HO<sub>2</sub></b>	558	597	<b>OH + O<sub>3</sub></b>	259	272
<b>H<sub>2</sub>O<sub>2</sub> + hv</b>	300	283	<b>OH + ISOP</b>	116	119
<b>Other</b>	117	133	<b>Other</b>	1488	1543

### 3.3.2 Comparison to other modelling studies

The results of the model regarding the two scheme configurations have been compared to the Spivakovsky et al. (2000) climatology and the modelling studies by Naik et al. (2013) and Lelieveld et al. (2016). The UPDATED scheme calculates and mean annual concentration of OH radical of  $10.5 \times 10^5$  molecules  $\text{cm}^{-3}$  and the OLD scheme  $10.2 \times 10^5$  molecules  $\text{cm}^{-3}$ . These results are very close to the low end of the mean of the multi-model comparison mean by Naik et al. (2013) for the year 2000, which is  $11.1 \pm 1.6 \times 10^5$  molecules  $\text{cm}^{-3}$ . Results are also very close to the mean tropospheric concentration as calculated by Lelieveld et al. (2016) for the year 2013, which is  $11.3 \times 10^5$  molecules  $\text{cm}^{-3}$ , and to the climatological distribution by Spivakovsky et al. (2000) which is  $11.6 \times 10^5$  molecules  $\text{cm}^{-3}$ . The difference between the two chemistry configurations is again really small. These results are summarized in the following table.

**Table 3.4: Annual mean concentrations of tropospheric OH radical for TM5-MP and other modelling studies**

<b>10<sup>5</sup> molecules/cm<sup>3</sup></b>	<b>OLD</b>	<b>UPDATED</b>	<b>Spivakovsky</b> <b>et al. 2000</b>	<b>Naik et</b> <b>al. 2013</b>	<b>Lelieveld</b> <b>et al.</b> <b>2016</b>
<b>OH conc.</b>	10.2	10.5	11.3	11.6	11.3

### 3.4 Carbon Monoxide

Carbon monoxide (CO) is an important trace gas for the atmospheric chemistry since is one of the major consumers of OH radicals. CO is either emitted directly to the atmosphere or produced secondarily by the oxidation of VOCs, especially methane (CH<sub>4</sub>). CO main primary emissions are from biomass burning sources as well as anthropogenic sources like industrial activity or fossil fuel burning.

The highest CO surface concentrations can be seen in areas with increased human and industrial activity like China and India with values >200ppb (**Figure 3.8; left**). Similar levels of CO concentrations appear in central Africa with those attributed mainly to biomass burning. Slightly lower concentrations of ~160ppb are calculated for central South America and eastern North America. In general, higher concentrations are observed in the NH than the SH attributed to increased human activity, in the NH, since the SH is mostly covered by sea. In addition, CO's lifetime of ~40 days, is sufficiently long to allow long range transport NH and SH, combined with its secondary source from CH<sub>4</sub> oxidation which is spread around the globe due to the very long lifetime of CH<sub>4</sub>, explains the significant concentrations (~100ppb NH, ~80ppb SH) are observed in areas that are far from the emission sources.

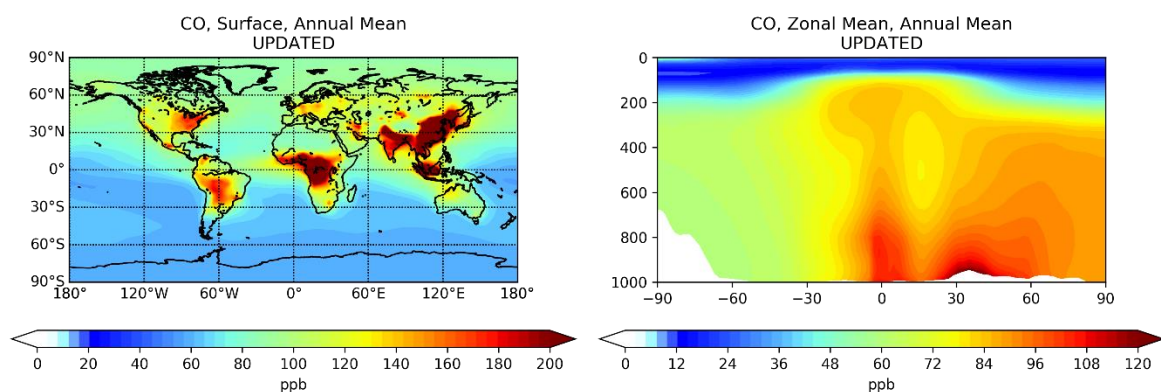


**Figure 3.8: Simulated annual mean CO concentrations for the updated MOGUNTIA scheme. Surface annual mean (left) and zonal annual mean (right)**

Regarding the zonal mean concentrations that the model calculated, the highest values of CO appear in the tropics and the NH, because of biomass burning and anthropogenic emissions. CO's transport can be clearly seen in the zonal mean distribution in **Figure 3.8** (right). It appears that CO is transported from the surface to the higher levels of the atmosphere to ~200hPa, especially in the tropics, where convection is strong, and the NH where the emissions are higher.

### 3.4.1 Comparison between the UPDATED and the OLD scheme

In **Figure 3.9** the differences between the two schemes are presented. The blue color indicates that the UPDATED scheme calculates lower CO concentrations than the OLD scheme. The largest difference is observed in the tropics and especially in the SH. The higher amounts of OH radicals that are calculated by the UPDATED scheme than in the OLD one lead to lower CO due to OH reaction with CO. The largest differences (~2-3ppb) appear in parts of the SH (South America, Indonesia). These are areas with increased vegetation and thus biogenic activity meaning that there are high isoprene emissions. For these areas the UPDATED scheme calculates higher OH radical concentrations than the OLD one. Zonal mean value differences appear to be higher in the SH maximizing at ~2-3ppb in the SH at ~500hPa and ~200hPa. This difference is attributed to the reaction of CO with OH radicals.

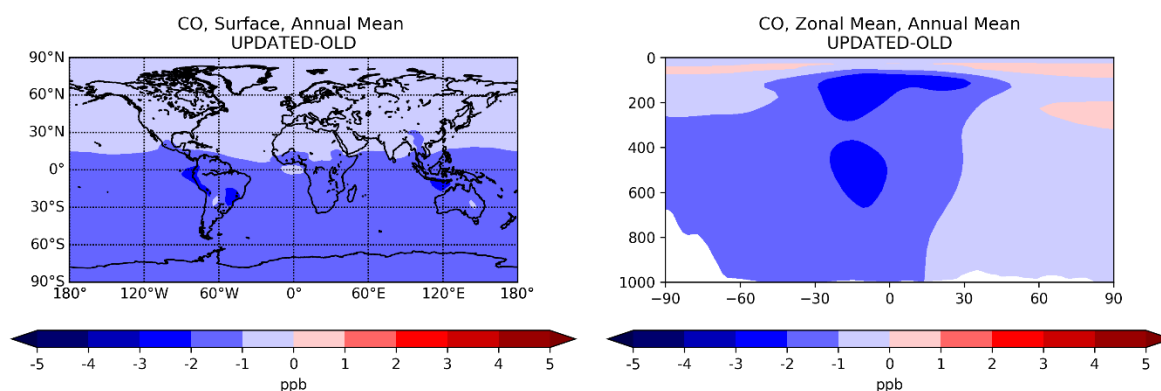


**Figure 3.9:** Difference between the UPDATED and the OLD MOGUNTIA scheme for CO concentrations. Surface annual mean difference (left) and zonal annual mean difference (right).

**Table 3.5:** Tropospheric budget of CO for the year 2006. Units are Tg(CO) yr<sup>-1</sup> except mentioned differently

<b>Production terms</b>	<b>OLD</b>	<b>UPDATED</b>	<b>Loss terms</b>	<b>OLD</b>	<b>UPDATED</b>
<b>Emissions</b>	1097	1097	<b>Deposition</b>	100	99
<b>Trop. chem. production</b>	1983	2025	<b>Trop. chem. loss</b>	2946	2997
<b>Strat. chem. production</b>	26	26	<b>Strat. chem. loss</b>	93	92

<b>Atmos. burden</b>	367	361	<b>Lifetime (days)</b>	44	43
--------------------------	-----	-----	----------------------------	----	----

### 3.4.2 Comparison to observations (CO)

In **Figure 3.10**, the model's performance in simulating the surface CO concentrations for the two simulations is presented, by comparing to flask observations for the year 2006. A mean underestimation of ~22.5ppb is calculated for the OLD scheme and a mean underestimation of ~24.2ppb for the UPDATED scheme, this difference between the two schemes is negligible. The model underestimates CO concentrations by ~20-50ppb in the NH for most sites (e.g. Barrow and Mace Head), in particular during springtime (March, April, May). The model presents an overall negative mean bias for the NH of ~30 ppb. At stations closer to the tropics (e.g. Mauna Loa, Tutuila) again a negative bias is found but with a better correlation (R= 0.9 and 0.76 respectively). On the other hand, in the SH (e.g. Cape Point and Cape Grim) and in Antarctica (e.g. South Pole and Syowa) a positive bias is calculated. Overall for the SH a small mean positive bias is found of ~1.1ppb.



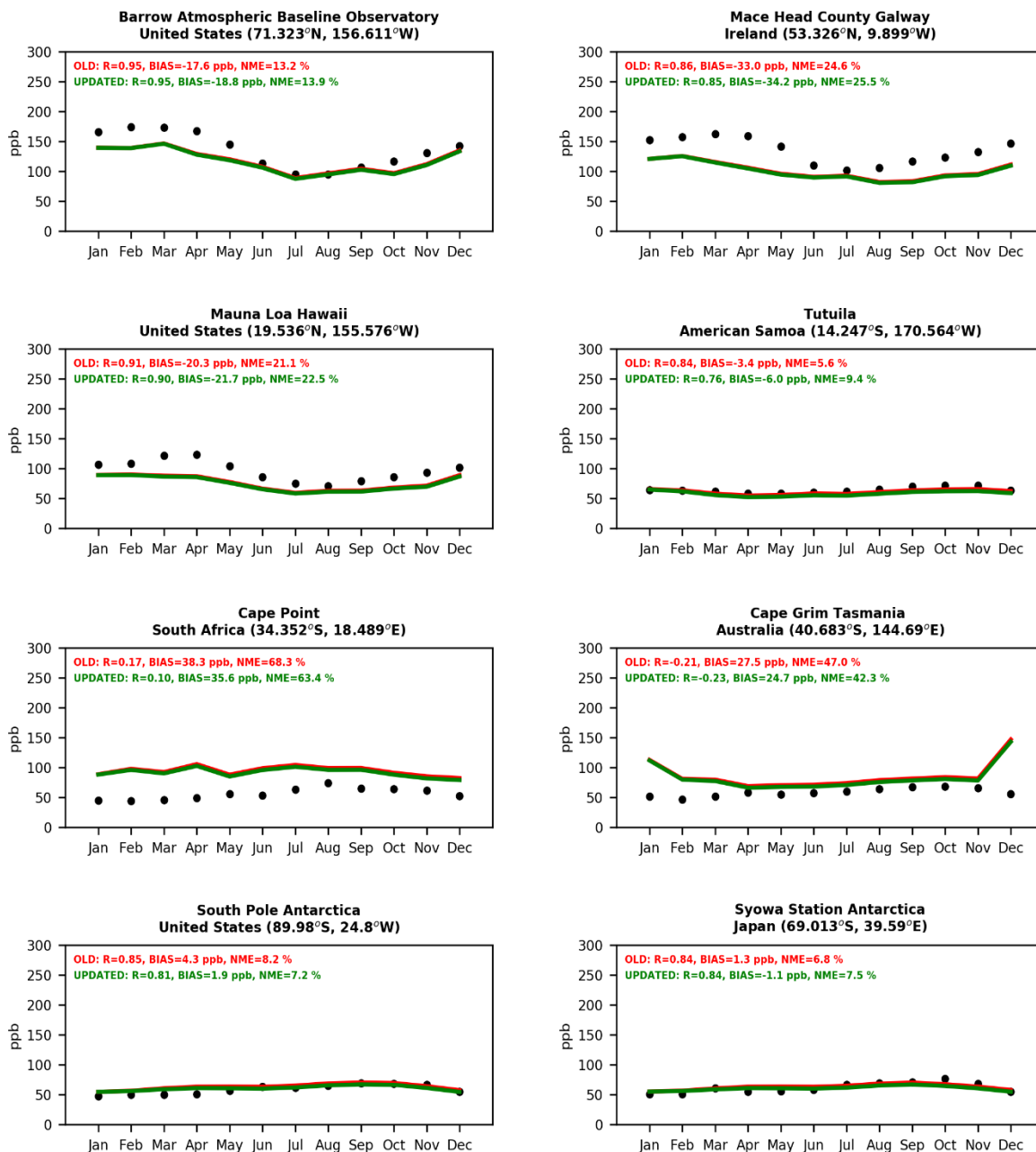


Figure 3.10: Monthly mean comparison of TM5-MP surface CO (ppb) against surface observations from the NOAA database for the two chemistry schemes (black dots), OLD (red line) and UPDATED (green line).

### 3.5 Isoprene epoxydiols

Isoprene epoxydiols (IEPOX) are compounds produced from isoprene oxidation and are responsible for the recycling of OH radicals under low  $\text{NO}_x$ . Isoprene is oxidized by OH radicals to produce isoprene peroxy radicals. Peroxy radicals may then, under low  $\text{NO}_x$  conditions, react with  $\text{HO}_2$  radicals in production of isoprene hydroperoxyl radicals. The

reaction of those hydroperoxyl radicals with OH radicals leads to isoprene epoxydiols with regeneration of a OH radical (see **Sect. 1**)

**Figure 3.11** shows the annual mean concentrations as simulated by the model. The highest amounts of IEPOX near the surface are calculated for the tropics and the Southern Hemisphere. Since IEPOX is produced through isoprene oxidation the highest concentrations appear in areas with high isoprene emissions (e.g. tropical forests). The zonal distribution shows maximum concentrations around the tropics and the SH extending upwards to ~600hPa. Furthermore, IEPOX has long enough lifetime to transport upwards to higher levels of the atmosphere up to ~200hPa with concentrations of ~15ppt. The model calculates the tropospheric production of IEPOX to be 168Tg yr<sup>-1</sup> as show in **Table 3.6**. Note that the model might overestimate IEPOX concentrations since the Secondary Organic Aerosol (SOA) formation from IEPOX is not yet implemented.

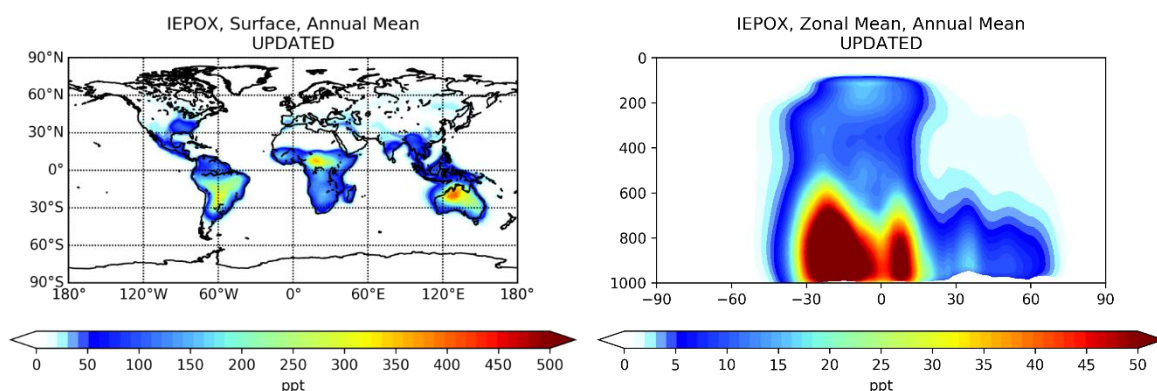


**Figure 3.11:** Simulated annual mean isoprene epoxydiol concentrations for the updated MOGUNTIA scheme. Surface annual mean (left) and zonal annual mean (right).

**Table 3.6:** Tropospheric budget of IEPOX for the year 2006

Production terms	MOGUNTIA	Loss terms	MOGUNTIA
Emissions	0	Deposition	30
Trop. chem. production	168	Trop. chem. loss	137
Atmos. Burden	209	Lifetime (hours)	11
Gg yr <sup>-1</sup>			

### 3.6 Hydro peroxy aldehydes

Hydro peroxy aldehydes (HPALDs) are another group of compounds formed as a result of the isoprene oxidation cascade. HPALDs are produced through the isomerization of isoprene peroxy radicals, more specifically through 1,6-H shift isomerization (see **Sect. 1**). These molecules are also important for the recycling of HO<sub>x</sub> species under low NO<sub>x</sub> conditions especially in forested areas. Their HO<sub>x</sub> recycling can take place by the photodissociation of HPALDs that produces OH and other smaller carbonyl compounds.

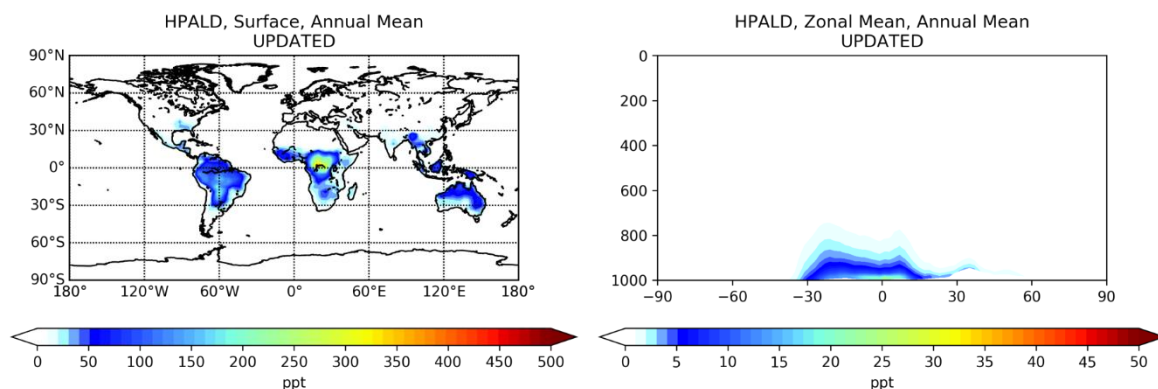


**Figure 3.12:** Simulated annual mean hydro peroxy aldehyde concentrations for the updated MOGUNTIA scheme. Surface annual mean (left) and zonal annual mean (right).

In **Figure 3.12** the annual mean values of HPALDs, as calculated by the model, can be seen. Again, since HPALDs are produced from isoprene oxidation products (such as IEPOX) the highest values appear in tropical areas and the southern hemisphere, i.e. in areas with increased vegetation cover and thus biogenic activity. Compared to IEPOX, HPALDs concentrations appear significantly because HPALDs can rapidly photo dissociate. This is illustrated on their zonal mean values as well. HPALDs are not transported high up to the middle and upper troposphere as IEPOX does but stay close to the surface because of their significantly shorter lifetime (**Table 3.7**).

**Table 3.7:** Tropospheric budget of HPALDs for the year 2006 in Tg yr<sup>-1</sup> except noted differently

<b>Production terms</b>	<b>MOGUNTIA</b>	<b>Loss terms</b>	<b>MOGUNTIA</b>
<b>Emissions</b>	0	<b>Deposition</b>	0.9
<b>Trop. chem. production</b>	88	<b>Trop. chem. loss</b>	87
<b>Atmos. Burden</b>	11	<b>Lifetime (hours)</b>	1
<b>Gg yr<sup>-1</sup></b>			

### 3.7 Impact of biogenic hydrocarbons (BVOCs) on tropospheric chemistry

We here investigate the impact of biogenic hydrocarbons contained in the MOGUNTIA chemistry scheme on important atmospheric tracers such as O<sub>3</sub>, OH radical and CO. For this purpose, we compared two simulations. The base simulation using the UPDATED MOGUNTIA scheme and one simulation for which the chemistry of terpenes and isoprene has been removed from the MOGUNTIA scheme further called BIOGENIC\_REMOVED.

#### 3.7.1 Ozone

In Figure 3.13 the differences in O<sub>3</sub> concentrations between the MOGUNTIA scheme and the BIOGENIC\_REMOVED scheme are presented. The differences in O<sub>3</sub> concentrations between the MOGUNTIA scheme and the BIOGENIC\_REMOVED scheme are also shown. The red color indicates the higher O<sub>3</sub> concentrations that are calculated by the MOGUNTIA scheme compared to those calculated with the BIOGENIC\_REMOVED scheme. The MOGUNTIA scheme seems to calculate higher concentrations of O<sub>3</sub> overall by up to ~8ppb. The highest negative differences between the two simulations (i.e. BIOGENIC\_REMOVED calculates higher O<sub>3</sub> concentration than the full scheme) appear over tropical America, Africa and Indonesia, areas where there is biogenic activity and thus isoprene and terpene emissions. Downwind these regions positive differences in O<sub>3</sub> are calculated. Isoprene and terpenes are precursors of RO<sub>2</sub> radicals, which contribute downwind surface regions in a high amount to O<sub>3</sub> production. RO<sub>2</sub> radicals from biogenic hydrocarbons are not present in the second scheme; this explains why in the full MOGUNTIA scheme more O<sub>3</sub> is calculated over the tropical oceans and the NH mid latitudes. The negative differences are most probably due to the reaction of O<sub>3</sub> with unsaturated hydrocarbons which dominate the areas with dense vegetation. Overall, the absence of isoprene and terpenes leads to higher O<sub>3</sub> concentrations for the BIOGENIC\_REMOVED scheme. Regarding zonal annual mean, the MOGUNTIA scheme calculates higher concentrations of O<sub>3</sub> in general with the highest difference being at ~200hPa (>12ppb).

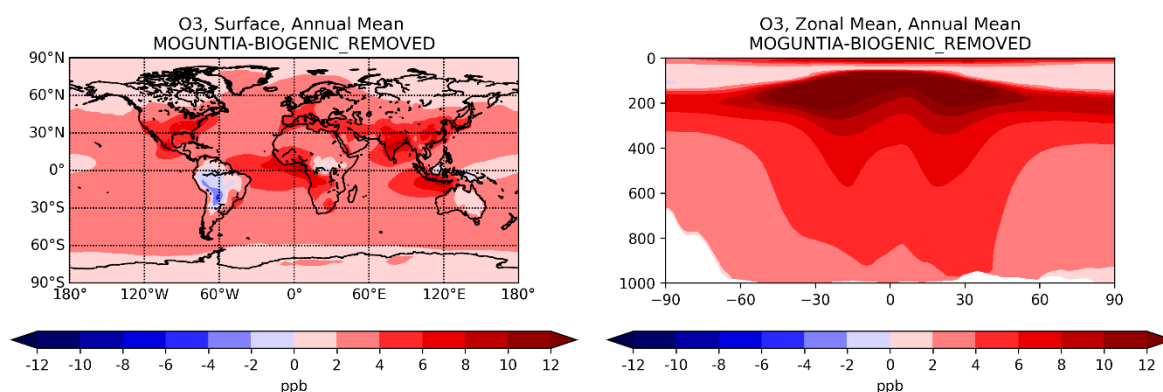


**Figure 3.13: Differences in O<sub>3</sub> concentrations between the MOGUNTIA scheme and the BIOGENIC\_REMOVED scheme. Annual mean surface concentrations (left) and annual zonal mean concentrations (right).**

**Table 3.8: Tropospheric budget of O<sub>3</sub> for the year 2006. Units in Tg(O<sub>3</sub>) yr<sup>-1</sup> except noted differently**

<b>Production terms</b>	<b>BIOGENIC REMOVED</b>	<b>MOGUNTIA</b>	<b>Loss terms Tg(O<sub>3</sub>) yr<sup>-1</sup></b>	<b>BIOGENIC REMOVED</b>	<b>MOGUNTIA</b>
<b>Stratospheric inflow*</b>	370	432	<b>Deposition</b>	842	927
<b>Trop. chem. production</b>	5222	5897	<b>Trop. chem. loss</b>	4749	5401
<b>Trop. burden</b>	346	382	<b>Trop. lifetime (days)</b>	23	22

\*sum of the deposition and the tropospheric chemical loss minus the production

### 3.7.2 Hydroxyl Radical

In **Figure 3.14** the results of the comparison between the MOGUNTIA and BIOGENIC\_REMOVED configuration regarding OH radical concentration are shown. The blue color indicates that the BIOGENIC\_REMOVED configuration calculates higher concentrations of OH radical.

The maximum near surface difference in OH concentrations is  $\sim 2.5\text{-}3.0 \times 10^6$  radicals  $\text{cm}^{-3}$ . As presented in the Fig. 3.14, higher differences in the OH concentrations are calculated for the tropical areas and the SH. This can be attributed to the absence of BVOCs in the BIOGENIC\_REMOVED configuration, which are a major sink for OH radical in these areas together with their oxidation products including carbon monoxide.

As for surface, regarding the zonal annual mean, the BIOGENIC\_REMOVED configuration calculates higher concentrations of OH radicals with the largest differences near the surface and at ~300hPa over the tropics. In altitudes above 200hPa the MOGUNTIA scheme following O<sub>3</sub> local maximum difference at this region (**Figure 3.13**, right) calculates slightly higher concentrations in the tropics ( $\sim 0.3\text{-}0.4 \times 10^6$  radicals  $\text{cm}^{-3}$ ).

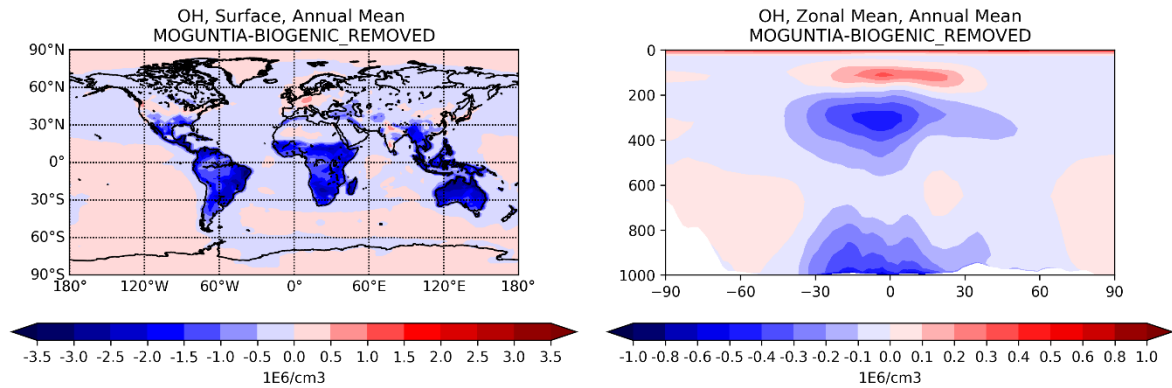


**Figure 3.14: Differences in OH radical concentrations between the MOGUNTIA scheme and the BIOGENIC\_REMOVED scheme. Annual mean surface concentrations (left) and annual zonal mean concentrations (right).**

Overall, the model calculates a global annual mean concentration, of OH radicals, of  $\sim 1.12 \times 10^6$  radicals  $\text{cm}^{-3}$  for the BIOGENIC\_REMOVED configuration. For the MOGUNTIA configuration the model calculates a global annual mean of  $\sim 1.05 \times 10^6$  radicals  $\text{cm}^{-3}$ . The highest difference is calculated for the tropics ( $30^\circ\text{N}\text{-}30^\circ\text{S}$ ) where the BIOGENIC\_REMOVED and the MOGUNTIA configurations calculate on average  $\sim 1.89 \times 10^6$  radicals  $\text{cm}^{-3}$  and  $\sim 1.75 \times 10^6$  radicals  $\text{cm}^{-3}$  respectively.

**Table 3.9: Concentrations for the BIOGENIC\_REMOVED and the MOGUNTIA configurations**

<b>10<sup>6</sup> radicals/cm<sup>3</sup></b>	<b>BIOGENIC_REMOVED</b>	<b>MOGUNTIA</b>	<b>Difference</b>
<b>North Hemisphere</b> ( <b>&gt;30°N</b> )	0.84	0.8	<b>5%</b>
<b>Tropics (30°N-30°S)</b>	1.89	1.75	<b>8%</b>
<b>South Hemisphere</b> ( <b>&gt;30°S</b> )	0.47	0.44	<b>7%</b>
<b>Global</b>	1.12	1.05	<b>7%</b>

The increase in OH radical concentration also affects the lifetime of VOCs such as CH<sub>4</sub> and HCHO which are oxidized by OH. The lifetime of both CH<sub>4</sub> and HCHO has been decreased due to the higher concentrations of OH calculated by the BIOGENIC\_REMOVED configuration. More specifically CH<sub>4</sub> chemical lifetime is calculated to be ~8 years using the MOGUNTIA configurations compared to ~7.3 years calculated by the BIOGENIC\_REMOVED configuration which is a decrease of ~9%. Regarding HCHO, MOGUNTIA calculates a lifetime of ~4.5h compared to BIOGENIC\_REMOVED which calculates ~4h, a decrease of 11%.

### 3.7.3 *Carbon monoxide*

In **Figure 3.15** the results regarding the comparison between the MOGUNTIA and BIOGENIC\_REMOVED configurations for the CO concentrations are presented. Red color indicates that MOGUNTIA calculates higher concentrations of CO than BIOGENIC\_REMOVED. The difference appears to be higher in the tropical and SH areas. This is attributed to the absence of BVOCs from the latter configuration. Isoprene and terpenes are oxidized to produce CO in the last stages of their oxidation. As can be seen the largest difference of ~60-80ppb is calculated over the Amazon forest, Central Africa and Indonesia/Australia, areas with high biogenic activity from vegetation. Furthermore, the atmospheric transport of CO leads to differences of ~20-40 ppb to be calculated over oceanic areas. Lastly, as can be seen in the annual zonal mean (**Figure 3.15**, right) the highest difference is calculated over the tropics and the SH to be ~20-30 ppb up to ~200 hPa altitude, with slightly lower differences of ~10-20 ppb calculated the NH and for latitudes >30° S.

The increase in the OH radicals which was discussed in the previous paragraph also affects CO and its lifetime. Regarding the MOGUNTIA configuration the model calculates a lifetime of ~42d for CO in contrast to the BIOGENIC\_REMOVED configuration which calculates ~39.5d, a decrease of ~6%. It is remarkable that the higher CO lifetime in the MOGUNTIA simulation is also favoring the buildup of CO from BVOC oxidation.

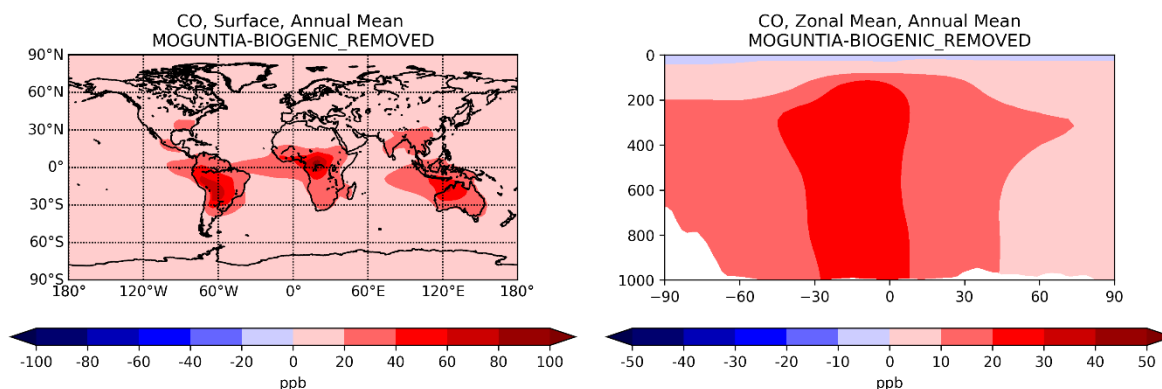


**Figure 3.15: Differences in CO concentrations between the MOGUNTIA scheme and the BIOGENIC\_REMOVED scheme. Annual mean surface concentrations (left) and annual zonal mean concentrations (right).**

**Table 3.10** and **Table 3.11** summarizes the key findings from the comparison of the two simulations (with and without BVOC chemistry) with regard to O<sub>3</sub> and CO budget terms as well as lifetimes of the key atmospheric constituents (CH<sub>4</sub>, HCHO, CO, O<sub>3</sub>)

**Table 3.10: CO and O<sub>3</sub> budget terms for the year 2006**

O <sub>3</sub>			CO		
Tg (O <sub>3</sub> ) yr <sup>-1</sup>	BIOGENIC REMOVED	MOGUNTIA	Tg(CO) yr <sup>-1</sup>	BIOGENIC REMOVED	MOGUNTIA
Stratospheric inflow	370	432	Net trop. chem.	-1081	-972
Net trop. Chem.	473	496	Trop. burden	259	331
Trop. burden	346	382			

**Table 3.11: Tropospheric lifetime of important atmospheric tracers. Units in days except noted differently**

Lifetime	BIOGENIC REMOVED	MOGUNTIA
CH <sub>4</sub>	7.3	8
HCHO (hours)	4	4.4
CO	40	43
O <sub>3</sub>	22	22.6



### 3.8 References

- Huijnen, V., Williams, J., Van Weele, M., Van Noije, T., Krol, M., Dentener, F., Segers, A., Houweling, S., Peters, W., De Laat, J., Boersma, F., Bergamaschi, P., Van Velthoven, P., Le Sager, P., Eskes, H., Alkemade, F., Scheele, R., Nédélec, P., Pätz, H.W., 2010. The global chemistry transport model TM5: Description and evaluation of the tropospheric chemistry version 3.0. *Geosci. Model Dev.* 3, 445–473. <https://doi.org/10.5194/gmd-3-445-2010>
- Lelieveld, J., Gromov, S., Pozzer, A., Taraborrelli, D., 2016. Global tropospheric hydroxyl distribution, budget and reactivity. *Atmos. Chem. Phys.* <https://doi.org/10.5194/acp-16-12477-2016>
- Naik, V., Voulgarakis, A., Fiore, A.M., Horowitz, L.W., Lamarque, J.-F., Lin, M., Prather, M.J., Young, P.J., Bergmann, D., Cameron-Smith, P.J., Cionni, I., Collins, W.J., Dalsøren, S.B., Doherty, R., Eyring, V., Faluvegi, G., Folberth, G.A., Josse, B., Lee, Y.H., MacKenzie, I.A., Nagashima, T., van Noije, T.P.C., Plummer, D.A., Righi, M., Rumbold, S.T., Skeie, R., Shindell, D.T., Stevenson, D.S., Strode, S., Sudo, K., Szopa, S., Zeng, G., 2013. Preindustrial to present-day changes in tropospheric hydroxyl radical and methane lifetime from the Atmospheric Chemistry and Climate Model Intercomparison Project (ACCMIP). *Atmos. Chem. Phys.* 13, 5277–5298. <https://doi.org/10.5194/acp-13-5277-2013>
- Spivakovsky, C.M., Logan, J.A., Montzka, S.A., Balkanski, Y.J., Foreman-Fowler, M., Jones, D.B.A., Horowitz, L.W., Fusco, A.C., Brenninkmeijer, C.A.M., Prather, M.J., Wofsy, S.C., McElroy, M.B., 2000. Three-dimensional climatological distribution of tropospheric OH: Update and evaluation. *J. Geophys. Res. Atmos.* 105, 8931–8980. <https://doi.org/10.1029/1999JD901006>
- Williams, J.E., Folkert Boersma, K., Le Sager, P., Verstraeten, W.W., 2017. The high-resolution version of TM5-MP for optimized satellite retrievals: Description and validation. *Geosci. Model Dev.* 10, 721–750. <https://doi.org/10.5194/gmd-10-721-2017>
- Williams, J.E., Van Velthoven, P.F.J., Brenninkmeijer, C.A.M., 2013. Quantifying the uncertainty in simulating global tropospheric composition due to the variability in global emission estimates of Biogenic Volatile Organic Compounds, *Atmospheric Chemistry and Physics*. <https://doi.org/10.5194/acp-13-2857-2013>

## 4 Conclusions

In the present work a detailed reaction scheme for isoprene was successfully implemented to the MOGUNTIA scheme in the global 3-dimensional chemistry transport model TM5-MP. The new isoprene scheme included two new species (IEPOX, HPALD) and the HO<sub>x</sub> recycling mechanism. Simulations were performed in order to compare the UPDATED to the OLD scheme, investigate the changes in the oxidation capacity of the atmosphere and examine the impact of IEPOX and HPALD chemistry on it. Another couple of simulations were performed in order to evaluate the impact of the BVOCs (isoprene and terpenes) in the oxidation capacity of the atmosphere. For that purpose, a simulation was performed where BVOCs chemistry was removed from the scheme.

Regarding the impact of IEPOX and HPALD chemistry alone, the oxidation capacity of the atmosphere was increased by ~3% globally by using the UPDATED scheme. The UPDATED scheme calculated higher concentrations regarding O<sub>3</sub> than the OLD scheme. The highest differences were calculated over the tropics and the SH because these are the areas with high concentrations of BVOCs and thus most affected by the chemistry changes in the scheme. CO concentrations were calculated to be lower for the UPDATED scheme than for the OLD one. Overall the differences between the two schemes regarding the studied species were very small. The model was evaluated by comparison of the model results to observations regarding O<sub>3</sub> and CO. For O<sub>3</sub> the model tends to overestimate the surface observations by ~16% with the differences between the two different schemes being negligible. For CO the model tends to underestimate observations by ~18% with the differences between the two schemes being again negligible. The increase in the calculated oxidation capacity due to consideration of IEPOX and HPALD chemistry led to an increase in OH and a decrease of the lifetime of CH<sub>4</sub> by ~4%, that of CO by ~5%, and of HCHO by ~2%.

Focusing on the impact of biogenic hydrocarbons in general, in the absence of BVOC the oxidation capacity (OH concentration) of the atmosphere was increased by an average of ~7%. The removal of BVOCs led to a decrease of O<sub>3</sub> concentrations and of CO concentrations when compared to the full scheme. The highest impact again was calculated for the tropics and in the SH, i.e. where high vegetation activity is present. Due to the increase in OH radical concentrations, CH<sub>4</sub> lifetime was decreased by ~9%, HCHO by ~11% and that of CO by ~6%.

The successful implementation of IEPOX species in the MOGUNTIA scheme allows to further improve the Secondary Organic Aerosol (SOA) formation in the model. Indeed, a

fraction of the isoprene derived SOA is produced by IEPOX which is not currently included in the model and can be the reason for the current overestimation of IEPOX concentrations by the model. The implementation of IEPOX-SOA in the TM5 is expected to contribute to better representation of both gas and aerosol tropospheric composition of organics involved in isoprene chemistry.

## 5 Appendix

Table 5.1: Photolysis reactions (J) in the MOGUNTIA chemistry scheme.

#	Reactants	Products <sup>#</sup>	Notes
<b><u>INORGANICS</u></b>			
J1	$O_3 + hv$	$\rightarrow O(^1D)$	1
J2	$H_2O_2 + hv$	$\rightarrow 2 OH$	1
J3	$NO_2 + hv$	$\rightarrow NO + O$	1
J4	$NO_3 + hv$	$\rightarrow NO_2 + O$	1
J5	$NO_3 + hv$	$\rightarrow NO$	1
J6	$N_2O_5 + hv$	$\rightarrow NO_2 + NO_3$	1
J7	$N_2O_5 + hv$	$\rightarrow NO + NO_3 + O$	1
J8	$HONO + hv$	$\rightarrow OH + NO$	1
J9	$HNO_3 + hv$	$\rightarrow NO_2 + OH$	1
J10	$HNO_4 + hv$	$\rightarrow NO_2 + HO_2$	1
<b><u>CARBON #1</u></b>			
J11	$HCHO + hv$	$\rightarrow CO$	1
J12	$HCHO + hv$	$\rightarrow CO + 2 HO_2$	1
J13	$CH_3OOH + hv$	$\rightarrow HCHO + HO_2 + OH$	1
J14	$CH_3ONO_2 + hv$	$\rightarrow HCHO + HO_2 + NO_2$	1
J15	$CH_3OONO_2 + hv$	$\rightarrow CH_3OO + NO_2$	1
J16	$CH_3OONO_2 + hv$	$\rightarrow HCHO + HO_2 + NO_3$	1
<b><u>CARBON #2</u></b>			
J17	$CH_3C(O)OONO_2 + hv$	$\rightarrow CH_3C(O)OO + NO_2$	J10
J18	$CH_3C(O)OONO_2 + hv$	$\rightarrow CH_3OO + NO_3 + CO_2$	J10
J19	$CH_3C(O)OOH + hv$	$\rightarrow CH_3C(O)OO + OH$	J13
J20	$C_2H_5OOH + hv$	$\rightarrow CH_3CHO + HO_2 + OH$	J13

J21	$C_2H_5ONO_2 + hv$	$\rightarrow HCHO + CO + HO_2 + NO_2$	1
J22	$HOCH_2CH_2OOH + hv$	$\rightarrow 2 HCHO + HO_2 + OH$	f 0.5 * J13
J23	$HOCH_2CH_2OOH + hv$	$\rightarrow HOCH_2CHO + HO_2 + OH$	(1 - f) 0.5 * J13
J24	$HOCH_2CH_2ONO_2 + hv$	$\rightarrow 2 HCHO + HO_2 + NO_2$	f 0.5 * JORGN
J25	$HOCH_2CH_2ONO_2 + hv$	$\rightarrow HOCH_2CHO + HO_2 + NO_2$	(1 - f) 0.5 * JORGN
J26	$CH_3CHO + hv$	$\rightarrow CH_3OO + CO + HO_2$	1
J27	$HOCH_2CHO + hv$	$\rightarrow CH_3OH + CO$	1
J28	$CHOCHO + hv$	$\rightarrow 2 CO + 2 HO_2$	1
J29	$CHOCHO + hv$	$\rightarrow HCHO + CO$	1
J30	$CHOCHO + hv$	$\rightarrow 2 CO$	1

### CARBON #3

J31	$CH_3C(O)CH_3 + hv$	$\rightarrow 2 CH_3OO + CO$	1
J32	$CH_3C(O)CH_3 + hv$	$\rightarrow CH_3C(O)OO + CH_3OO$	1
J33	$HOCH_2C(O)CH_3 + hv$	$\rightarrow CH_3C(O)OO + HCHO + HO_2$	1
J34	$CH_3C(O)CH_2OOH + hv$	$\rightarrow 0.3 CH_3C(O)CHO + 0.7(CH_3C(O)OO + HCHO) + OH$	J13
J35	$n-C_3H_7OOH + hv$	$\rightarrow C_2H_5CHO + HO_2 + OH$	0.5 * J13
J36	$n-C_3H_7ONO_2 + hv$	$\rightarrow C_2H_5CHO + HO_2 + NO_2$	1
J37	$i-C_3H_7OOH + hv$	$\rightarrow CH_3C(O)CH_3 + HO_2 + OH$	0.5 * J13
J38	$i-C_3H_7ONO_2 + hv$	$\rightarrow CH_3C(O)CH_3 + HO_2 + NO_2$	1
J39	$C_2H_5CHO + hv$	$\rightarrow C_2H_5OO + CO + HO_2$	1
J40	$HOC_3H_6OOH + hv$	$\rightarrow CH_3CHO + HCHO + HO_2$	J13
J41	$CH_3COCHO + hv$	$\rightarrow CH_3C(O)OO + CO + HO_2$	1

### CARBON >= #4

J42	$C_4H_9OOH + hv$	$\rightarrow 0.67(CH_3CH_2COCH_3 + HO_2) + 0.33(C_2H_5OO + CH_3CHO) + OH$	J13
J43	$C_4H_9ONO_2 + hv$	$\rightarrow 0.67(CH_3CH_2COCH_3 + HO_2) + 0.33(C_2H_5OO + CH_3CHO) + NO_2$	JORGN

J44	$\text{CH}_3\text{CH}_2\text{C}(\text{O})\text{CH}_3 + h\nu$	$\rightarrow \text{CH}_3\text{C}(\text{O})\text{OO} + \text{C}_2\text{H}_5\text{OO}$	1
J45	$\text{CH}_3\text{CH}(\text{OOH})\text{COCH}_3 + h\nu$	$\rightarrow \text{CH}_3\text{CHO} + \text{CH}_3\text{C}(\text{O})\text{OO} + \text{OH}$	J13
J46	$\text{CH}_3\text{CH}(\text{ONO}_2)\text{COCH}_3 + h\nu$	$\rightarrow \text{CH}_3\text{CHO} + \text{CH}_3\text{C}(\text{O})\text{OO} + \text{NO}_2$	J <sub>ORGN</sub>
<b><u>ISOPRENE</u></b>			
J47	$\text{ISOPOOH} + h\nu$	$\rightarrow \text{HCHO} + 0.64 \text{ MVK} + 0.36 \text{ MACR} + \text{HO}_2 + \text{OH}$	13
J48	$\text{ISOPONO}_2 + h\nu$	$\rightarrow \text{HCHO} + 0.64 \text{ MVK} + 0.36 \text{ MACR} + \text{HO}_2 + \text{NO}_2$	J <sub>ORGN</sub>
J49	$\text{MACR} + h\nu$	$\rightarrow 0.5 \text{ MACROO} + 0.5 \text{ HCHO} + 0.175 \text{ CH}_3\text{C}(\text{O})\text{OO} + 0.325 \text{ CH}_3\text{OO} + 0.825 \text{ CO} + \text{HO}_2$	1
J50	$\text{MACROOH} + h\nu$	$\rightarrow \text{CH}_3\text{COCH}_2\text{OH} + \text{CO} + \text{HO}_2 + \text{OH}$	J13
J51	$\text{MACRONO}_2 + h\nu$	$\rightarrow \text{CH}_3\text{COCH}_2\text{OH} + \text{CO} + \text{HO}_2 + \text{NO}_2$	J <sub>ORGN</sub>
J52	$\text{MVK} + h\nu$	$\rightarrow 0.6 (\text{C}_3\text{H}_6 + \text{CO}) + 0.4 (\text{CH}_3\text{C}(\text{O})\text{OO} + \text{CH}_3\text{OO} + \text{HCHO})$	1
J53	$\text{MVKOOH} + h\nu$	$\rightarrow 0.7(\text{CH}_3\text{C}(\text{O})\text{OO} + \text{HOCH}_2\text{CHO}) + 0.3(\text{MGLY} + \text{HCHO} + \text{HO}_2) + \text{OH}$	J13
J54	$\text{MVKONO}_2 + h\nu$	$\rightarrow 0.7(\text{CH}_3\text{C}(\text{O})\text{OO} + \text{HOCH}_2\text{CHO}) + 0.3(\text{MGLY} + \text{HCHO} + \text{HO}_2) + \text{NO}_2$	J <sub>ORGN</sub>
J55	$\text{CH}_3\text{C}(\text{O})\text{C}(\text{O})\text{CH}_3 + h\nu$	$\rightarrow 2 \text{ CH}_3\text{C}(\text{O})\text{OO}$	1
J56	$\text{CH}_3\text{C}(\text{O})\text{COOH} + h\nu$	$\rightarrow \text{CH}_3\text{C}(\text{O})\text{OO} + \text{HO}_2 + \text{CO}_2$	1
J57	$\text{HPALD} + h\nu$	$\rightarrow 0.5 \text{ HOCH}_2\text{C}(\text{O})\text{CH}_3 + 0.5 \text{ CH}_3\text{COCHO} + 0.25 \text{ HOCH}_2\text{CHO} + 0.25 \text{ CHOCHO} + \text{HCHO} + \text{HO}_2 + \text{OH}$	4, 5
J58	$\text{O}_2 + h\nu$	$\rightarrow \text{O}_3$	1

# The reaction products  $\text{O}_2$ ,  $\text{H}_2$ , and  $\text{H}_2\text{O}$  are not shown.

<sup>1</sup> <http://iupac.pole-ether.fr>

<sup>2</sup> Atkinson, (1997):

- $R_1 = 2.7 \times 10^{14} \exp(-6350/T)$   
 $R_2 = 6.3 \times 10^{14} \exp(-550/T)$

$$f = R_1 / (R_1 + R_2 \times [\text{O}_2])$$

<sup>3</sup> J<sub>ORGN</sub> is calculated based on average of  $\sigma$ -values for 1-C<sub>4</sub>H<sub>9</sub>ONO<sub>2</sub> and 2-C<sub>4</sub>H<sub>9</sub>ONO<sub>2</sub> as in Williams et al. (2012)

<sup>4</sup> Browne et al. (2014)

<sup>5</sup> Peeters and Müller (2010)

**Table 5.2: Thermal reactions (K) in MOGUNTIA chemistry scheme.**

#	Reactants	Products <sup>#</sup>	Rate expression <sup>s</sup>	Ref.
<b><u>INORGANICS</u></b>				
K0a	O( <sup>1</sup> D) (+ M)	O	$3.3 \times 10^{-11} \exp(55/T) [\text{O}_2] + 2.5 \times 10^{-11} \exp(110/T) [\text{N}_2]$	1
K0b	O( <sup>1</sup> D) + H <sub>2</sub> O	OH + OH	$1.63 \times 10^{-10} \exp(60/T)$	1
K1	O <sub>3</sub> + OH	→ HO <sub>2</sub>	$1.7 \times 10^{-12} \exp(-940/T)$	1
K2	HO <sub>2</sub> + O <sub>3</sub>	→ OH	$2.03 \times 10^{-16} (T/300)^{4.57} \exp(693/T)$	1
K3	HO <sub>2</sub> + OH	→ H <sub>2</sub> O	$4.8 \times 10^{-11} \exp(250/T)$ $2.2 \times 10^{-13} \exp(600/T)$	1
K4	HO <sub>2</sub> + HO <sub>2</sub>	→ H <sub>2</sub> O <sub>2</sub>	$1.9 \times 10^{-33} [\text{N}_2] \exp(980/T)$ $1.4 \times 10^{-21} [\text{H}_2\text{O}] \exp(2200/T)$	1
K5	H <sub>2</sub> O <sub>2</sub> + OH	→ HO <sub>2</sub>	$2.9 \times 10^{-12} \exp(-160/T)$	1
K6	HO <sub>2</sub> + NO	→ NO <sub>2</sub> + HO	$3.45 \times 10^{-12} \exp(270/T)$	1
K7	NO + O <sub>3</sub>	→ NO <sub>2</sub>	$2.07 \times 10^{-12} \exp(-1400/T)$	1
K8	NO + NO <sub>3</sub>	→ 2NO <sub>2</sub>	$1.8 \times 10^{-11} \exp(110/T)$	1
K9	NO <sub>2</sub> + O <sub>3</sub>	→ NO <sub>3</sub>	$1.4 \times 10^{-13} \exp(-2470/T)$ $7.4 \times 10^{-31} \times (T/300)^{-2.4} [\text{N}_2]$	1
K10	OH + NO {+ M}	→ HONO	$3.3 \times 10^{-11} (T/300)^{0.3}$ $F_c = 0.81$ $3.2 \times 10^{-30} (T/300)^{-4.5} [\text{N}_2]$	1
K11	OH + NO <sub>2</sub> {+ M}	→ HONO <sub>2</sub>	$3.0 \times 10^{-11}$ $F_c = 0.41$ $3.6 \times 10^{-30} (T/300)^{-4.1} [\text{N}_2]$	1
K12	NO <sub>2</sub> + NO <sub>3</sub> {+ M}	→ N <sub>2</sub> O <sub>5</sub>	$1.9 \times 10^{-12} (T/300)^{0.2}$ $F_c = 0.35$ $1.4 \times 10^{-31} (T/300)^{-3.1} [\text{N}_2]$	1
K13	NO <sub>2</sub> + HO <sub>2</sub>	→ HO <sub>2</sub> NO <sub>2</sub>	$4.0 \times 10^{-12}$ $F_c = 0.40$	1



K14	$\text{HO}_2 + \text{NO}_3$	$\rightarrow \text{OH} + \text{NO}_2$	$4.0 \times 10^{-12}$	1
K15	$\text{HONO} + \text{OH}$	$\rightarrow \text{NO}_2$	$2.5 \times 10^{-12} \exp(260/T)$ $2.4 \times 10^{-14} \exp(460/T)$	1
K16	$\text{HNO}_3 + \text{OH}$	$\rightarrow \text{NO}_3$	$6.5 \times 10^{-34} \exp(1335/T)$ $2.7 \times 10^{-17} \exp(2199/T)$	1
K17	$\text{HO}_2\text{NO}_2 + \text{OH}$	$\rightarrow \text{NO}_2$	$1.9 \times 10^{-12} \exp(270/T)$ $4.1 \times 10^{-5} \exp(-10650/T)[\text{N}_2]$	1
K18	$\text{HO}_2\text{NO}_2$	$\rightarrow \text{HO}_2 + \text{NO}_2$	$6.0 \times 10^{15} \exp(-11170/T)$ $F_c = 0.40$ $1.3 \times 10^{-3} (T/300)^{-3.5} \exp(-11000/T)[\text{N}_2]$	1
K19	$\text{N}_2\text{O}_5$	$\rightarrow \text{NO}_2 + \text{NO}_3$	$9.7 \times 10^{14} (T/300)^{0.1} \exp(-11080/T)$ $F_c = 0.35$	1
K20	$\text{OH} + \text{H}_2$	$\rightarrow \text{HO}_2$	$7.7 \times 10^{-12} \exp(-2100/T)$	1
<b><u>CARBON #1</u></b>				
K21	$\text{CH}_4 + \text{OH}$	$\rightarrow \text{CH}_3\text{OO}$	$2.45 \times 10^{-12} \exp(-1775/T)$ $3.8 \times 10^{-13} \exp(780/T)^*$	2
K22	$\text{CH}_3\text{OO} + \text{HO}_2$	$\rightarrow \text{CH}_3\text{OOH}$	$(1 - 1/(1 + 498.0 \exp(-1160/T)))$	1, 3
K23	$\text{CH}_3\text{OO} + \text{HO}_2$	$\rightarrow \text{HCHO}$	$3.8 \times 10^{-13} \exp(780/T)^*$ $(1/(1 + 498.0 \exp(-1160/T)))$	1, 3
K24	$\text{CH}_3\text{OO} + \text{NO}$	$\rightarrow 0.999 (\text{HCHO} + \text{HO}_2 + \text{NO}_2) + 0.001 \text{CH}_3\text{ONO}_2$	$2.3 \times 10^{-12} \exp(360/T)$ $2.5 \times 10^{-30} (T/300)^{-5.5} [\text{N}_2]$	1, 3
K25	$\text{CH}_3\text{OO} + \text{NO}_2$	$\rightarrow \text{CH}_3\text{O}_2\text{NO}_2$	$1.8 \times 10^{-11}$ $F_c = 0.36$	1
K26	$\text{CH}_3\text{OO} + \text{NO}_3$	$\rightarrow \text{HCHO} + \text{NO}_2$	$1.2 \times 10^{-12}$ $7.4 \exp(-520/T) \times$	1
K27	$\text{CH}_3\text{OO} + \text{CH}_3\text{OO}$	$\rightarrow 2\text{HCHO} + 2\text{HO}_2$	$1.03 \times 10^{-13} \exp(365/T)$	1, 3
K28	$\text{CH}_3\text{OO} + \text{CH}_3\text{OO}$	$\rightarrow \text{CH}_3\text{OH} + \text{HCHO}$	$(1 - 7.4 \exp(-520/T) \times$	1, 3

			$1.03 \times 10^{-13} \exp(365/T)$	
K29	$\text{CH}_3\text{OOH} + \text{OH}$	$\rightarrow \text{HCHO} + \text{OH}$	$0.4 \times 5.3 \times 10^{-12} \exp(190/T)$	1
K30	$\text{CH}_3\text{OOH} + \text{OH}$	$\rightarrow \text{CH}_3\text{OO}$	$0.6 \times 5.3 \times 10^{-12} \exp(190/T)$	1
K31	$\text{CH}_3\text{ONO}_2 + \text{OH}$	$\rightarrow \text{HCHO} + \text{NO}_2$	$4.0 \times 10^{-13} \exp(-845/T)$	1
			$9.0 \times 10^{-5} \exp(-9690/T) [\text{N}_2]$	
K32	$\text{CH}_3\text{OONO}_2$	$\rightarrow \text{CH}_3\text{O}_2 + \text{NO}_2$	$1.1 \times 10^{16} \exp(-10560/T)$	1
			$F_c = 0.40$	
K33	$\text{HCHO} + \text{OH}$	$\rightarrow \text{CO} + \text{HO}_2$	$5.4 \times 10^{-12} \exp(135/T)$	1
K34	$\text{HCHO} + \text{NO}_3$	$\rightarrow \text{CO} + \text{HO}_2 + \text{HNO}_3$	$2.0 \times 10^{-12} \exp(-2440/T)$	1
K35	$\text{CH}_3\text{OH} + \text{OH}$	$\rightarrow \text{HCHO} + \text{HO}_2$	$2.85 \times 10^{-12} \exp(-345/T)$	1
K36	$\text{CH}_3\text{OH} + \text{NO}_3$	$\rightarrow \text{HCHO} + \text{HO}_2 + \text{HNO}_3$	$9.4 \times 10^{-13} \exp(-2650/T)$	1
K37	$\text{HCOOH} + \text{OH}$	$\rightarrow \text{CO}_2 + \text{HO}_2$	$4.5 \times 10^{-13}$	1
			$5.9 \times 10^{-33} (300/T)^{1.4}$	
			$1.1 \times 10^{-12} (300/T)^{-1.3}$	
K38	$\text{CO} + \text{OH}$	$\rightarrow \text{CO}_2 + \text{HO}_2$	$1.5 \times 10^{-13} (300/T)^{-0.6}$	2
			$2.9 \times 10^9 (300/T)^{-6.1}$	
	<b><u>CARBON #2</u></b>			
K39	$\text{C}_2\text{H}_6 + \text{OH}$	$\rightarrow \text{C}_2\text{H}_5\text{OO}$	$6.9 \times 10^{-12} \exp(-1000/T)$	1
K40	$\text{C}_2\text{H}_5\text{OO} + \text{HO}_2$	$\rightarrow \text{C}_2\text{H}_5\text{OOH}$	$6.4 \times 10^{-13} \exp(710/T)$	1
K41	$\text{C}_2\text{H}_5\text{OO} + \text{NO}$	$\rightarrow \text{CH}_3\text{CHO} + \text{HO}_2 + \text{NO}_2$	$(1 - \text{RTC}2\text{P}) \times 2.55 \times 10^{-12} \exp(380/T)$	1, 4
K42	$\text{C}_2\text{H}_5\text{OO} + \text{NO}$	$\rightarrow \text{C}_2\text{H}_5\text{ONO}_2$	$\text{RTC}2\text{P} \times 2.55 \times 10^{-12} \exp(380/T)$	1, 4
K43	$\text{C}_2\text{H}_5\text{OO} + \text{CH}_3\text{OO}$	$\rightarrow \text{CH}_3\text{CHO} + \text{HCHO} + 2\text{HO}_2$	$0.8 \times (6.4 \times 10^{-14} \times 1.03 \times 10^{-13} \exp(365/T))^{0.5}$	3
K44	$\text{C}_2\text{H}_5\text{OO} + \text{CH}_3\text{OO}$	$\rightarrow 0.5 \text{CH}_3\text{CHO} + 0.5 \text{CH}_3\text{CH}_2\text{OH} + \text{CH}_3\text{OH}$	$0.2 \times (6.4 \times 10^{-14} \times 1.03 \times 10^{-13} \exp(365/T))^{0.5}$	3
K45	$\text{C}_2\text{H}_5\text{OOH} + \text{OH}$	$\rightarrow \text{C}_2\text{H}_5\text{OO}$	$1.90 \times 10^{-12} \exp(190/T)$	1
K46	$\text{C}_2\text{H}_5\text{OOH} + \text{OH}$	$\rightarrow \text{CH}_3\text{CHO} + \text{OH}$	$6.0 \times 10^{-12}$	3
K47	$\text{C}_2\text{H}_5\text{ONO}_2 + \text{OH}$	$\rightarrow \text{CH}_3\text{CHO} + \text{NO}_2$	$6.7 \times 10^{-13} \exp(-395/T)$	1
K48	$\text{CH}_3\text{CHO} + \text{OH}$	$\rightarrow \text{CH}_3\text{C}(\text{O})\text{OO}$	$4.7 \times 10^{-12} \exp(345/T)$	1

K49	$\text{CH}_3\text{CHO} + \text{NO}_3$	$\rightarrow \text{CH}_3\text{C(O)OO} + \text{HNO}_3$	$1.4 \times 10^{-12} \exp(-1860/T)$	1
K50	$\text{CH}_3\text{C(O)OO} + \text{HO}_2$	$\rightarrow \text{CH}_3\text{C(O)OOH}$	$0.41 * 5.2 \times 10^{-13} \exp(980/T)$	3
K51	$\text{CH}_3\text{C(O)OO} + \text{HO}_2$	$\rightarrow \text{CH}_3\text{COOH} + \text{O}_3$	$0.15 * 5.2 \times 10^{-13} \exp(980/T)$	3
K52	$\text{CH}_3\text{C(O)OO} + \text{HO}_2$	$\rightarrow \text{CH}_3\text{O}_2 + \text{CO}_2 + \text{OH}$	$0.44 * 5.2 \times 10^{-13} \exp(980/T)$	3
K53	$\text{CH}_3\text{C(O)OO} + \text{NO}$	$\rightarrow \text{CH}_3\text{OO} + \text{CO}_2 + \text{NO}_2$	$7.5 \times 10^{-12} \exp(290/T)$	1
			$3.28 \times 10^{-28} (T/300)^{-6.87} [\text{N}_2]$	
K54	$\text{CH}_3\text{C(O)OO} + \text{NO}_2$	$\rightarrow \text{CH}_3\text{C(O)OONO}_2$	$1.125 \times 10^{-11} (T/300)^{-1.105}$	1
			$F_c = 0.3$	
K55	$\text{CH}_3\text{C(O)OO} + \text{NO}_3$	$\rightarrow \text{CH}_3\text{OO} + \text{NO}_2$	$4.0 \times 10^{-12}$	2
K56	$\text{CH}_3\text{C(O)OO} + \text{CH}_3\text{OO}$	$\rightarrow \text{CH}_3\text{C(O)OOH} + \text{HCHO}$	$0.9 * 2.0 \times 10^{-12} \exp(500/T)$	2
K57	$\text{CH}_3\text{C(O)OO} + \text{CH}_3\text{OO}$	$\rightarrow \text{CH}_3\text{COOH} + \text{HCHO}$	$0.1 * 2.0 \times 10^{-12} \exp(500/T)$	2
K58	$\text{CH}_3\text{C(O)OO} + \text{CH}_3\text{C(O)OO}$	$\rightarrow 2 (\text{CH}_3\text{OO} + \text{CO}_2)$	$2.9 \times 10^{-12} \exp(500/T)$	2
K59	$\text{CH}_3\text{C(O)OO} + \text{CH}_3\text{COCH}_2\text{O}_2$	$\rightarrow \text{CH}_3\text{COOH} + \text{CH}_3\text{COCHO}$	$2.5 \times 10^{-12}$	2
K60	$\text{CH}_3\text{C(O)OO} + \text{CH}_3\text{COCH}_2\text{O}_2$	$\rightarrow \text{CH}_3\text{OO} + \text{CH}_3\text{COCH}_2\text{OH} + \text{CO}_2$	$2.5 \times 10^{-12}$	2
K61	$\text{CH}_3\text{C(O)OO} + \text{C}_2\text{H}_5\text{OO}$	$\rightarrow \text{CH}_3\text{CHO} + 2 \text{CH}_3\text{OO}$	$0.7 * 4.4 \times 10^{-13} \exp(1070/T)$	1, 3
K62	$\text{CH}_3\text{C(O)OO} + \text{C}_2\text{H}_5\text{OO}$	$\rightarrow \text{CH}_3\text{CHO} + \text{CH}_3\text{COOH}$	$0.3 * 4.4 \times 10^{-13} \exp(1070/T)$	1, 3
K63	$\text{CH}_3\text{C(O)OONO}_2 + \text{OH}$	$\rightarrow \text{HCHO} + \text{CO} + \text{NO}_2$	$3.0 \times 10^{-14}$	1
			$1.1 \times 10^{-5} \exp(-10100/T) [\text{N}_2]$	
K64	$\text{CH}_3\text{C(O)OONO}_2$	$\rightarrow \text{CH}_3\text{C(O)OO} + \text{NO}_2$	$1.9 \times 10^{17} \exp(-14100/T)$	1
			$F_c = 0.3$	
K65	$\text{CH}_3\text{C(O)OONO}_2$	$\rightarrow \text{CH}_3\text{ONO}_2 + \text{CO}_2$	$2.1 \times 10^{12} \exp(-12525/T)$	5
K66	$\text{CH}_3\text{C(O)OOH} + \text{OH}$	$\rightarrow \text{CH}_3\text{C(O)OO}$	$1.1 \times 10^{-11}$	3
			$8.6 \times 10^{-29} (T/300)^{-3.1} [\text{N}_2]$	
K67	$\text{C}_2\text{H}_4 + \text{OH}$	$\rightarrow \text{HOCH}_2\text{CH}_2\text{OO}$	$9.0 \times 10^{-12} (T/300)^{-0.85}$	1

			$Fc = 0.48$	
K68	$C_2H_4 + NO_3$	$\rightarrow HOCH_2CH_2ONO_2$	$3.3 \times 10^{-12} \exp(-2880/T)$	1
K69	$C_2H_4 + O_3$	$\rightarrow 1.37 HCHO + 0.63 CO + 0.13 HO_2 + 0.13 OH$	$6.82 \times 10^{-15} \exp(-2500/T)$	1
K70	$HOCH_2CH_2OO + HO_2$	$\rightarrow HOCH_2CH_2OOH$	$1.3 \times 10^{-11}$	1
K71	$HOCH_2CH_2OO + NO$	$\rightarrow NO_2 + 2HCHO + HO_2$	$(1-RTC2P) \times f \times 2.7 \times 10^{-12} \exp(360/T)$	3
K72	$HOCH_2CH_2OO + NO$	$\rightarrow NO_2 + HOCH_2CHO + HO_2$	$(1-RTC2P) \times (1-f) \times 2.7 \times 10^{-12} \exp(360/T)$	3
K73	$HOCH_2CH_2OO + NO$	$\rightarrow HOCH_2CH_2ONO_2$	$RTC2P \times 2.7 \times 10^{-12} \exp(360/T)$	1
K74	$HOCH_2CH_2OO + CH_3OO$	$\rightarrow HOCH_2CHO + HCHO + 2HO_2$	$0.8 * (7.8 \times 10^{14} \exp(1000/T)) * 1.03 \times 10^{-13} \exp(365/T)^{0.5}$	3
K75	$HOCH_2CH_2OO + CH_3OO$	$\rightarrow HOCH_2CHO + CH_3OH$	$0.2 * (7.8 \times 10^{14} \exp(1000/T)) * 1.03 \times 10^{-13} \exp(365/T)^{0.5}$	3
K76	$HOCH_2CH_2OOH + OH$	$\rightarrow HOCH_2CH_2OO$	K45	
K77	$HOCH_2CH_2OOH + OH$	$\rightarrow HOCH_2CHO + OH$	$1.38 \times 10^{-11}$	3
K78	$HOCH_2CH_2ONO_2 + OH$	$\rightarrow HOCH_2CHO + NO_2$	K47	
K79	$C_2H_2 + OH$	$\rightarrow 0.636(CHOCHO + OH) + 0.364(HCOOH + CO + HO_2)$	$5.0 \times 10^{-30} (T/300)^{-1.5} [N_2]$ $1.0 \times 10^{-12}$	1
			$Fc = 0.37$	
K80	$C_2H_2 + NO_3$	$\rightarrow 0.635 CHOCHO + 0.365(HCOOH + CO) + HNO_3$	$1.0 \times 10^{-16}$	1
K81	$C_2H_2 + O_3$	$\rightarrow 0.635 CHOCHO + 0.365(HCOOH + CO)$	$1.0 \times 10^{-20}$	1
K82	$HOCH_2CHO + OH$	$\rightarrow HCHO + CO_2$	$6.4 \times 10^{-12}$	1
K83	$HOCH_2CHO + OH$	$\rightarrow CHOCHO + HO_2$	$1.6 \times 10^{-12}$	1
K84	$CHOCHO + OH$	$\rightarrow 2CO + HO_2$	$3.1 \times 10^{-12} \exp(340/T)$	1
K85	$CHOCHO + NO_3$	$\rightarrow 2CO + HO_2 + HNO_3$	$4.0 \times 10^{-16}$	1
K86	$CH_3COOH + OH$	$\rightarrow CH_3OO + CO_2$	$4.0 \times 10^{-14} \exp(850/T)$	1

K87	$\text{CH}_3\text{CH}_2\text{OH} + \text{OH}$	$\rightarrow 0.95 (\text{CH}_3\text{CHO} + \text{HO}_2) + 0.05 \text{HOCH}_2\text{CH}_2\text{OO}$	$3.0 \times 10^{-12} \exp(20/T)$	1
<b><u>CARBON #3</u></b>				
K88	$\text{C}_3\text{H}_8 + \text{OH}$	$\rightarrow 0.264 n\text{-C}_3\text{H}_7\text{O}_2 + 0.736 i\text{-C}_3\text{H}_7\text{O}_2$	$7.6 \times 10^{-12} \exp(-585/T)$	1, 3
K89	$n\text{-C}_3\text{H}_7\text{O}_2 + \text{HO}_2$	$\rightarrow n\text{-C}_3\text{H}_7\text{OOH}$	$0.52 \times 2.91 \times 10^{-13} \exp(1300/T)$	3
K90	$n\text{-C}_3\text{H}_7\text{O}_2 + \text{NO}$	$\rightarrow \text{C}_2\text{H}_5\text{CHO} + \text{HO}_2 + \text{NO}_2$	$(1 - \text{RTC3P}) \times 2.9 \times 10^{-12} \exp(350/T)$	1, 4
K91	$n\text{-C}_3\text{H}_7\text{O}_2 + \text{NO}$	$\rightarrow n\text{-C}_3\text{H}_7\text{ONO}_2$	$\text{RTC3P} \times 2.9 \times 10^{-12} \exp(350/T)$	1, 4
K92	$n\text{-C}_3\text{H}_7\text{O}_2 + \text{CH}_3\text{OO}$	$\rightarrow \text{C}_2\text{H}_5\text{CHO} + \text{CH}_3\text{OH}$	$0.8 \times (3.5 \times 10^{-13} \times 3.0 \times 10^{13})^{0.5}$	3
K93	$n\text{-C}_3\text{H}_7\text{O}_2 + \text{CH}_3\text{OO}$	$\rightarrow \text{C}_2\text{H}_5\text{CHO} + \text{HCHO} + 2\text{HO}_2$	$0.2 \times (3.5 \times 10^{-13} \times 3.0 \times 10^{13})^{0.5}$	3
K94	$n\text{-C}_3\text{H}_7\text{OOH} + \text{OH}$	$\rightarrow n\text{-C}_3\text{H}_7\text{O}_2$	K76	
K95	$n\text{-C}_3\text{H}_7\text{OOH} + \text{OH}$	$\rightarrow \text{C}_2\text{H}_5\text{CHO} + \text{OH}$	$1.66 \times 10^{-11}$	3
K96	$n\text{-C}_3\text{H}_7\text{ONO}_2 + \text{OH}$	$\rightarrow \text{C}_2\text{H}_5\text{CHO} + \text{NO}_2$	$5.8 \times 10^{-13}$	1
K97	$i\text{-C}_3\text{H}_7\text{O}_2 + \text{HO}_2$	$\rightarrow i\text{-C}_3\text{H}_7\text{OOH}$	K89	
K98	$i\text{-C}_3\text{H}_7\text{O}_2 + \text{NO}$	$\rightarrow \text{CH}_3\text{COCH}_3 + \text{HO}_2 + \text{NO}_2$	$(1 - \text{RTC3S}) * 2.7 \times 10^{-12} \exp(360/T)$	1, 4
K99	$i\text{-C}_3\text{H}_7\text{O}_2 + \text{NO}$	$\rightarrow i\text{-C}_3\text{H}_7\text{ONO}_2$	$\text{RTC3S} * 2.7 \times 10^{-12} \exp(360/T)$	1, 4
K100	$i\text{-C}_3\text{H}_7\text{O}_2 + \text{CH}_3\text{OO}$	$\rightarrow \text{CH}_3\text{COCH}_3 + \text{HCHO} + 2\text{HO}_2$	$0.8 * (1.03 \times 10^{-13} \exp(365/T)) * 1.6 \times 10^{-12} \exp(-2200/T)^{0.5}$	3
K101	$i\text{-C}_3\text{H}_7\text{O}_2 + \text{CH}_3\text{OO}$	$\rightarrow \text{CH}_3\text{COCH}_3 + \text{CH}_3\text{OH}$	$0.2 * (1.03 \times 10^{-13} \exp(365/T)) * 1.6 \times 10^{-12} \exp(-2200/T)^{0.5}$	3
K102	$i\text{-C}_3\text{H}_7\text{OOH} + \text{OH}$	$\rightarrow i\text{-C}_3\text{H}_7\text{O}_2$	$1.9 \times 10^{-12} \exp(190/T)$	3
K103	$i\text{-C}_3\text{H}_7\text{OOH} + \text{OH}$	$\rightarrow \text{CH}_3\text{COCH}_3 + \text{OH}$	$1.66 \times 10^{-11}$	3
K104	$i\text{-C}_3\text{H}_7\text{ONO}_2 + \text{OH}$	$\rightarrow \text{CH}_3\text{COCH}_3 + \text{NO}_2$	$6.2 \times 10^{-13} \exp(-230/T)$	1
K105	$\text{C}_2\text{H}_5\text{CHO} + \text{OH}$	$\rightarrow \text{CH}_3\text{C}(\text{O})\text{OO} + \text{CO}$	$4.9 \times 10^{-12} \exp(405/T)$	1
K106	$\text{C}_2\text{H}_5\text{CHO} + \text{NO}_3$	$\rightarrow \text{CH}_3\text{C}(\text{O})\text{OO} + \text{CO} + \text{HNO}_3$	$6.3 \times 10^{-15}$	1

K107	$\text{CH}_3\text{COCH}_3 + \text{OH}$	$\rightarrow \text{CH}_3\text{COCH}_2\text{OO}$	$8.8 \times 10^{-12}\text{exp}(-1320/T) +$ $1.7 \times 10^{-14}\text{exp}(423/T)$	1
K108	$\text{CH}_3\text{COCH}_2\text{OO} +$ $\text{NO}$	$\rightarrow \text{CH}_3\text{COCHO} + \text{NO}_2 + \text{HO}_2$	$2.7 \times 10^{-13}\text{exp}(360/T)$	3
K109	$\text{CH}_3\text{COCH}_2\text{OO} +$ $\text{HO}_2$	$\rightarrow \text{CH}_3\text{COCH}_2\text{OOH}$	$1.36 \times 10^{-13}\text{exp}(1250/T)$	3
K110	$\text{CH}_3\text{COCH}_2\text{OOH} +$ $\text{OH}$	$\rightarrow 0.7 \text{CH}_3\text{COCHO} + 0.3 \text{CH}_3\text{COCH}_2\text{OO} + \text{OH}$	$1.90 \times 10^{-12}\text{exp}(190/T)$	3
K111	$\text{C}_3\text{H}_6 + \text{OH}$	$\rightarrow \text{HOC}_3\text{H}_6\text{OO}$	$8 \times 10^{-27}(T/300)^{-3.5}[\text{N}_2]$ $3.0 \times 10^{-11}(T/300)^{-1.0}$ $F_c = 0.5$	1
K112	$\text{C}_3\text{H}_6 + \text{NO}_3$	$\rightarrow 0.35 n\text{-C}_3\text{H}_7\text{ONO}_2 + 0.65 i\text{-C}_3\text{H}_7\text{ONO}_2$	$4.6 \times 10^{-13}\text{exp}(-1155/T)$	1, 3
K113	$\text{C}_3\text{H}_6 + \text{O}_3$	$\rightarrow 0.62 \text{HCHO} + 0.62 \text{CH}_3\text{CHO} + 0.38 \text{CH}_3\text{OO}$ $+ 0.56 \text{CO} + 0.36 \text{HO}_2 + 0.36 \text{OH} + 0.2 \text{CO}_2$	$5.77 \times 10^{-15}\text{exp}(-1880/T)$	1, 3
K114	$\text{HOC}_3\text{H}_6\text{OOH} + \text{OH}$	$\rightarrow 0.928 \text{CH}_3\text{COCH}_2\text{OH} + 0.072 \text{HOC}_3\text{H}_6\text{OO} +$ $0.928 \text{OH}$	$2.44 \times 10^{-11} + 1.9 \times 10^{-12}\text{exp}(190/T)$	3
K115	$\text{HOC}_3\text{H}_6\text{OO} + \text{HO}_2$	$\rightarrow \text{HOC}_3\text{H}_6\text{OOH}$	K89	3
K116	$\text{HOC}_3\text{H}_6\text{OO} + \text{NO}$	$\rightarrow \text{CH}_3\text{CHO} + \text{HCHO} + \text{HO}_2 + \text{NO}_2$	$(1 - 0.35R_{TC3P} - 0.65R_{TC3S})^*$ $2.55 \times 10^{-12}\text{exp}(380/T)$	1, 3
K117	$\text{HOC}_3\text{H}_6\text{OO} + \text{NO}$	$\rightarrow 0.35 n\text{-C}_3\text{H}_7\text{ONO}_2 + 0.65 i\text{-C}_3\text{H}_7\text{ONO}_2$	$(0.35R_{TC3P} + 0.65R_{TC3S})^*$ $2.55 \times 10^{-12}\text{exp}(380/T)$	1, 3
K118	$\text{HOC}_3\text{H}_6\text{OO} +$ $\text{CH}_3\text{OO}$	$\rightarrow \text{CH}_3\text{CHO} + 2\text{HCHO} + 2\text{HO}_2$	$0.8 * 6.0 \times 10^{-13}$	3
K119	$\text{HOC}_3\text{H}_6\text{OO} +$ $\text{CH}_3\text{OO}$	$\rightarrow \text{CH}_3\text{COCH}_2\text{OH} + \text{CH}_3\text{OH}$	$0.2 * 6.0 \times 10^{-13}$	3
K120	$\text{CH}_3\text{COCH}_2\text{OH} +$ $\text{OH}$	$\rightarrow \text{CH}_3\text{COCHO} + \text{HO}_2$	$1.6 \times 10^{-12}\text{exp}(305/T)$	1
K121	$\text{CH}_3\text{COCHO} + \text{OH}$	$\rightarrow \text{CH}_3\text{C(O)OO} + \text{CO}$	$1.9 \times 10^{-12}\text{exp}(575/T)$	1
K122	$\text{CH}_3\text{COCHO} + \text{NO}_3$	$\rightarrow \text{CH}_3\text{C(O)OO} + \text{CO} + \text{HNO}_3$	$5.0 \times 10^{-16}$	1
K123	$\text{CH}_3\text{C(O)COOH} +$ $\text{OH}$	$\rightarrow \text{CH}_3\text{C(O)OO} + \text{CO}_2$	$8.0 \times 10^{-13}$	3

**CARBON >= #4**

K124	$C_4H_{10} + OH$	$\rightarrow C_4H_9OO$	$9.8 \times 10^{-12} \exp(-425/T)$	3
K125	$C_4H_{10} + NO_3$	$\rightarrow C_4H_9OO + HNO_3$	$2.8 \times 10^{-12} \exp(-3280/T)$	1
K126	$C_4H_9OO + HO_2$	$\rightarrow C_4H_9OOH$	$0.625 * 2.91 \times 10^{-13} \exp(1300/T)$	3
K127	$C_4H_9OO + NO$	$\rightarrow NO_2 + 0.67(CH_3CH_2COCH_3 + HO_2) + 0.33(C_2H_5OO + CH_3CHO)$	$(1 - RTC4P) \times 8.3 \times 10^{-12}$	1, 4
K128	$C_4H_9OO + NO$	$\rightarrow C_4H_9ONO_2$	$RTC4P \times 8.3 \times 10^{-12}$	1, 4
K129	$C_4H_9OO + CH_3OO$	$\rightarrow HCHO + HO_2 + 0.67(CH_3CH_2C(O)CH_3 + HO_2) + 0.33(CH_3CHO + CH_3CH_2OO)$	$0.8 * 1.3 \times 10^{-12}$	3
K130	$C_4H_9OO + CH_3OO$	$\rightarrow CH_3CH_2COCH_3 + CH_3OH$	$0.2 * 1.3 \times 10^{-12}$	3
K131	$C_4H_9OOH + OH$	$\rightarrow C_4H_9OO$	$1.90 \times 10^{-12} \exp(190/T)$	3
K132	$C_4H_9OOH + OH$	$\rightarrow CH_3CH_2COCH_3 + OH$	$2.15 \times 10^{-11}$	3
K133	$C_4H_9ONO_2 + OH$	$\rightarrow CH_3CH_2COCH_3 + NO_2$	$8.6 \times 10^{-13}$	1
K134	$CH_3CH_2COCH_3 + OH$	$\rightarrow CH_3CH(OO)COCH_3$	$1.5 \times 10^{-12} \exp(-90/T)$	1
K135	$CH_3CH(OO)COCH_3 + HO_2$	$\rightarrow CH_3CH(OOH)COCH_3$	K126	
K136	$CH_3CH(OO)COCH_3 + NO$	$\rightarrow CH_3CHO + CH_3C(O)OO + NO_2$	$(1 - RTC4S) \times 2.55 \times 10^{-12} \exp(380/T)$	1, 4
K137	$CH_3CH(OO)COCH_3 + NO$	$\rightarrow CH_3CH(ONO_2)COCH_3$	$RTC4S \times 2.55 \times 10^{-12} \exp(380/T)$	1, 4
K138	$CH_3CH(OOH)COCH_3 + OH$	$\rightarrow CH_3CH(OO)COCH_3$	K131	
K139	$CH_3CH(OOH)COCH_3 + OH$	$\rightarrow CH_3C(O)C(O)CH_3 + OH$	$1.88 \times 10^{-11}$	3
K140	$CH_3CH(ONO_2)COCH_3 + OH$	$\rightarrow CH_3C(O)C(O)CH_3 + NO_2$	$1.2 \times 10^{-12}$	1
<b><u>ISOPRENE</u></b>				
K141	$ISOP + OH$	$\rightarrow 0.98 \text{ ISOPOO} + 0.0003 \text{ ELVOC} + 0.007 \text{ SVOC}$	$2.7 \times 10^{-11} \exp(390/T)$	1, 3
K142	$ISOP + NO_3$	$\rightarrow ISOPONO_2$	$2.95 \times 10^{-12} \exp(-450/T)$	1, 3
K143	$ISOP + O_3$	$\rightarrow 0.98 * (0.3 \text{ MACR} + 0.3 \text{ MACROO} + 0.2 \text{ MVK} + 0.2 \text{ MVKOO} + 0.78 \text{ HCHO} +$	$1.05 \times 10^{-14} \exp(-2000/T)$	1, 3

			0.22CO + 0.125 HO <sub>2</sub> + 0.125OH) + 0.0001 ELVOC + 0.009 SVOC		
K144	ISOPOO + HO <sub>2</sub>	→	ISOPOOH	$2.06 \times 10^{-13} \exp(1300/T)$	3, 7
K145	ISOPOO + NO	→	HCHO + 0.64MVK + 0.36MACR + HO <sub>2</sub> + NO <sub>2</sub>	$(1-RTC5S) * 2.7 \times 10^{-12} \exp(360/T)$	3
K146	ISOPOO + NO	→	ISOPONO <sub>2</sub>	$RTC5S * 2.7 \times 10^{-12} \exp(360/T)$	3
K147	ISOPOO + NO <sub>3</sub>	→	HCHO + 0.64MVK + 0.36MACR + HO <sub>2</sub> + NO <sub>2</sub>	$2.3 \times 10^{-12}$	3
K148	ISOPOO + CH <sub>3</sub> OO	→	0.64MVK + 0.36MACR + 2HCHO + 2HO <sub>2</sub>	$0.8 * 2.65 \times 10^{-12}$	3
K149	ISOPOO + CH <sub>3</sub> OO	→	0.64MVK + 0.36MACR + HCHO + CH <sub>3</sub> OH	$0.2 * 2.65 \times 10^{-12}$	3
K150	ISOPOO	→	HPALD + HO <sub>2</sub>	$4.12 \times 10^8 \exp(-7700/T)$	6, 7
K151	ISOPOOH + OH	→	IEPOX + OH	$1.9 \times 10^{-11} \exp(-390/T)$	8
K152	ISOPOOH + OH	→	ISOPOO	$0.7 * 3.8 \times 10^{-12} \exp(-200/T)$	8
K153	ISOPOOH + OH	→	0.64 CH <sub>3</sub> COCHO + 0.64 HOCH <sub>2</sub> CHO + 0.36 HOCH <sub>2</sub> C(O)CH <sub>3</sub> + 0.36 CHOCHO + OH	$0.3 * 3.8 \times 10^{-12} \exp(-200/T)$	8, 9
K154	ISOPONO <sub>2</sub> + OH	→	0.64 CH <sub>3</sub> COCHO + 0.64 HOCH <sub>2</sub> CHO + 0.36 HOCH <sub>2</sub> C(O)CH <sub>3</sub> + 0.36 CHOCHO + NO <sub>2</sub>	$1.77 \times 10^{-11} \exp(-500/T)$	8
K155	HPALD + OH	→	0.5 HOCH <sub>2</sub> C(O)CH <sub>3</sub> + 0.5 CH <sub>3</sub> C(O)CHO + 0.25 HOCH <sub>2</sub> CHO + 0.25 CHOCHO + HCHO + HO <sub>2</sub> + OH	$4.6 \times 10^{-11}$	6
K156	IEPOX + OH	→	IEPOXOO	$5.78 \times 10^{-11} \exp(-400/T)$	8
K157	IEPOXOO + HO <sub>2</sub>	→	0.725 HOCH <sub>2</sub> C(O)CH <sub>3</sub> + 0.275 HOCH <sub>2</sub> CHO + 0.275 HOCH <sub>2</sub> CHO + 0.275 CH <sub>3</sub> C(O)CHO + 1.125 OH + 0.825 HO <sub>2</sub> + 0.2 CO <sub>2</sub> + 0.375 CH <sub>2</sub> O + 0.074 HCOOH + 0.251 CO	$7.4 \times 10^{-13} \exp(700/T)$	8
K158	IEPOXOO + NO	→	0.725 HOCH <sub>2</sub> C(O)CH <sub>3</sub> + 0.275 HOCH <sub>2</sub> CHO + 0.275 HOCH <sub>2</sub> CHO + 0.275 CH <sub>3</sub> C(O)CHO + 1.125 OH + 0.825 HO <sub>2</sub> + 0.2 CO <sub>2</sub> + 0.375 CH <sub>2</sub> O + 0.074 HCOOH + 0.251 CO + NO <sub>2</sub>	$2.7 \times 10^{-12} \exp(360/T)$	3
K159	IEPOXOO + NO <sub>3</sub>	→	0.725 HOCH <sub>2</sub> C(O)CH <sub>3</sub> + 0.275 HOCH <sub>2</sub> CHO + 0.275 HOCH <sub>2</sub> CHO + 0.275 CH <sub>3</sub> C(O)CHO + 1.125 OH + 0.825 HO <sub>2</sub> + 0.2 CO <sub>2</sub> + 0.375 CH <sub>2</sub> O + 0.074 HCOOH + 0.251 CO + NO <sub>2</sub>	$1.74 * 2.3 \times 10^{-12}$	3
K160	MVK + OH	→	MVKOO	$2.6 \times 10^{-12} \exp(610/T)$	1



K161	MVK + NO <sub>3</sub>	→ 0.65 HCOOH + 0.65 MGLY + 0.35 HCHO + 0.35 CH <sub>3</sub> C(O)OOH + HNO <sub>3</sub>	6.0 x 10 <sup>-16</sup>	1
K162	MVK + O <sub>3</sub>	→ 0.38 CH <sub>3</sub> COCHO + 0.2088 CH <sub>3</sub> C(O)OO + 0.26 CH <sub>3</sub> COCOHOH + 0.26 CO + 0.0432 CH <sub>3</sub> COOH + 0.108 CH <sub>3</sub> CHO + 0.62 HCHO + 0.48 CO <sub>2</sub> + 0.54 HO <sub>2</sub> + 0.1008 OH	8.5 x 10 <sup>-16</sup> exp(-1520/T)	1, 3
K163	MVKOO + HO <sub>2</sub>	→ MVKOOH	K144	
K164	MVKOO + NO	→ 0.295 CH <sub>3</sub> C(O)CHO + 0.295 HCHO + 0.670 CH <sub>3</sub> CHO + 0.670 GLYAL + 0.295 HO <sub>2</sub> + 0.965 NO <sub>2</sub> + 0.0352 MVKONO <sub>2</sub>	2.6 x 10 <sup>-12</sup> exp(380/T)	3
K165	MVKOOH + OH	→ CH <sub>3</sub> C(O)CHO + CO + 2HO <sub>2</sub> + OH	2.55 x 10 <sup>-11</sup>	3
K166	MVKOOH + OH	→ MVKOO	1.9 x 10 <sup>-12</sup> exp(190/T)	3
K167	MVKONO <sub>2</sub> + OH	→ CH <sub>3</sub> C(O)CHO + CO + HO <sub>2</sub> + NO <sub>2</sub>	1.33 x 10 <sup>-12</sup>	3
K168	MACR + OH	→ MACROO	8.0 x 10 <sup>-12</sup> exp(380/T)	1
K169	MACR + NO <sub>3</sub>	→ MACROO + HNO <sub>3</sub>	3.4 x 10 <sup>-15</sup>	1
K170	MACR + O <sub>3</sub>	→ 0.90 CH <sub>3</sub> COCHO + 0.5 HCHO + 0.5 CO + 0.14 HO <sub>2</sub> + 0.24 OH	1.4 x 10 <sup>-15</sup> exp(-2100/T)	1, 3
K171	MACROO + HO <sub>2</sub>	→ MACROOH	0.625 * 2.91 x 10 <sup>-13</sup> exp(1300/T)	3
K172	MACROO + NO	→ 0.987 (CH <sub>3</sub> COCH <sub>2</sub> OH + CO + NO <sub>2</sub> + HO <sub>2</sub> ) + 0.013 MACRONO <sub>2</sub>	K164	1, 3
K173	MACROOH + OH	→ CH <sub>3</sub> COCH <sub>2</sub> OH + CO + OH	3.77 x 10 <sup>-11</sup>	
K174	MACROOH + OH	→ MACROO	K166	
K175	MACRONO <sub>2</sub> + OH	→ MGLY + CO + HO <sub>2</sub> + NO <sub>2</sub>	4.34 x 10 <sup>-12</sup>	3
<b><u>TERPENES</u></b>				
K176	TERP + OH	→ 0.81 TERPOO + 0.05 ELVOC + 0.14 SVOC	0.5 * 1.34 x 10 <sup>-11</sup> exp(410/T) +	1, 10
K177	TERP + NO <sub>3</sub>	→ TERPOO + HNO <sub>3</sub>	0.5 * 1.62 x 10 <sup>-11</sup> exp(460/T) 0.5 * 1.2 x 10 <sup>-12</sup> exp(490/T) + 0.5 * 2.5 x 10 <sup>-12</sup>	1, 10
K178	TERP + O <sub>3</sub>	→ 0.915 MACR + 0.36 MVK + 0.24 PRV + 1.68 HCHO + 0.16 CO + 0.6 HCOOH + 0.08 C <sub>3</sub> H <sub>6</sub> + 0.68 OH + 0.05 ELVOC + 0.14 SVOC	0.5 * 8.22 x 10 <sup>-16</sup> exp(-640/T) + 0.5 * 1.39 x 10 <sup>-15</sup> exp(- 1280/T)	1, 10

K179	TERPOO + HO <sub>2</sub>	→ 2 ISOPOOH	K144
K180	TERPOO + NO	→ 2 (HCHO + 0.64MVK + 0.36MACR + HO <sub>2</sub> ) + NO <sub>2</sub>	K145
K181	TERPOO + NO	→ 2 ISOPONO <sub>2</sub>	K146
K182	TERPOO + NO <sub>3</sub>	→ 2 (HCHO + 0.64MVK + 0.36MACR + HO <sub>2</sub> ) + NO <sub>2</sub>	K147
K183	TERPOO + CH <sub>3</sub> OO	→ 2 (0.64MVK + 0.36MACR + 2HCHO + 2HO <sub>2</sub> )	K148
K184	TERPOO + CH <sub>3</sub> OO	→ 2 (0.64MVK + 0.36MACR + HCHO + CH <sub>3</sub> OH)	K149

**AROMATICS**

			A1 * 1.8 x 10 <sup>-12</sup> exp(340/T) +	
K185	AROM + OH	→ AROMOO + HO <sub>2</sub>	A2 * 1.72 x 10 <sup>-11</sup> + A3 * 2.3 x 10 <sup>-12</sup> exp(-190/T)	1, 11
K186	AROM + NO <sub>3</sub>	→ AROMOO + HNO <sub>3</sub>	A1 * 7.8 x 10 <sup>-17</sup> + A2 * 3.54 x 10 <sup>-16</sup>	1, 11
K187	AROM + O <sub>3</sub>	→ AROMOO	A1 * 1.0x 10 <sup>-21</sup> + A2 * (2.4 x 10 <sup>-13</sup> exp(-5586/T) + 5.37 x 10 <sup>-13</sup> exp(-6039/T) + 1.91 x 10 <sup>-13</sup> exp(-5586/T))/3	1, 11, 12
K188	AROMOO + HO <sub>2</sub>	→ C <sub>4</sub> H <sub>9</sub> OOH + CHOCHO + HCHO	K126	
K189	AROMOO + NO	→ NO <sub>2</sub> + 0.67CH <sub>3</sub> CH <sub>2</sub> COCH <sub>3</sub> + 0.67 HO <sub>2</sub> + 0.33C <sub>2</sub> H <sub>5</sub> OO + 0.33CH <sub>3</sub> CHO + CHOCHO + HCHO	K127	
K190	AROMOO + NO	→ C <sub>4</sub> H <sub>9</sub> ONO <sub>2</sub> + CHOCHO + HCHO	K128	
K191	AROMOO CH <sub>3</sub> OO	+ → HCHO + HO <sub>2</sub> + 0.67(CH <sub>3</sub> CH <sub>2</sub> C(O)CH <sub>3</sub> + HO <sub>2</sub> ) + 0.33(CH <sub>3</sub> CHO + CH <sub>3</sub> CH <sub>2</sub> OO) + CHOCHO + HCHO	K129	
K192	AROMOO CH <sub>3</sub> OO	+ → CH <sub>3</sub> CH <sub>2</sub> COCH <sub>3</sub> + CH <sub>3</sub> OH + CHOCHO + HCHO	K130	

**SO<sub>x</sub>**

K193	SO <sub>2</sub> + OH	→ HO <sub>2</sub> + H <sub>2</sub> SO <sub>4</sub>	3.3 x 10 <sup>-31</sup> (T/300) <sup>-4.3</sup> [N <sub>2</sub> ] 1.6 x 10 <sup>-12</sup> (T/300) <sup>-0.7</sup>	2
------	----------------------	--	--	---

			$F_c = 0.6$	
K194	DMS + OH	→ CH <sub>3</sub> OO + HCHO + SO <sub>2</sub>	$1.1 \times 10^{-11} \exp(-240/T)$	2
K195	DMS + OH	→ 0.75 CH <sub>3</sub> OO + 0.75 HCHO + 0.75 SO <sub>2</sub> + 0.25 MSA	$1.0 \times 10^{-39} [\text{O}_2] \exp(5820/T) / (1 + 5.0 \times 10^{-30} [\text{O}_2] \exp(6280/T))$	2
K196	DMS + NO <sub>3</sub>	→ CH <sub>3</sub> OO + HCHO + SO <sub>2</sub> + HNO <sub>3</sub>	$1.9 \times 10^{-13} \exp(520/T)$	2
	<b><u>NH<sub>x</sub></u></b>			
K197	NH <sub>3</sub> + OH	→ NH <sub>2</sub> + HO <sub>2</sub>	$1.7 \times 10^{-12} \exp(-710/T)$	2
K198	NH <sub>2</sub> + O <sub>2</sub>	→ NH <sub>2</sub> O <sub>2</sub>	$6.0 \times 10^{-21}$	2
K199	NH <sub>2</sub> + O <sub>3</sub>	→ NH <sub>2</sub> O <sub>2</sub>	$4.3 \times 10^{-12} \exp(-930/T)$	2
K200	NH <sub>2</sub> + OH	→ NH <sub>2</sub> O <sub>2</sub>	$3.4 \times 10^{-11}$	2
K201	NH <sub>2</sub> + HO <sub>2</sub>	→ NH <sub>3</sub>	$3.4 \times 10^{-11}$	2
K202	NH <sub>2</sub> + NO	→ NH <sub>2</sub> O <sub>2</sub> + NO <sub>2</sub>	$4.0 \times 10^{-12} \exp(450/T)$	2
K203	NH <sub>2</sub> + NO <sub>2</sub>	→ NH <sub>2</sub> O <sub>2</sub> + NO	$2.1 \times 10^{-12} \exp(650/T)$	2
K204	NH <sub>2</sub> O <sub>2</sub> + O <sub>3</sub>	→ NH <sub>2</sub>	K199	
K205	NH <sub>2</sub> O <sub>2</sub> + HO <sub>2</sub>	→ NH <sub>2</sub>	K201	
K206	NH <sub>2</sub> O <sub>2</sub> + NO	→ NH <sub>2</sub> + NO <sub>2</sub>	K202	

# The reaction products O<sub>2</sub>, H<sub>2</sub>, and H<sub>2</sub>O are not shown.

<sup>1</sup> The chemical kinetic data and mechanistic information was taken from the website of the IUPAC Task Group on Atmospheric Chemical Kinetic Data Evaluation: [www.iupac-kinetic.ch.cam.ac.uk](http://www.iupac-kinetic.ch.cam.ac.uk)

<sup>2</sup> The chemical kinetic data and mechanistic information was taken from the website of the NASA Panel for Data Evaluation (Evaluation No. 18, JPL Publication 15-10) <http://jpldataeval.jpl.nasa.gov>

<sup>3</sup> The chemistrymechanistic information was taken from the Master Chemical Mechanism (MCM v3.2):

- for non-aromatic schemes: Jenkin et al. (1997); Saunders et al. (2003)
- for the isoprene scheme: Jenkin et al. (2015)
- for aromatic schemes: Jenkin et al. (2003); Bloss et al. (2005)
- and via website: <http://mcm.leeds.ac.uk/MCM>

<sup>4</sup> Atkinson (1997):

- $R_1 = 2.7 \times 10^{14} \exp(-6350/T)$   
 $R_2 = 6.3 \times 10^{-14} \exp(-550/T)$

$$f = R_1 / (R_1 + R_2 \times [\text{O}_2])$$

- $R_1 = 1.94 \times 10^{-22} [\text{AIR}] \exp(0.972 \times N_c)$   
 $R_2 = 0.826 \times (T/300)^{-8.1}$

$$A = 1/(1 + \log_{10}(R_1/R_2)^2)$$

$$\text{RTC}(N_c)P = 0.4 \times R_1 / (1 + R_1/R_2) 0.411^A$$

$$\text{RTC}(N_c)S = R_1 / (1 + R_1/R_2) 0.411^A$$

where  $N_c$  is the number of carbons (i.e., 1-5)

<sup>5</sup> Orlando et al. (1992); Poisson et al. (2000)

<sup>6</sup> Peeters and Müller (2010)

<sup>7</sup> Crouse et al. (2011)

<sup>8</sup> Paulot et al. (2009)

<sup>9</sup> Browne et al. (2014)

<sup>10</sup> Average of  $\alpha$ - and  $\beta$ -pinene

<sup>11</sup> A1, A2, A3 represents the relative contributions of *ortho*-, *meta*-, and *para*-xylene, toluene and benzene (roughly 0.4, 0.6 and 0.4, respectively, for the year 2006)

<sup>12</sup> Average of *ortho*-, *meta*- and *para*-isomers of xylene

**Table 5.3: Selection of effective Henry law coefficients ( $H^*$ ) used in TM5-MP for the MOGUNTIA chemical scheme.**

Trace gas	$H^*$ ( $M \text{ atm}^{-1}$ )	$\Delta H R^{-1}$ (K)	Reference
CH <sub>3</sub> OOH, <i>n</i> -C <sub>3</sub> H <sub>7</sub> OOH, <i>i</i> -C <sub>3</sub> H <sub>7</sub> OOH, CH <sub>3</sub> COCH <sub>2</sub> OH, C <sub>4</sub> H <sub>9</sub> OOH, MEKOOH, ISOPOOH, MVKOOH, MACROOH	2.9 x 10 <sup>2</sup>	5200	1
CH <sub>3</sub> ONO <sub>2</sub> ,	2.0	4700	1
CH <sub>3</sub> OONO <sub>2</sub>	2.0	4700	1
HCHO	3.2 x 10 <sup>3</sup>	6800	1
CH <sub>3</sub> OH	2.0 x 10 <sup>2</sup>	5600	1
HCOOH	8.8 x 10 <sup>3</sup>	6100	1
CH <sub>3</sub> CH <sub>2</sub> OOH	3.3	6000	1
CH <sub>3</sub> CH <sub>2</sub> ONO <sub>2</sub>	1.6	5400	1
HOCH <sub>2</sub> CH <sub>2</sub> OOH	1.7 x 10 <sup>6</sup>	9700	1
HOCH <sub>2</sub> CH <sub>2</sub> ONO <sub>2</sub>	3.9 x 10 <sup>4</sup>		1
CH <sub>3</sub> CHO	13	5900	1
CH <sub>3</sub> COOH	8.3 x 10 <sup>2</sup>	5300	1
HOCH <sub>2</sub> CHO	4.1 x 10 <sup>4</sup>	4600	1
CHOCHO	4.19 x 10 <sup>5</sup>	7500	1
CH <sub>3</sub> CH <sub>2</sub> OH	190	6400	1
CH <sub>3</sub> COOH	4.0 x 10 <sup>3</sup>	6200	1
<i>n</i> -C <sub>3</sub> H <sub>7</sub> ONO <sub>2</sub>	1.1	5500	1
<i>i</i> -C <sub>3</sub> H <sub>7</sub> ONO <sub>2</sub>	0.78	5400	1
HOC <sub>3</sub> H <sub>6</sub> OOH	1.7 x 10 <sup>6</sup>	9700	1
CH <sub>3</sub> COCH <sub>3</sub>	27	5500	1
CH <sub>3</sub> CH <sub>2</sub> CHO	9.9	4300	1
CH <sub>3</sub> COCHO	3.2 x 10 <sup>3</sup>	7500	1
CH <sub>3</sub> C(O)COOH	3.1 x 10 <sup>5</sup>	5100	1
C <sub>4</sub> H <sub>9</sub> ONO <sub>2</sub>	1	5800	1
MEK	18	5700	1

MEKONO <sub>2</sub>	0.7	5200	1
CH <sub>3</sub> COCOCH <sub>3</sub>	73	5700	1
ISOPONO <sub>2</sub> , MACRONO <sub>2</sub> , MVKONO <sub>2</sub>	1.7 x 10 <sup>4</sup>	9200	2
IEPOX	9.1 x 10 <sup>4</sup>	6600	3
HPALD	2.3		1
MVK	26	4800	1
MACR	4.8	4300	1

<sup>1</sup> Sander (2015) and references therein; <sup>2</sup> Ito et al. (2007) for all biogenic hydroxy nitrates; <sup>3</sup> Browne et al. (2014), as for H<sub>2</sub>O<sub>2</sub>

## 5.1 References

- Atkinson, R., 1997. Gas-phase tropospheric chemistry of volatile organic compounds: 1. Alkanes and alkenes. *J. Phys. Chem. Ref. Data*. <https://doi.org/10.1063/1.556012>
- Bloss, C., Wagner, V., Bonzanini, A., Jenkin, M.E., Wirtz, K., Martin-Reviejo, M., Pilling, M.J., 2005. Evaluation of detailed aromatic mechanisms (MCMv3 and MCMv3.1) against environmental chamber data. *Atmos. Chem. Phys.* 5, 623–639. <https://doi.org/10.5194/acp-5-623-2005>
- Browne, E.C., Wooldridge, P.J., Min, K.E., Cohen, R.C., 2014. On the role of monoterpene chemistry in the remote continental boundary layer. *Atmos. Chem. Phys.* <https://doi.org/10.5194/acp-14-1225-2014>
- Crouse, J.D., Paulot, F., Kjaergaard, H.G., Wennberg, P.O., 2011. Peroxy radical isomerization in the oxidation of isoprene. *Phys. Chem. Chem. Phys.* <https://doi.org/10.1039/c1cp21330j>
- Ito, A., Sillman, S., Penner, J.E., 2007. Effects of additional nonmethane volatile organic compounds organic nitrates, and direct emissions of oxygenates organic species of global tropospheric chemistry. *J. Geophys. Res. Atmos.* <https://doi.org/10.1029/2005JD006556>
- Jenkin, M.E., Saunders, S.M., Pilling, M.J., 1997. The tropospheric degradation of volatile organic compounds: A protocol for mechanism development. *Atmos. Environ.* [https://doi.org/10.1016/S1352-2310\(96\)00105-7](https://doi.org/10.1016/S1352-2310(96)00105-7)
- Jenkin, M.E., Saunders, S.M., Wagner, V., Pilling, M.J., 2003. Protocol for the development of the Master Chemical Mechanism, MCM v3 (Part B): tropospheric degradation of aromatic volatile organic compounds. *Atmos. Chem. Phys.* 3, 181–193. <https://doi.org/10.5194/acp-3-181-2003>
- Jenkin, M.E., Young, J.C., Rickard, A.R., 2015. The MCM v3.3.1 degradation scheme for isoprene. *Atmos. Chem. Phys.* <https://doi.org/10.5194/acp-15-11433-2015>
- Orlando, J.J., Tyndall, G.S., Calvert, J.G., 1992. Thermal decomposition pathways for peroxyacetyl nitrate (PAN): Implications for atmospheric methyl nitrate levels. *Atmos. Environ. Part A, Gen. Top.* [https://doi.org/10.1016/0960-1686\(92\)90468-Z](https://doi.org/10.1016/0960-1686(92)90468-Z)
- Paulot, F., Crouse, J.D., Kjaergaard, H.G., Kroll, J.H., Seinfeld, J.H., Wennberg, P.O., 2009. Isoprene photooxidation: New insights into the production of acids and organic nitrates. *Atmos. Chem. Phys.* <https://doi.org/10.5194/acp-9-1479-2009>
- Peeters, J., Müller, J.F., 2010. HOx radical regeneration in isoprene oxidation via peroxy radical isomerisations. II: Experimental evidence and global impact. *Phys. Chem. Chem. Phys.* 12, 14227–14235. <https://doi.org/10.1039/c0cp00811g>
- Poisson, N., Kanakidou, M., Crutzen, P.J., 2000. Impact of non-methane hydrocarbons on tropospheric chemistry and the oxidizing power of the global troposphere: 3-Dimensional modelling results. *J. Atmos. Chem.* 36, 157–230. <https://doi.org/10.1023/A:1006300616544>
- Saunders, S.M., Jenkin, M.E., Derwent, R.G., Pilling, M.J., 2003. Protocol for the development of the Master Chemical Mechanism, MCM v3 (Part A): Tropospheric degradation of non-aromatic volatile organic compounds. *Atmos. Chem. Phys.* [75](https://doi.org/10.5194/acp-3-</a></p></div><div data-bbox=)

161-2003